

# ACCURATE EVALUATION OF TRANSIENTS ON DOUBLE CIRCUIT EHV TRANSMISSION LINES

A Thesis Submitted  
in partial Fulfilment of the Requirements  
for the Degree of  
DOCTOR OF PHILOSOPHY

by  
R. BALASUBRAMANIAN

TK

to the

DEPARTMENT OF ELECTRICAL ENGINEERING  
INDIAN INSTITUTE OF TECHNOLOGY KANPUR  
JUNE, 1976

Dedicated to

my parents

1917

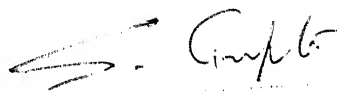
ILLINOIS  
CENTRAL LIBRARY  
51191  
Acc. No. A .....

27 SEP 1977

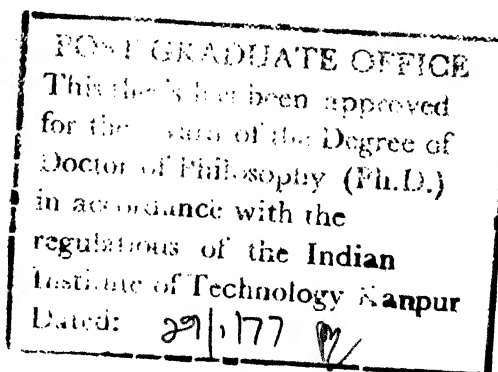
EE-1976-D-BAL-ACC

## CERTIFICATE

Certified that this work, 'Accurate Evaluation of Transients on Double Circuit EHV Transmission Lines' by R. Balasubramanian, has been carried out under my supervision and that this work has not been submitted elsewhere for a degree.



Dr. S. Gupta  
Assistant Professor  
Department of Electrical Engineering  
Indian Institute of Technology  
Kanpur





## ACKNOWLEDGEMENTS

With deep sense of gratitude, the author thanks Dr. S. Gupta for his guidance and comments.

The author wishes to express his deep gratitude to Dr. V.R. Sastry for making some invaluable suggestion in the early part of this work.

The author is grateful to the Indian Institute of Technology, Kanpur and in particular to the Computer Centre for providing the facilities to carry out this work.

The author also expresses his gratitude to the authorities of Bharat Heavy Electrical Limited (Consulting Services) for the encouragement given by them during the final stages of this work.

Thanks are also due to Mr. K.N. Tewari for his cooperation in typing this thesis.

## TABLE OF CONTENTS

LIST OF TABLES	vii	
LIST OF FIGURES	ix	
LIST OF SYMBOLS	xii	
SYNOPSIS	xii	
CHAPTER 1	INTRODUCTION	1
1.1	Transients on Transmission Lines	1
1.2	Lumped Parameter Method	3
1.3	Lattice Diagram Method	4
1.4	Uram and Miller's Method	5
1.5	Fourier Transform Method	6
1.6	Dommel's Method	8
1.7	Finite Difference Method	10
1.8	Objectives and Outlines of the Thesis	11
CHAPTER 2	MODIFIED FOURIER TRANSFORM METHOD	17
2.1	Introduction	17
2.2	Theory of the Method	17
2.3	Three Phase Systems - Modal Analysis	23
2.4	Mathematical Model for Energisation Study	26
2.5	Numerical Example	30
2.6	Conclusions	32

CHAPTER 3	MODELLING OF A DOUBLE CIRCUIT LINE FOR TRANSIENT STUDIES	33
3.1	Introduction	33
3.2	Modal Transformation for a Double Circuit Line	34
3.2.1	Transposed line	39
3.2.2	Untransposed line	40
3.3	Conclusions	41
CHAPTER 4	FAULT INITIATING TRANSIENT ON A DOUBLE CIRCUIT TRANSMISSION LINE	42
4.1	Introduction	42
4.2	Simulation of Fault	44
4.3	Evaluation of Transient Response for the Injected Voltages	46
4.4	Verification of the Computer Program	51
4.5	System Used for the Study	51
4.6	Computation Results	55
4.6.1	Fault overvoltages on single circuit and double circuit lines	55
4.6.2	Transposed versus untransposed line	57
4.6.3	Effect of incorporating frequency dependence of line parameters	57
4.6.4	Overvoltages for off-centre fault locations	59
4.7	Conclusions	64
CHAPTER 5	ENERGISING TRANSIENT ON A DOUBLE CIRCUIT TRANSMISSION LINE	66
5.1	Introduction	66
5.2	Problem Description	66
5.3	First Circuit Energisation	67
5.4	Computational Results	72

5.4.1	Transposed line versus untransposed line	73
5.4.2	Single circuit versus double circuit line representations	73
5.5	Simulation of Second Circuit Energisation	75
5.5.1	Calculation of Steady State Response	78
5.5.2	Calculation of Transient Response for the Injected Voltages	82
5.6	Computational Results	83
5.6.1	Transposed versus untransposed configurations	84
5.6.2	Single versus double circuit line representations	84
5.7	Effect of Incorporation of Frequency Dependence of Line Parameters	88
5.8	Conclusions	88
CHAPTER 6	EXTENSION OF URAM AND MILLER'S METHOD FOR DOUBLE CIRCUIT LINE ENERGISATION TRANSIENT ANALYSIS	90
6.1	Introduction	90
6.2	Extension of Uram and Miller's Method for Double Circuit Line Transients	91
6.3	First Circuit Energisation Transient	94
6.4	Second Circuit Energisation	99
6.5	Computational Results	102
6.6	Conclusions	106
CHAPTER 7	ENERGISATION TRANSIENT DUE TO SEQUENTIAL CLOSING OF CIRCUIT BREAKER POLES	108
7.1	Introduction	108
7.2	Incorporation of Sequential Closing of Circuit Breaker Poles in Fourier Transform Method	109

7.3	Development of Algorithm for Handling Sequential Closing	113
7.4	Numerical Evaluation of the Modified Fourier Transform	117
7.5	Single Circuit Line Examples	120
7.5.1	Verification of Computer Program	120
7.5.2	Effect of Incorporating Frequency Dependence of Line Parameters	124
7.6	Energisation Transient on a Double Circuit Line	125
7.7	Computational Results	134
7.7.1	Double Circuit versus Single Circuit Lines	134
7.7.2	Transposed versus Untransposed Lines	136
7.7.3	The Effect of Frequency Dependence of Line Parameters	136
7.8	Conclusions	141
CHAPTER 8	SUMMARY AND CONCLUSIONS	142
8.1	Conclusions	142
8.2	Summary	152
	LIST OF REFERENCES	156
APPENDIX A	SYSTEM DATA	164
APPENDIX B	LINE PARAMETERS CALCULATION - CARSON'S FORMULAE	165
APPENDIX C	SYSTEM DATA - BOONYUBOL'S EXAMPLE	166
APPENDIX D	SYSTEM DATA FOR FAULT STUDIES	167
APPENDIX E	URAM AND MILLER'S METHOD - THEORY	169
APPENDIX F	FLOW CHART FOR COMPUTATION OF SEQUENTIAL CLOSING TRANSIENTS BY MODIFIED FOURIER TRANSFORM METHOD	175
APPENDIX G	OBRA-LUCKNOW LINE DATA	180
	CURRICULUM VITAE	181

## LIST OF TABLES

Table No.		Page
4.1	Table showing the maximum peak voltages for various cases of fault initiating transients on double circuit lines	59
4.2	Table showing the maximum peak voltages for various locations of the fault	62

## LIST OF FIGURES

Figure No.	Caption	Page
2.1.1	System diagram with source representation	29
2.1.2	System diagram with equivalent current source	29
2.2	Energising transient voltage waveforms at receiving end	31
4.1	Principle of superposition used for fault simulation	45
4.2	Fault point voltage waveforms of Boonyubol's example	52
4.3	Line configuration	53
4.4	Fault transient on transposed single circuit and double circuit lines - fault at mid span on phase-a	56
4.5	Fault transients on transposed and untransposed lines - fault at mid span on phase-a	58
4.6	Effect of frequency dependence of line parameters on fault transients - transposed line - fault at mid span on phase-a	60
4.7	Effect of frequency dependence of line parameters on fault transients - untransposed line - fault at mid span on phase-a	61
4.8	Effect of change in fault location to quarter span - transposed line-without frequency dependence	63
5.1.1	System diagram with source representation	69
5.1.2	System diagram with equivalent current source	69
5.2	Voltage transients at receiving end - first circuit energisation - second circuit open	74

5.3	Receiving end voltage waveforms for untransposed double and single circuit lines - first circuit energisation - second circuit open	76
5.4	Principle of superposition used for energisation studies	77
5.5	Voltage transients at receiving end - second circuit energisation - first circuit in steady state	85
5.6	Receiving end voltage waveforms for untransposed double and single circuit lines - second circuit energisation - first circuit in steady state	87
6.1	Single line diagram - first circuit energisation - second circuit open	95
6.2	Principle of superposition used for simulation of second circuit energisation - first circuit in steady state	100
6.3	Comparison of voltage waveforms at receiving end by Uram and Miller and modified Fourier transform methods - first circuit energisation - second circuit open	104
6.4	Voltage waveforms at receiving end - second circuit energisation - first circuit open	105
7.1	Numerical evaluation of Fourier transform of a function	119
7.2	System diagram of the example	122
7.3	Comparison of voltage waveforms at receiving end by Uram and Miller and modified Fourier transform methods - UPSEB single circuit line sequential energisation	123
7.4	Effect of frequency dependence of line parameters on sequential energisation transients of a transposed single circuit line	126



7.5	System diagram for calculation of transient response for injected voltage - sequential closing	129
7.6	Comparison of voltage waveforms at receiving end following sequential closing for transposed single and double circuit lines	135
7.7	Comparison of receiving end voltage waveforms following sequential closing for transposed and untransposed lines	137
7.8	Effect of frequency dependence of line parameters on voltage transients due to sequential closing for transposed double circuit line	139
7.9	Effect of frequency dependence of line parameters on voltage transients due to sequential closing for untransposed double circuit line	140

## LIST OF SYMBOLS

$t$	=	time
$\omega$	=	angular frequency
$a$	=	'smoothing' factor
$\underline{i}(x,t)$	=	current vector at instant $t$ , $x$ units away from the line end
$\underline{v}(x,t)$	=	voltage vector at instant $t$ , $x$ units away from the line end
$\underline{V}(x,\omega)$	=	modified Fourier transform of $\underline{v}(x,t)$
$\underline{I}(x,\omega)$	=	modified Fourier transform of $\underline{i}(x,t)$
$[R]$	=	resistance per unit length matrix of the line
$[L]$	=	inductance per unit length matrix of the line
$[C]$	=	capacitance per unit length matrix of the line
$[Z]$	=	transformed series impedance per unit length matrix of the line
$[Y]$	=	transformed shunt admittance per unit length matrix of the line
$[P]$	=	$[Z][Y]$
$[\gamma]$	=	the diagonal propagation constant matrix
$[Q]$	=	modal transformation matrix, which makes $[Q]^{-1}[P][Q]$ diagonal
$\Omega$	=	integration range in the truncated inverse modified Fourier integral
$l$	=	length of the line
$R_s$	=	source resistance
$L_s$	=	source inductance

Any other symbol used is explained at the place where it appears.

## SYNOPSIS

R. BALASUBRAMANIAN  
Ph.D.

Department of Electrical Engineering  
Indian Institute of Technology, Kanpur  
June 1976

ACCURATE EVALUATION OF TRANSIENTS ON  
DOUBLE CIRCUIT EHV TRANSMISSION LINES

An overhead transmission line is subjected to overvoltage transients due to lightning, switching operations or faults. Among these, the overvoltages caused by the lightning is independent of the operating voltage of the line, whereas the overvoltages due to the switching operations or faults depend on the operating voltage of the line. Therefore, of late as the transmission voltages are increasing, the studies of switching and fault transients have gained more importance. Accurate calculation of these overvoltages permits reduction of safety margins and eventually reduces the cost of insulation of transmission lines and associated equipments.

The various methods of calculating these overvoltage transients, described in the literature may be broadly classified into the lumped parameter methods (including the Transient Network Analyser studies), time domain methods such as Lattice Diagram method, Uram and Miller's method and finite difference method and transform techniques. In this thesis, the modified Fourier transform method, first applied to the power system transient studies by Mullineaux et al and later by Battisson et al and Wedepohl and Mohamad, has been made use of. Briefly

the Fourier transform method of calculating the transient involves solving the transformed differential equations of the transmission line for transformed voltage and current at any point on the line, satisfying the boundary conditions at the ends of the line by the method of modal analysis and the transformation of the response to the time domain by performing the truncated numerical integration. The resistance and inductance matrices of a transmission line are in reality frequency dependent because of the variation of the conductor resistance with frequency due to the skin effect phenomenon and the finite conductivity of the earth return path. Hence an exact study of transients on transmission lines calls for the inclusion of the effect of frequency dependence of line parameters. The Fourier transform method, being a frequency domain method, has the special advantage that the frequency dependence of line parameters can be directly incorporated without involving almost any additional computational effort.

The double circuit transmission line is a common feature of any power system. In the published literature, except for some TNA studies, the double circuit line transients have not been studied. Most of the double circuit lines have their conductors placed at mirror symmetrical positions with respect to a vertical plane. For a transposed double circuit line whose conductors are so symmetrically located, a frequency independent modal transformation is shown to exist in this thesis. For the untransposed double circuit line of

the above structure, the eigen-value, eigen-vector analysis of two  $3 \times 3$  matrices are to be performed at each frequency in the integration range to arrive at the modal transformation matrix.

The objective of this thesis is to study the fault and energising transients on a typical double circuit line, using the modified Fourier transform method.

The energisation and re-energisation overvoltages on a transmission line can be contained within the limit as low as 1.5 p.u. by various control methods such as the multi-step resistance closing, controlling the timing of the closure of the individual poles of the circuit breakers etc. When such effective methods of controlling the energisation and re-energisation transient overvoltages are employed, the overvoltages that arise due to fault initiation may become the limiting factor. Ninety percent or more of the faults experienced by a power system are single line to ground faults. In the event of a single line to ground fault, transient overvoltages of the order of 2 p.u. may be experienced by the sound phases. This calls for an accurate calculation of transients due to single line to ground fault initiation. Various authors have studied this problem. Kimbark and Legate have used the TNA to evaluate the fault initiating transient on a single circuit three phase line and have presented a Lattice Diagram approach for a theoretical study of the problem with certain approximations. Later exhaustive analogue computer aided studies of the problem

have been reported. Bonnyubol et al have made use of the Laplace Transform method and evaluated the fault transient, employing the 'Residue Theorem' for the inverse Laplace transformation. Except for a few TNA studies, in all the above studies, only single circuit lines have been considered. Moreover the lines have been assumed to be transposed and the effect of frequency dependence of line parameters has not been investigated. In this thesis, the modified Fourier transform method has been applied to study the transient due to the initiation of single line to ground fault at any intermediate point on a double circuit transmission line. The need for the modelling of a double circuit line for fault transient studies has been established by comparing the fault transients on single and double circuit lines. A typical 400 KV double circuit line has been considered, taking into account the mutual coupling between the two circuits. For the line, fed on both the ends by inductive sources, the mid span fault transients have been evaluated, assuming the line to be both transposed and untransposed. The effect of frequency dependence of line parameters on the fault transient overvoltages for both the transposed and untransposed configurations of the line has been investigated. The fault location is changed to various off-centre points and the fault transients have been studied. The mid span fault has been found to give rise to the maximum peak overvoltage.

The energisation of a double circuit line involves closing of both the circuits. In practice, there is bound

to be a time delay between the closing of the first and second circuits of a double circuit line. This delay is atleast a few seconds if not a few minutes. During this period, the transient due to the energisation of the first circuit would have died down and the first circuit would be in steady state. Thus essentially two transients are involved in the study of the energisation of a double circuit line (viz.) (i) the transient due to the closing of the first circuit, keeping the second circuit unenergised; (ii) the transient due to the closing of the second circuit when the first circuit is already in steady state. The thesis presents the calculation procedure and the results of the above mentioned studies on a double circuit line. A typical 400 KV double circuit line, open at the receiving end has been considered and the voltage waveforms at the open receiving end, subsequent to energisation from an inductive source have been calculated for both transposed and untransposed configurations of the line. The effect of the frequency dependence of line parameters has been incorporated in the studies by using the Carson's formulae for the calculation of the line parameter matrices.

## CHAPTER 1

### INTRODUCTION

#### 1.1 TRANSIENTS ON TRANSMISSION LINES

The study of electrical transient phenomenon in power systems has gained great importance, especially with the increasing voltages of the transmission systems. The transient overvoltages are developed in a power system either due to internal or external causes. Lightning overvoltage is an example of the externally developed overvoltage and therefore the overvoltage caused by lightning is independent of the operating voltage of the transmission system. Internally developed overvoltages are usually caused by the switching operations (either the opening or closing of the circuit breakers) and fault initiation or clearing. The overvoltages due to these depend on the operating voltage of the system and other system parameters. In earlier days when the system voltages were lower, the overvoltages due to lightning were higher than those due to switching or faults. Nowadays, in high voltage systems, the overvoltages caused by switching or faults are higher than those due to lightning. Therefore, the basic insulation level (BIL) of a power system is being determined more by the behaviour of the system under switching and fault conditions than by its response to lightning surges.



The cost of insulation of equipment and transmission lines in a high voltage system is very high. When the BIL cannot be determined accurately, the factor of safety has to be rather high. However, accurate determination of the BIL permits the reduction of this factor of safety and thereby the cost of insulation can also be made an optimum. Further, once the magnitude of the overvoltages that can arise in a system is known, methods of controlling them within limits can be developed. An accurate analysis requires an exact modelling of the system components and the physical phenomena involved in the study and similarly an accurate method of solution has to be employed.

When a switching operation or fault takes place, the elements of the power system are subjected to voltages and currents, having a wide frequency range, which may extend from 50 Hz to 100 KHz. The resistance and inductance matrices of a transmission line are, in reality, frequency dependent due to the skin effect phenomenon and the finite conductivity of the earth return path. Many of the EHV transmission lines are untransposed and even if a line is transposed, an ideal transposition is not practically realizable. Hence an exact study of transients on transmission line calls for the inclusion of the effect of frequency dependence of line parameters and handling of the untransposed lines.

There are various methods of calculating these overvoltage transients on a transmission network, available in the literature. These may be broadly classified into lumped parameter method, lattice diagram method, Uram and Miller's method, Fourier transform method, Dommel's method and finite difference method. Brief description of these methods and their salient features are presented in the following sections.

## 1.2 LUMPED PARAMETER METHOD

In the lumped parameter method, the transmission line is represented by a number of lumped T or  $\pi$  sections and the differential equations of the resulting equivalent network are solved either with a transient network analyser or a digital computer.

The favourable features of the method are its simplicity and its ability to handle untransposed lines and nonlinear elements directly.

On the other hand, for achieving good accuracy in the results, a large number of line sections are required in this method and this correspondingly increases the storage requirements. The frequency dependence of line parameters cannot be incorporated in the method. Further, the computations are to be carried out in stages right from the initial state. In other words, the response at

any particular instant cannot be directly found out without going through the calculations in stages from the initial state.

### 1.3 LATTICE DIAGRAM METHOD

The Lattice diagram was first introduced by Bewley [1]. The application of this method to large scale single and three phase systems has been done by Barthold and Carter [2], Bickford and Doepal [3] and others. In this method, lines and cables are specified by their surge impedances and surge travel times and the reflected and refracted voltages and currents at junctions and terminations are calculated by the use of reflection and refraction coefficients. To reduce the computational effort, the lumped parameters such as the transformers, shunt reactors etc. are represented as transmission line stubs of appropriate reactance values with the terminals kept open or shorted.

The advantages of this method are that it is simple, takes less computational effort and can handle large systems.

On the contrary, in this method, the frequency dependence of line parameters cannot be incorporated. Line losses can be taken into account only approximately by an attenuation factor. Representation of lumped parameter elements by stub lines leads to inaccuracy if proper

values of surge impedance and travel time for these stubs are not chosen. A lot of data such as the reflection coefficient array, travel time array, the magnitudes of the forward and backward waves are to be stored. Hence the memory requirement is quite high.

#### 1.4 URAM AND MILLER'S METHOD

The Uram and Miller's method [4,5] is a time domain method based on Laplace transform technique. In this method, by making certain assumptions, an incremental solution of the transmission line equations is made possible. Here the voltage and current at each instant of time and at any point on the transmission line, subsequent to a switching operation, can be expressed in terms of the values of some four functions at that instant (which can be interpreted as the forward and backward waves). Among these four functions, two are determined by the terminal conditions existing at the ends of the line and the other two are just the attenuated delayed functions of these two functions. For the case of a line, which was unenergised before the switching operation, the delayed functions take zero values initially till the time equal to the travel time of the line and this facilitates the starting of an incremental solution of the problem. For the three phase case, the functions become vectors of order 3, the components of which correspond to the modal

quantities. The method basically uses Laplace transform technique. The transformed transmission line equation is decoupled into modal components with the help of a constant modal transformation matrix. Such a transformation exists only for the transposed line and hence the applicability of the method is restricted to the transposed lines only. With the other assumption that the resistance offered by the line for the various modes is much less, when compared to the inductive reactance offered by the line for the various modes at all frequencies, the inversion of the response in the Laplace domain to time domain by analytical means is made possible.

The favourable features of the method are that it involves less computational effort and takes less computer time.

But this method cannot take into account the effect of frequency dependence of line parameters directly. The untransposed lines cannot be handled by the method. Computations are to be carried out in stages, starting from the initial state. Nonlinearities cannot be handled directly.

## 1.5 FOURIER TRANSFORM METHOD

The Fourier transform method has been applied for studying the transients on transmission lines by Day, Mullinaux et al [6-8], Battisson et al [9] and Wedepohl and Mohamed [10]. The method involves solving the Fourier

transformed differential equations of the transmission line for transformed voltage and current at any point on the line, satisfying the boundary conditions at the ends of the line by modal analysis and the transformation of the response to time domain by numerically performing the inverse integral. A modified version of the Fourier transform, which includes a negative exponential term in the basic transform pair relationships makes the integral over the infinite range numerically stable. The infinite integral is truncated at a finite large value for the purpose of performing the numerical integration and the resulting unwanted oscillation (Gibb's oscillation) in the process is avoided by introducing a factor to the integrand. As the method involves calculation of the frequency response in the whole frequency range, the additional calculation of the modal transformation matrix at each frequency to handle the untransposed line case and the calculation of the line parameter values at each frequency to be used in the transients computations are straightforward.

This method does not involve any assumption and represents all the components in a detailed manner. Incorporation of the frequency dependence of line parameters in the method is direct and does not involve any additional computations but for the calculation of just

the parameters at each frequency. Calculation of the solution just at any desired instant or period can be done and does not have to be carried out in stages right from the initial conditions. Handling of lumped parameter elements is very simple. There is no difficulty in studying the untransposed line cases by doing the eigenvalue, eigenvector analysis at each frequency to arrive at the modal transformation matrix at that frequency.

## 1.6 DOMMEL'S METHOD

The Dommel's solution procedure [11,12] adopts the method of characteristics [13,14] for the transmission line and the trapezoidal rule of integration for the lumped parameter elements. According to the method of characteristics, for an imaginary observer, moving along the transmission line in the forward direction with a velocity equal to that of the travelling waves initiated on the line, following a disturbance, the expression  $(v + z i)$  remains constant, where  $v$  and  $i$  are the voltage and current respectively at any point on the line and  $z$  is the surge impedance of the line. Also for an observer, moving along the line with the same velocity in the backward direction, the expression  $(v - z i)$  remains constant. Forcing these conditions, the current and voltage at both the ends of the line can be expressed in terms of the surge impedance of the line and the past values of the

voltages and currents at these terminals, prior to a period equal to the travel time of the line. The application of the trapezoidal rule of integration for the lumped parameters facilitates expressing the currents and voltages at the terminals of these elements at each instant of time in terms of the values of these currents and voltages an interval earlier and in terms of the values of the parameters. Once each component of the network is replaced by its equivalent circuit described above, the nodal equations for the whole network at each instant of time can be written and they can be solved for the unknown node voltages, knowing the past history of the system over a time span equal to the travel time for the transmission line and just the previous step value for lumped parameter elements. The line losses can be represented by lumped resistances at the ends and at the middle of the line. For solving the nodal equations of large scale networks, the application of the well developed optimally ordered triangularization and the sparsity techniques reduces the storage requirement considerably.

This method is well suited for large scale system problems especially because of the availability of the well developed sparsity techniques. It can handle nonlinearities. The method is quite general and hence the development of a general purpose program is possible.



On the other hand, there is no direct way of incorporating the frequency dependence of line parameters in this method. Computations are to be carried out in stages, starting from the initial state. As the method represents the lossy nature of the line by lumped parameter elements, to that extent the modelling is not accurate.

### 1.7 FINITE DIFFERENCE METHOD

The finite difference method has been applied for solving the electrical transient problems by Stafford et al [15] and Raghavan and Sastry [16,17]. In this method for determining the voltage and current on the transmission line, which is a function of both distance and time, the partial differential equations of the line are converted to difference equations, adopting a central, forward or backward difference scheme. The distance-time space of the transmission line is divided into a number of lattice points and the difference equations are solved simultaneously step by step to arrive at the voltage and current at each lattice point, satisfying the boundary conditions at the ends of the line.

The nonlinearities and untransposed lines can be handled by this method.

However, proper choice of time step and distance step is very crucial for ensuring numerical stability. The

method requires large storage. Frequency dependence of line parameters cannot be directly incorporated.

## 1.8 OBJECTIVES AND OUTLINE OF THE THESIS

The objective of this thesis is mainly to develop and extend the modified Fourier transform method for solving the electrical transients on double circuit transmission lines. A double circuit line is a part and parcel of any power system. In the existing literature, the electrical transients on double circuit lines have been studied mostly using the Transient Network Analyser. This thesis presents the development of a detailed model for a double circuit line and analyses the transients on them due to fault initiation and line energisation by the modified Fourier transform method. The modified Fourier transform method has been rated as one of the more accurate methods for solving these problems as it can be applied to a detailed transmission line model with ease. The distributed nature of all the parameters of the line is preserved in the analysis. The effect of frequency dependence of line parameters can be accounted for easily in the method almost with no additional computational effort. The case of the untransposed line can also be handled by this method.

Also the relevant theory for extending the Uram and Miller's method for studying the electrical transients

on transposed double circuit transmission lines is developed and presented in the thesis. As this method assumes a simpler model for the transmission line, it takes relatively less computer time and gives fairly accurate results. However, it can be used only for a transposed line and without incorporating the effects of frequency dependence of line parameters.

In this chapter a general introduction to the study of electrical transients on transmission systems has been given together with a brief description, and the salient features of the various methods that have been reported in the literature for evaluating these transients.

Chapter 2 describes the theory of the modified Fourier transform method as applied to the study of electrical transients on three phase power systems. The concepts of matrix functions and modal decomposition, proposed by Wedepohl and Mohamed [10], are made use of in the solution procedure. A typical 400 KV single circuit line, open at the receiving end is considered and the transient voltage waveform at the receiving end arising due to its energisation is computed. A comparison of voltage waveforms at the open receiving end for the transposed and untransposed configurations of the line is done.

A mathematical model of a double circuit transmission line, suitable for electrical transient studies is developed

in Chapter 3. It is shown in this chapter that for a transposed double circuit line of mirror symmetric conductor configuration with respect to a vertical plane, there exists a constant modal transformation matrix, which holds good at each frequency of the integration range.

An EHV transmission line is subjected to high overvoltages due to its energisation and re-energisation on trapped charge. Effective ways of restricting these overvoltages to low values, such as multistep resistance switching, controlling the timing of the closure of the individual poles of the circuit breaker etc. have been developed and are implemented in practice to limit these overvoltages to less than 2 p.u. When such methods are employed for controlling switching overvoltages, the overvoltages that arise due to fault initiation and fault clearing may dominate the scene over the switching overvoltages. Because of this, the study of fault transients on transmission lines is of importance. In Chapter 4, the application of the modified Fourier transform method for evaluating the overvoltage transients, arising on the sound phases of a transmission line due to a single phase to ground fault at any intermediate point on the line is described. The mathematical model, developed in Chapter 3 for a double circuit line is used to study the transient overvoltages on the sound phases due to a single phase to

ground fault on one circuit of a typical 400 KV double circuit line. A comparison of fault overvoltages for the transposed and untransposed configurations of the line is made. The effect of frequency dependence of line parameters on the fault initiating transient is studied for both the transposed and untransposed double circuit lines. The fault transient is evaluated for various intermediate fault locations.

The modified Fourier transform method is applied to compute the energisation transients on a double circuit line in Chapter 5. The model, developed in Chapter 3 for the double circuit line is used in these studies. The energisation of the first circuit with the second circuit remaining unenergised as well as the energisation of the second circuit when the first circuit is operating in steady state are considered. In these studies, it is assumed that all the three poles of the circuit breaker of each circuit get closed simultaneously. This simplifies the analysis and helps in getting an idea of the magnitudes of the overvoltages involved. A 400 KV line example is considered and the energisation transient at its open receiving end is computed for both the transposed and untransposed configurations of the line.

The extension of the Uram and Miller's method of solving the electrical transients for a double circuit

line is done in Chapter 6. The existence of a constant modal transformation matrix, independent of frequency, for a transposed double circuit line, as shown in Chapter 3, has made the application of this method for this problem possible. This being a time domain method, it takes much less computer time but can handle only transposed lines and the frequency dependence of line parameters cannot be directly incorporated. The method is applied to the same 400 KV double circuit line example as of Chapter 5. The results, obtained for the example for both the first and second circuit energisation are presented.

In Chapter 7, the effect of the nonsimultaneous closing of the circuit breaker poles on the energisation transients is investigated. The theory of the modified Fourier transform method is extended for analysing the energisation transients on double circuit lines, incorporating the sequential closing of breaker poles. The same 400 KV double circuit line example as of Chapters 5 and 6 is considered and the energising transients are evaluated for both the transposed and untransposed configurations of the line. The effect of frequency dependence of line parameters on the transients is investigated.

In the concluding chapter 8, the results of the various chapters of the thesis are reviewed, conclusions are drawn and problems for further research are outlined.

## CHAPTER 2

### MODIFIED FOURIER TRANSFORM METHOD

#### 2.1 INTRODUCTION

The theory of the modified Fourier transform method and its application for solving the electrical transient problems [9,10] have been described in this chapter. This method has been adopted in this work with a view to represent the transmission line and other components in a detailed manner so that the transients can be evaluated more accurately. It is easy to incorporate the effect of frequency dependence of line parameters in this method of transients evaluation. The method takes all the parameters of the transmission line to be distributed and can handle untransposed lines. To illustrate the method, an example of a single circuit line has been considered and the results of the energisation study are presented.

#### 2.2 THEORY OF THE METHOD

The solution of the transients on multiconductor transmission lines is complicated by the fact that the partial differential equations describing the behaviour of the system are 4-dimensional (3-dimensions in space and the time dimension). By making the assumption that only plane-wave propagation takes place, it is possible to separate the two space variables mutually at right



angles to the direction of propagation and to express them in terms of equivalent impedances, as described by Carson [18]. This leaves space variable in the direction of propagation and the time variable alone in the analysis. With this assumption, the voltage and current at any point on a transmission line are determined by the partial differential equations

$$-\frac{\partial v(x,t)}{\partial x} = R i(x,t) + L \frac{\partial i(x,t)}{\partial t} \quad (2.1)$$

$$-\frac{\partial i(x,t)}{\partial x} = G v(x,t) + C \frac{\partial v(x,t)}{\partial t} \quad (2.2)$$

where  $v(x,t)$ ,  $i(x,t)$  are the voltage and current respectively at the point,  $x$  units away from the end at time 't'

$R$  is the resistance/unit length of the line

$L$  is the inductance/unit length of the line

$G$  is the conductance to ground/unit length of the line

and  $C$  is the capacitance to ground/unit length of the line.

For a transmission line, usually  $G$  is negligibly small and hence (2.2) takes the form

$$-\frac{\partial i(x,t)}{\partial x} = C \frac{\partial v(x,t)}{\partial t} \quad (2.3)$$

When equations (2.1) and (2.3) are Fourier transformed, they become full differential equations in transformed voltage and current.

The Fourier transform pair is defined by the expressions

$$F(\omega) = \int_0^{\infty} f(t) e^{-j\omega t} dt \quad (2.4)$$

$$f(t) = \frac{1}{2\pi} \int_{-\infty}^{\infty} F(\omega) e^{j\omega t} d\omega \quad (2.5)$$

Equations (2.1) and (2.3), when Fourier transformed take the form

$$-\frac{dV(x, \omega)}{dx} = [R + j\omega L] I(x, \omega) \quad (2.6)$$

$$-\frac{dI(x, \omega)}{dx} = j\omega C V(x, \omega) \quad (2.7)$$

Differentiating equation (2.6) with respect to  $x$  and substituting for  $\frac{dI(x, \omega)}{dx}$  from equation (2.7), we get

$$\frac{d^2 V(x, \omega)}{dx^2} = [R + j\omega L] j\omega C V(x, \omega) \quad (2.8)$$

Solution of the above equation can be written as

$$V(x, \omega) = \cosh \gamma x \cdot A + \sinh \gamma x \cdot B \quad (2.9)$$

where  $\gamma = ([R + j\omega L] j\omega C)^{\frac{1}{2}}$

and  $A$  and  $B$  are arbitrary constants, which are determined by the terminal conditions, existing at the ends of the line.

From equation (2.6), the expression for transformed current can be obtained as

$$I(x, \omega) = -\left[\frac{j\omega C}{(R + j\omega L)}\right]^{\frac{1}{2}} [\cosh \gamma x \cdot B + \sinh \gamma x \cdot A] \quad (2.10)$$

Once the boundary conditions are known in the frequency domain, the arbitrary constants A and B can be evaluated and the transformed voltage and current at any point on the line can be found out with the help of equations(2.9) and (2.10). As this response in frequency domain is a complicated expression involving hyperbolic functions, it can be transformed back to time domain only by numerically evaluating the inverse integral of the form (2.5). The above mentioned conventional Fourier transform technique is not suitable for the evaluation of this integral numerically, as the integrand in this form is not quite stable numerically. A negative exponential term, when introduced to the integrand makes it numerically stable and hence a modified version of the transform is preferred for the calculations.

The modified Fourier transform pair is given by the expressions

$$V(x,\omega) = \int_0^{\infty} v(x,t) e^{-(a+j\omega)t} dt \quad (2.11)$$

$$v(x,t) = \frac{1}{2\pi} \int_{-\infty}^{\infty} V(x,\omega) e^{(a+j\omega)t} d\omega \quad (2.12)$$

where a is a positive constant, sufficiently large to ensure that the above integrals converge.

When the modified Fourier transform is applied instead of the conventional Fourier transform,

equations (2.6) and (2.7) get modified to the form

$$-\frac{dV(x, \omega)}{dx} = [R + (a + j\omega)L] I(x, \omega) \quad (2.13)$$

$$-\frac{dI(x, \omega)}{dx} = (a + j\omega)C V(x, \omega) \quad (2.14)$$

Putting these equations together, we get

$$\frac{d^2V(x, \omega)}{dx^2} = Z Y V(x, \omega) \quad (2.15)$$

where  $Z = R + (a + j\omega)L$   
and  $Y = (a + j\omega)C$ .

The general solution for transformed voltage and current at any point on the line can now be written as

$$V(x, \omega) = \cosh \gamma x \cdot A + \sinh \gamma x \cdot B \quad (2.16)$$

$$I(x, \omega) = -(Y/Z)^{\frac{1}{2}} [\cosh \gamma x \cdot B + \sinh \gamma x \cdot A] \quad (2.17)$$

where now  $\gamma = \{ [R + (a + j\omega)L](a + j\omega)C \}^{\frac{1}{2}}$ .

The boundary conditions, when substituted in equations (2.16) and (2.17) determine the constants A and B. The final step is to evaluate the integral (2.12) to arrive at the response in time domain.

For evaluating the above integral numerically, the infinite range is, in practice, truncated at a large finite value, say  $\Omega$ . To effect economy in computation, a half range form of the Fourier integral can be used and in that

case the integral to be evaluated takes the form

$$v(x,t) = \frac{2e^{at}}{\pi} \int_0^{\Omega} \text{Real Part}[V(x,\omega)] \cos \omega t \, d\omega$$

The truncation of the infinite range of the integral at a finite value has been found to give rise to unwanted oscillations, known as Gibb's oscillation in the solution. To eliminate these oscillations, a weighting function known as sigma factor is introduced to the integrand. With the introduction of this factor, the integral reads as

$$v(x,t) = \frac{2e^{at}}{\pi} \int_0^{\Omega} \text{Real Part}[V(x,\omega)] \cos \omega t \frac{\sin(\frac{\pi \omega}{\Omega})}{(\frac{\pi \omega}{\Omega})} d\omega \quad (2.18)$$

A set of suitable parameters ( $\Omega$ ,  $\Delta\omega$  and  $a$ ) to achieve accuracy and economy in computation, while evaluating numerically the above integral has been reported [6-8].

Accuracy in representation of the rise time of the response is determined, in main, by the choice of  $\Omega$ . For a good representation, it is significant to choose  $\Omega$  so that the calculated rise time is less than 10 percent of the travel time of the transmission line.

$$\text{i.e. } T < \tau/10$$

It has been found, in practice, that the inaccuracy in the rise time is principally in the range  $\Omega T > 4$ . So the above criterion implies choosing  $\Omega$  so that

$$\Omega T > 4$$

$$\text{i.e. } \Omega > 40/\tau$$

It has been confirmed by experience that the angular frequency interval  $\Delta\omega = \Omega/500$  is a good choice.

While the parameter 'a' can be used to 'smoothen' the term  $V(a, \omega)$  in the integrand, the 'Cos $\omega t$ ' term oscillates with a period in  $\omega$  of  $2\pi/t$ . For taking into account this oscillation, introduced to the integrand accurately, it is desirable to choose  $\Delta\omega$ , so that at least 4 points occur in each quarter cycle

$$\text{i.e. } 16\Delta\omega < 2\pi/t$$

In other words, the period over which the response is calculated should be restricted for a particular value of  $\Delta\omega$  chosen so that

$$\text{period of calculation} < 0.4/\Delta\omega$$

## 2.3 THREE PHASE SYSTEMS - MODAL ANALYSIS

The theory involved in applying the modified Fourier transform method for solving the transients on single phase systems has been presented in the previous section. When this is extended to a 3 phase system, the voltages and currents become vectors and the line parameters become matrices.

Now the matrix differential equation, which has to be solved to arrive at the transformed voltage vector at any point on the line takes the form

$$\frac{d^2 \underline{V}(x, \omega)}{dx^2} = [P] \underline{V}(x, \omega) \quad (2.19)$$

$$\begin{aligned} \text{where } [P] &= [Z][Y] \\ [Z] &= [R] + (a + j\omega)[L] \\ \text{and } [Y] &= (a + j\omega)[C] \end{aligned}$$

For solving the coupled matrix differential equation (2.19), the concept of matrix function is to be made use of. By the concept of matrix function, if a mathematical operation is to be performed on a square matrix, the resulting matrix after the operation can be obtained by doing the operation individually on the eigenvalues (modal values) of the matrix and by pre-multiplying and post-multiplying the diagonal matrix, having these operated eigenvalues as diagonal elements, by the eigenvector (or modal transformation) matrix and its inverse respectively.

Symbolically,

$$f([A]) = [Q] f([\lambda]) [Q]^{-1}$$

Using this property, the solution of equation (2.19) can be written as

$$V(x, \omega) = [\cosh \psi x] \underline{A} + [\sinh \psi x] \underline{B} \quad (2.20)$$

$$\text{where } [\psi] = [Q][\gamma][Q]^{-1}$$

$$[\cosh \psi x] = [Q][\cosh \gamma x][Q]^{-1}$$

$$[\sinh \psi x] = [Q][\sinh \gamma x][Q]^{-1}$$

$[\gamma]$  is the diagonal matrix, whose diagonal elements are the square roots of the eigenvalues of matrix  $[P] = [Z][Y]$

$[Q]$  is the modal transformation matrix, which makes

$$[Q]^{-1}[P][Q] \text{ diagonal}$$

and  $\underline{A}$  and  $\underline{B}$  are arbitrary constant vectors, which can be evaluated by the terminal conditions of the line.

The general current vector solution can now be determined as

$$\underline{I}(x, \omega) = -[Z]^{-1}[\psi] \{ [\cosh \psi x] \underline{B} + [\sinh \psi x] \underline{A} \} \quad (2.21)$$

When the boundary conditions are forced into equations (2.20) and (2.21), the constant vectors  $\underline{A}$  and  $\underline{B}$  are determined and hence the transformed voltage and current vectors at any point on the line is completely determined. Then the final step of evaluating the inverse integral of each of the phase components of the transformed response separately for the 3 phase case yields the phase voltages and currents in time domain.

In the above analysis, if the transmission line is transposed, the computation of the eigenvalues  $\gamma$ 's and eigenvector  $[Q]$  becomes unnecessary, as for this case a constant modal transformation, which holds good at each frequency in the integration range exists. For the transposed line, the line parameter matrices and hence the matrix  $[P]$  have a special structure, in which all the diagonal elements are equal and all the off-diagonal elements are equal. Though the values of these diagonal and off-diagonal elements vary with frequency, still at



each frequency this special structure of equality of diagonal and off-diagonal elements is preserved. The eigenvalues of such a matrix  $[P]$  are the one corresponding to the ground or zero sequence mode, given by (diagonal element + 2 x off-diagonal element) and the other two (repeated ones) corresponding to the aerial modes given by (diagonal element - off-diagonal element). An eigenvector matrix for the matrix  $[P]$  of such a structure [4] is given by

$$[Q] = \begin{bmatrix} 1 & 1 & 0 \\ 1 & 0 & 1 \\ 1 & -1 & -1 \end{bmatrix} \quad (2.22)$$

When the line is untransposed, the matrix  $[P]$  does not possess this special structure. Hence for this case the eigenvalue, eigenvector analysis has to be performed at each frequency to arrive at the matrices  $[Q]$  and  $[\gamma]$ , which hold good only at that frequency.

## 2.4 MATHEMATICAL MODEL FOR ENERGISATION STUDY

In this section, the development of an algorithm for computing the transient following the energisation of a single circuit, three phase line [10], applying the theory of the previous two sections is described. The algorithm assumes simultaneous closing of the circuit breaker poles during energisation.

Supposing the transformed voltages at the sending and receiving ends of a transmission line are known, forcing of these conditions in the general voltage vector solution expression (2.20) yields

$$\underline{A} = \underline{V}_S \quad (2.23)$$

$$[\text{Cosh} \psi \ell] \underline{V}_S + [\text{Sinh} \psi \ell] \underline{B} = \underline{V}_R$$

where  $\ell$  is the length of the line,

$$\text{i.e. } \underline{B} = [\text{Cosech } \psi \ell] \underline{V}_R - [\text{Coth } \psi \ell] \underline{V}_S \quad (2.24)$$

From (2.21), (2.23) and (2.24), the transforms of currents at the terminals of the line can be expressed in terms of the terminal transformed voltages as follows:

$$\begin{bmatrix} \underline{I}_S \\ \underline{I}_R \end{bmatrix} = \begin{bmatrix} [Y_{11}] & [Y_{12}] \\ [Y_{12}] & [Y_{11}] \end{bmatrix} \begin{bmatrix} \underline{V}_S \\ \underline{V}_R \end{bmatrix} \quad (2.25)$$

$$\text{where } [Y_{11}] = [Z]^{-1} [\psi] [\text{Coth } \psi \ell]$$

$$\text{and } [Y_{12}] = -[Z]^{-1} [\psi] [\text{Cosech } \psi \ell]$$

In the above equation, the matrix relating the terminal voltages to the terminal currents can be interpreted as the short circuit admittance parameter matrix of the line, viewed as a two port network.

Supposing a shunt element is added at one of the terminals of the transmission line, then the short circuit admittance matrix of the resulting overall set up can be

obtained by just adding to the self admittance term, corresponding to the particular terminal of the transmission line, the admittance value of the added shunt element.

For simulating the energisation of the line from a constant voltage source having a source impedance, conversion of the voltage source with the series impedance to its equivalent current source with the appropriate shunt admittance facilitates the application of the modified short circuit admittance parameter matrix (obtained as described above) in the analysis.

Figure 2 .1.1 and 2.1.2 give the system set up with voltage source and with the equivalent current source respectively.

Referring to Figure 2.1.2 when the shunt elements corresponding to the source admittances are added at the sending end terminals, the short circuit admittance parameter of the system takes the form

$$\begin{bmatrix} ([Y_{11}] + [Y_s]) & [Y_{12}] \\ [Y_{12}] & [Y_{11}] \end{bmatrix} \quad (2.26)$$

where

$$[Y_s] = \begin{bmatrix} 1/[R_s + (a + j\omega)L_s] & 0 & 0 \\ 0 & 1/[R_s + (a + j\omega)L_s] & 0 \\ 0 & 0 & 1/[R_s + (a + j\omega)L_s] \end{bmatrix} \quad (2.27)$$

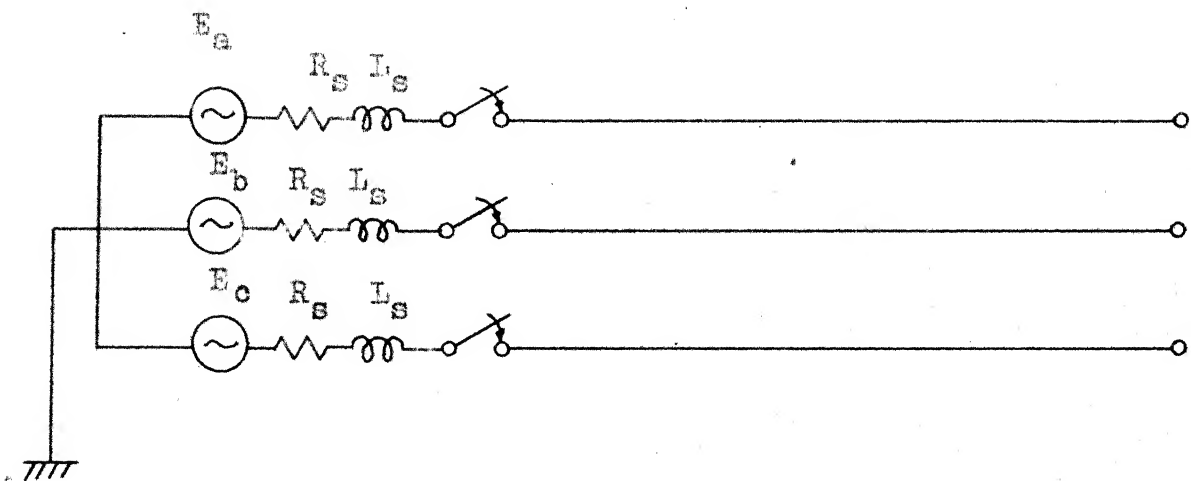


FIGURE 2.1.1: SYSTEM DIAGRAM WITH SOURCE REPRESENTATION

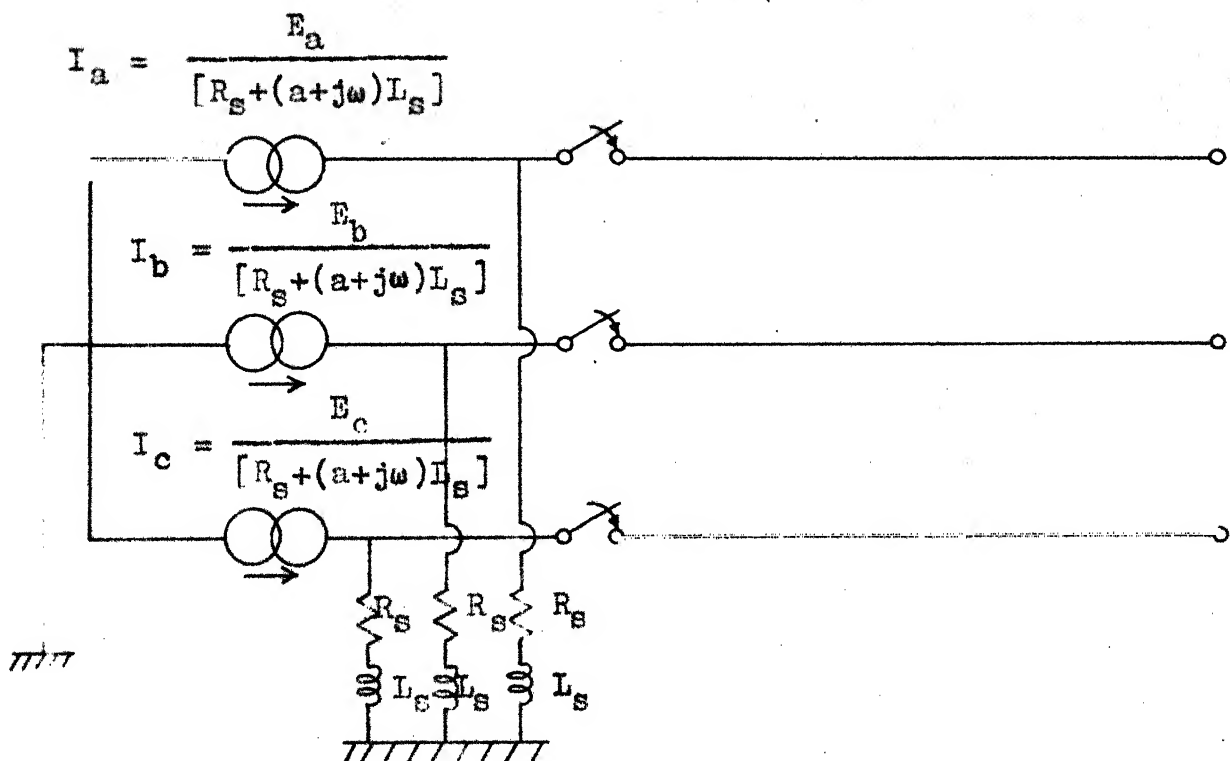


FIGURE 2.1.2: SYSTEM DIAGRAM WITH EQUIVALENT CURRENT SOURCE.

Now the desired response is calculated for the injected current vector at the sending end

$$\underline{I}_s = \begin{bmatrix} E_A / [R_s + (a + j\omega)L_s] \\ E_B / [R_s + (a + j\omega)L_s] \\ E_C / [R_s + (a + j\omega)L_s] \end{bmatrix} \quad (2.28)$$

where  $E_A$ ,  $E_B$  and  $E_C$  are the modified Fourier transform of the source voltages of the three phases, which are analytically known.

Considering the case of a line, open at the receiving end, equation (2.25), when the boundary conditions are substituted take the form

$$\begin{bmatrix} \underline{I}_s \\ \underline{0} \end{bmatrix} = \begin{bmatrix} ([Y_{11}] + [Y_s]) & [Y_{12}] \\ [Y_{12}] & [Y_{11}] \end{bmatrix} \begin{bmatrix} \underline{V}_s \\ \underline{V}_R \end{bmatrix} \quad (2.29)$$

From the above equation, expressions for  $\underline{V}_s$  and  $\underline{V}_R$  can be obtained in terms of  $\underline{I}_s$  as follows:

$$\underline{V}_s = \{ [Y_{11}] + [Y_s] - [Y_{12}][Y_{11}]^{-1}[Y_{12}] \}^{-1} \underline{I}_s \quad (2.30)$$

$$\underline{V}_R = \{ [Y_{12}] - ([Y_{11}] + [Y_s])[Y_{12}]^{-1}[Y_{11}] \}^{-1} \underline{I}_s \quad (2.31)$$

## 2.5 NUMERICAL EXAMPLE

The above algorithm is applied to study the transient following the energisation of a typical 400KV single circuit, three phase line, open at the receiving end and the results of the study are presented in this

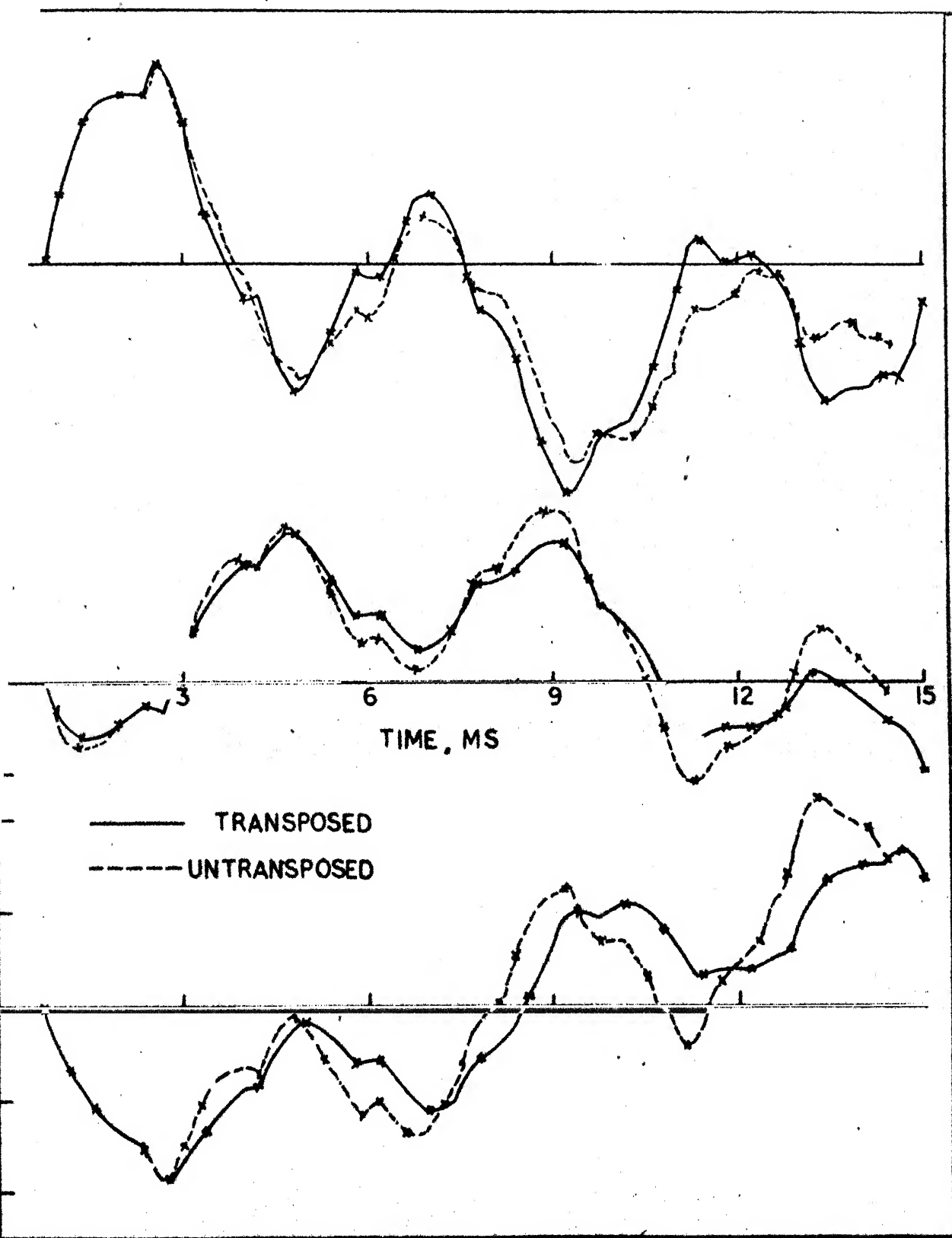


FIGURE 2.1: THE RISING TRANSIENT VOLTAGE WAVES AT  
REMOVING END.

section. The source has been assumed to be purely inductive. The effect of the presence of earth wire is included by making the necessary correction to the phase parameter matrices of the line. The line parameters and other system data are given in Appendix A.

The phase voltage waveforms at the open receiving end, following the energisation for the transposed and untransposed configurations of the line are compared in Figure 2.2. All the three poles of the circuit breaker are assumed to close simultaneously at the instant when the source voltage of phase-A is at its peak value. A maximum peak of  $-2.45$  p.u. is observed to occur on phase- A at  $9.2$  m.secs. for the case of the transposed line, whereas the maximum peak for the case of the untransposed line is  $2.22$  p.u. on phase- C at  $13.26$  m.secs.

## 2.6 CONCLUSIONS

The theory of modified Fourier transform method for studying the electrical transients on transmission lines has been presented in this chapter. A typical  $400\text{KV}$ , single circuit, three phase line example has been considered and the transients following its energisation from an inductive source has been evaluated for both the cases of transposed and untransposed configurations of the line. The extension of the theory for evaluating the energisation and fault initiating transients on double circuit transmission lines is described in the following chapters.

## CHAPTER 3

### MODELLING OF A DOUBLE CIRCUIT LINE FOR TRANSIENT STUDIES

#### 3.1 INTRODUCTION

In this chapter, a model of a double circuit transmission line, suitable for transient studies is developed. This model is used in the subsequent chapters for analysing transients due to energisation and fault initiation. The double circuit line is a part and parcel of any power system. So far, in the literature, except for a few studies using Transient Network Analyser (TNA) [19], the double circuit line transients have not been reported.

The study of transients on a transmission line involves solving of the polyphase wave equations. The first step in the solution procedure is to decompose the equation to modal components. The transformation matrix for this purpose is to be obtained by performing the eigenvalue, eigenvector analysis of the line propagation coefficient matrix.

In any practical power system, most of the double circuit lines have got a mirror symmetric conductor configuration with respect to a vertical plane. This gives most economical tower configuration. For such a special conductor configuration, a saving in the computation of the eigenvalues and eigenvector can be



and followed [20]. In the case of an ideally transposed double circuit line of mirror-symmetric conductor configuration, a constant modal transformation matrix, which holds good at all frequencies can be shown to exist.

## 3.2.1 MODAL TRANSFORMATION FOR A DOUBLE CIRCUIT TRANSMISSION LINE

The line parameter matrices of a double circuit transmission line, whose conductor configuration is mirror-symmetric with respect to a vertical plane are symmetrical. The matrix  $[P]$  of the line, which is given by  $[Z][Y]$  will, therefore also be symmetrical. Further the matrix  $[P]$  or the line parameter matrices, when partitioned, take the special form

$$[M] = \begin{bmatrix} [M_a] & [M_b] \\ [M_b] & [M_a] \end{bmatrix}$$

In the case of  $[P]$ , this may be written as

$$[P] = \begin{bmatrix} [P_a] & [P_b] \\ [P_b] & [P_a] \end{bmatrix} \quad (3.1)$$

whereas  $[P_a]$  and  $[P_b]$  are matrices of order 3. These submatrices  $[P_a]$  and  $[P_b]$  are symmetrical. However, their diagonal elements are unequal. Similarly, their off-diagonal elements are also unequal.

The eigenvalues of the matrix  $[P]$  are obtained by solving the polynomial equation

$$\det([P] - \lambda_i [U_2]) = 0 \quad (3.2)$$

for the six values  $\lambda_i$ ;  $i = 1, 2, \dots, 6$ , where  $[U_2]$  is unit matrix of order 6.

Since the determinant of a matrix product is equal to the product of the determinants of the component matrices, taken in any order, if we choose a particular regular matrix

$$[K] = \begin{bmatrix} [U] & -[U] \\ [U] & [U] \end{bmatrix} \quad (3.3)$$

where  $[U]$  is unit matrix of order 3, the equation for finding the eigenvalues can be written as

$$\det\{[K]^{-1}([P] - \lambda_i [U_2]) [K]\} = 0 \quad (3.4)$$

It can be verified that the matrix product

$$[K]^{-1}([P] - \lambda_i [U_2])[K] = \begin{bmatrix} ([P_a] + [P_b] - \lambda_{si} [U]) & [0] \\ [0] & ([P_a] - [P_b] - \lambda_{di} [U]) \end{bmatrix}$$

$$\text{where } [0] = \begin{bmatrix} 0 & 0 & 0 \\ 0 & 0 & 0 \\ 0 & 0 & 0 \end{bmatrix},$$

$\lambda_{si}$ ;  $i = 1, 2, 3$  are the eigenvalues of the matrix  $([P_a] + [P_b])$

and  $\lambda_{di}$ ;  $i = 1, 2, 3$  are the eigenvalues of the matrix  $([P_a] - [P_b])$ .

Therefore, equation (3.4) becomes

$$\det \begin{bmatrix} ([P_a] + [P_b] - \lambda_{si}[U]) & [0] \\ [0] & ([P_a] - [P_b] - \lambda_{di}[U]) \end{bmatrix} = 0$$

$$\text{i.e. } \det ([P_a] + [P_b] - \lambda_{si}[U]) \det ([P_a] - [P_b] - \lambda_{di}[U]) = 0 \quad (3.5)$$

Hence the eigenvalues of the matrix  $[P]$  can be obtained by solving the equations

$$\det ([P_a] + [P_b] - \lambda_{si}[U]) = 0 \quad \text{for } \lambda_{si} ; i=1, 2, 3$$

$$\text{and } \det ([P_a] - [P_b] - \lambda_{di}[U]) = 0 \quad \text{for } \lambda_{di} ; i=1, 2, 3$$

separately.

The eigenvector matrix  $[Q]$  of the matrix  $[P]$  is to be obtained by solving the matrix equation

$$[P][Q] = [\lambda][Q] \quad (3.6)$$

where  $[\lambda]$  is the diagonal eigenvalue matrix of matrix  $[P]$ .

Equation (3.6) can be manipulated to the form

$$[K]^{-1}[P][K][K]^{-1}[Q] = [K]^{-1}[\lambda][K][K]^{-1}[Q]$$

where the matrices  $[K]$  and  $[K]^{-1}$  are the same as described earlier.

We have seen that

$$[K]^{-1}([P]-[\lambda])[K] = \begin{bmatrix} ([P_a]+[P_b]-[\lambda_s]) & [0] \\ [0] & ([P_a]-[P_b]-[\lambda_d]) \end{bmatrix}$$

where  $[\lambda_s]$  is the diagonal eigenvalue matrix of the matrix  $([P_a]+[P_b])$  and  $[\lambda_d]$  is the diagonal eigenvalue matrix of the matrix  $([P_a]-[P_b])$ .

Let  $[K]^{-1} [Q]$  be denoted by  $[Q']$ . Then

$$\begin{bmatrix} ([P_a]+[P_b]-[\lambda_s]) & [0] \\ [0] & ([P_a]-[P_b]-[\lambda_d]) \end{bmatrix} \begin{bmatrix} [Q'_{11}] & [Q'_{12}] \\ [Q'_{21}] & [Q'_{22}] \end{bmatrix} = \begin{bmatrix} [0] & [0] \\ [0] & [0] \end{bmatrix} \quad (3.7)$$

where  $[Q'_{11}]$ ,  $[Q'_{12}]$ ,  $[Q'_{21}]$  and  $[Q'_{22}]$  are submatrices, obtained after partitioning of matrix  $[Q']$  for conformable multiplication in the above equation.

From equation (3.7), it is evident that

$$\text{if } \det([P_a]+[P_b]-[\lambda_s]) = 0$$

$$\text{and } \det([P_a]-[P_b]-[\lambda_d]) \neq 0,$$

$$\text{then } [Q'_{21}] = [0]$$

and  $[Q'_{11}]$  is obtained by solving the matrix equation

$$([P_a]+[P_b]-[\lambda_s])[Q'_{11}] = [0].$$

Similarly if  $\det([P_a] - [P_b] - [\lambda_d]) = 0$   
 and  $\det([P_a] + [P_b] - [\lambda_s]) \neq 0$ ,  
 then  $[Q'_{12}] = [0]$

and  $[Q'_{22}]$  is obtained by solving the matrix equation

$$([P_a] - [P_b] - [\lambda_d])[Q'_{22}] = [0].$$

Thus  $[Q']$  takes the form

$$[Q'] = \begin{bmatrix} [Q'_{11}] & [0] \\ [0] & [Q'_{22}] \end{bmatrix}$$

The above form of the matrix  $[Q']$  is very useful. It contains only the self term  $[Q'_{11}]$  and  $[Q'_{22}]$ . The mutual terms  $[Q'_{12}]$  and  $[Q'_{21}]$  are zero. This fact is of particular importance in the present calculations. Therefore,

$$\begin{aligned} [Q] = [K][Q'] &= \begin{bmatrix} [U] & -[U] \\ [U] & [U] \end{bmatrix} \begin{bmatrix} [Q'_{11}] & [0] \\ [0] & [Q'_{22}] \end{bmatrix} \\ &= \begin{bmatrix} [Q'_{11}] & -[Q'_{22}] \\ [Q'_{11}] & [Q'_{22}] \end{bmatrix} \end{aligned} \quad (3.8)$$

The above matrix  $[Q]$  again contains only the self term  $[Q'_{11}]$  and  $[Q'_{22}]$  and the mutual terms  $[Q'_{12}]$  and  $[Q'_{21}]$  are not present. Therefore, the problem of solving the transient on a double circuit line can be reduced to the

solution of two single circuit lines, decoupled from each other. Thus, all operations and manipulations can be carried out independently on each circuit as if the other does not exist. Only when the composite parameters are required, the independent values are combined by means of matrix  $[K]$ .

### 3.2.1 Transposed Line:

For an ideally transposed line, the submatrix  $[P_a]$  takes the particular form, in which all the diagonal elements are equal and all the off-diagonal elements are also equal. In addition, all the elements of the submatrix  $[P_b]$  are also equal. Hence the matrices  $([P_a] + [P_b])$  and  $([P_a] - [P_b])$  will also have the structure, in which all the diagonal elements are equal and all the off-diagonal elements are equal. The diagonal and off-diagonal elements of these matrices  $([P_a] + [P_b])$  and  $([P_a] - [P_b])$  (which are dependent upon the line parameter matrices) vary in magnitude with the frequency. However, the diagonal elements of each of these matrices separately will be equal. Similarly, the off-diagonal elements of each of these matrices will also be separately equal.

e.g.

$$\begin{bmatrix} \alpha & \beta & \beta \\ \beta & \alpha & \beta \\ -\beta & \beta & \alpha \end{bmatrix}$$

For a 3x3 matrix of such a structure, there exists a frequency independent eigenvector matrix (vide Section 2.3)

$$\begin{bmatrix} 1 & 1 & 0 \\ 1 & 0 & 1 \\ 1 & -1 & -1 \end{bmatrix}$$

Hence for the case of an ideally transposed double circuit line, the matrices  $[Q'_{11}]$  and  $[Q'_{22}]$  in equation (3.8) take the frequency independent form

$$[Q'_{11}] = [Q'_{22}] = \begin{bmatrix} 1 & 1 & 0 \\ 1 & 0 & 1 \\ 1 & -1 & -1 \end{bmatrix}$$

Thus a transformation matrix, which decouples the  $[P]$  matrix for the case of the transposed double circuit line at each frequency, inspite of the variation of  $[P]$  matrix with frequency, is given by

$$\begin{bmatrix} 1 & 1 & 0 & -1 & -1 & 0 \\ 1 & 0 & 1 & -1 & 0 & -1 \\ 1 & -1 & -1 & -1 & 1 & 1 \\ 1 & 1 & 0 & 1 & 1 & 0 \\ 1 & 0 & 1 & 1 & 0 & 1 \\ 1 & -1 & -1 & 1 & -1 & -1 \end{bmatrix}$$

### 3.2.2 Untransposed Line:

For the case of an untransposed double circuit line, the eigenvalue, eigenvector analyses [21] for the matrices  $([P_a] + [P_b])$  and  $([P_a] - [P_b])$  are to be performed at each frequency to obtain the modal transformation matrix  $[Q]$ .

### 3.3 CONCLUSIONS

This chapter describes the development of a modal transformation matrix for a double circuit transmission line of mirror symmetric conductor configuration with respect to a vertical plane. If the double circuit line is ideally transposed, it has been shown that a constant modal transformation matrix, independent of frequency, exists. This reduces the computational effort, needed for the calculation of transients in the case of a transposed double circuit line. This model has been made use of for analysing energising and fault transients on double circuit lines in the subsequent chapters.



## CHAPTER 4

### FAULT INITIATING TRANSIENT ON A DOUBLE CIRCUIT TRANSMISSION LINE

#### 4.1 INTRODUCTION

Switching overvoltages on an EHV transmission line arise due to energisation and re-energisation of the line. In practice, it is desirable to contain these overvoltages to a value as low as possible in order to reduce the cost of insulation. The various control methods such as the multistep resistance switching, controlling the timing of the closure of the individual poles of the circuit breaker etc. are effective in restricting these overvoltages to a value as low as 1.5 p.u. When such effective methods of controlling overvoltages are employed, the overvoltages that arise due to fault initiation may become a limiting factor. Ninety percent or more of the faults, experienced by a power system are single line to ground faults. In the event of a single line to ground fault, transient overvoltages of the order of 2 p.u. may be experienced by the sound phases. This calls for an accurate evaluation of transients on a transmission line due to single line to ground fault initiation.

The transient due to fault initiation on single circuit transmission line has been studied by various authors. Kimbark and Legate [22] have used the TNA to

evaluate the fault transient and have presented a lattice diagram approach for a theoretical study of the problem with certain approximations. Later exhaustive analogue computer studies of the problem have been reported [23,24]. Boonyubol et al [25] have made use of the Laplace transform method and have calculated the fault transient, employing the residue theorem for the inverse Laplace transformation. In all the above studies, the lines were assumed to be ideally transposed and the line parameters, computed at a single frequency have been assumed to remain constant in the whole frequency range.

The double circuit transmission line is a common feature of any power system. In this chapter, the application of modified Fourier transform method for studying the transients due to fault initiation on a double circuit line is described. A typical double circuit line has been considered, taking into account the mutual coupling between the two circuits. A single line to ground fault is applied on phase 'a' at any point along its length and the resulting overvoltages on the sound phases are calculated. Both the cases of an ideally transposed line and a completely untransposed line are considered. For the case of an ideally transposed double circuit line, a frequency independent modal transformation exists, as shown in Chapter 3 and hence the calculation of the transient for this case involves much

less computation. The frequency dependence of line parameters is included, using Carson's formulae [18] (Appendix B).

#### 4.2 SIMULATION OF FAULT

The principle of superposition has been applied for simulating fault on the transmission line. The system considered is linear and therefore superposition can be applied to the problem. Initially before the fault occurs, the line has been assumed to be under steady state.

The steps involved in the simulation of fault can be explained with the help of Figure 4.1 as follows:

(i) First assuming the fault not to be present, the voltage at the fault point and the required response at any point of interest on the line are determined as functions of time. As the line is in steady state, these functions are pure sinusoids at power frequency.

(ii) As the second step, the voltage at the fault point on the faulted phase, calculated in step (i) is injected as cancellation voltage with reversed polarity, across the faulted phase and ground, at the same point. The source voltages at the ends of the line are short circuited. Now the transient response of the line to this injected voltage alone is calculated as a function of time, starting from the instant of fault initiation (taken as zero time).

(iii) The superposition of these two responses gives the total response as a function of time, subsequent to the initiation of the fault.

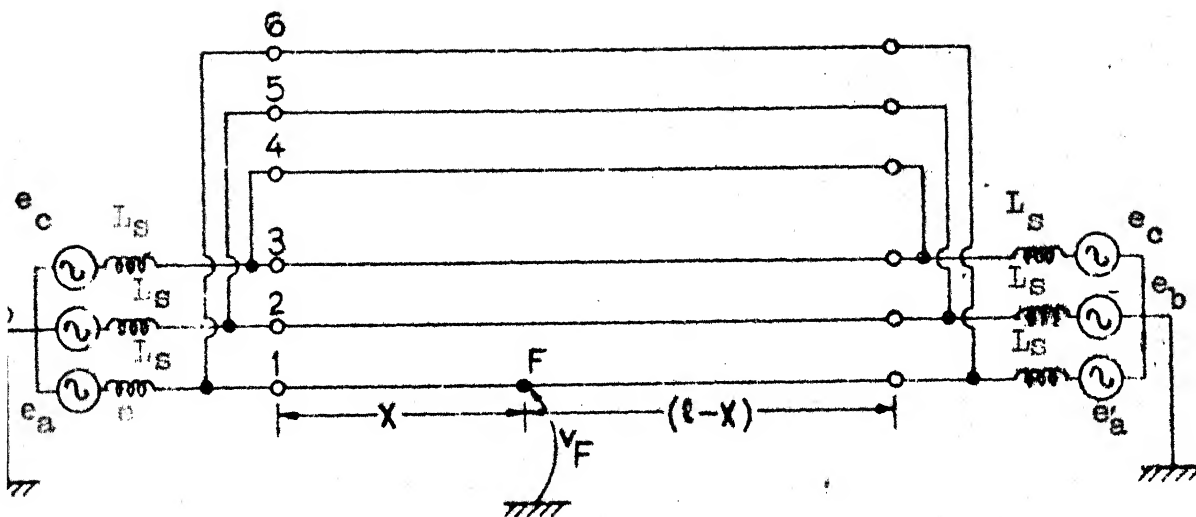


FIGURE 4.1.1

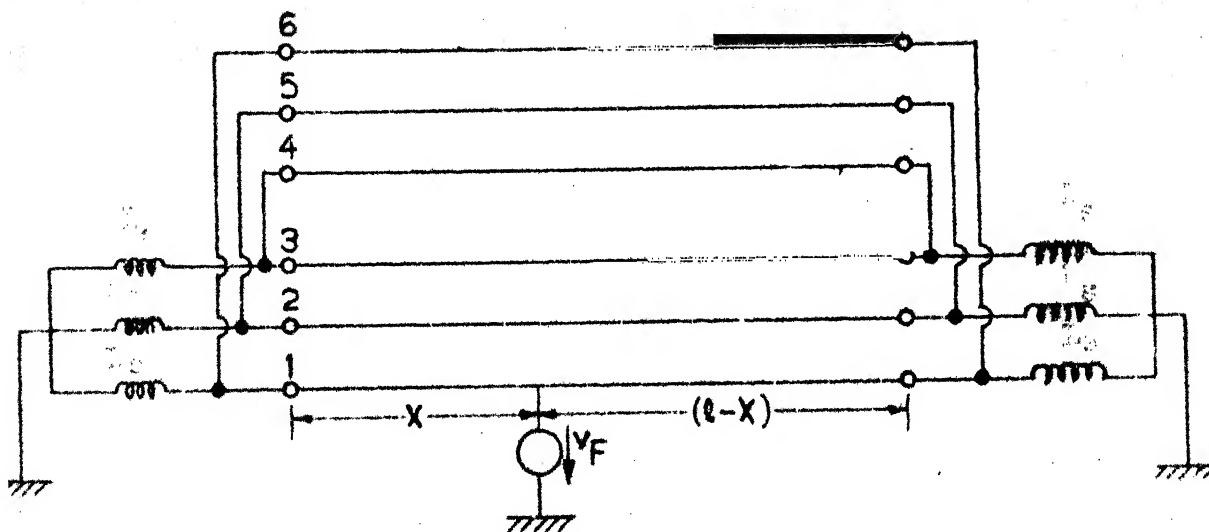


FIGURE 4.1.2

PRINCIPLE OF SUPERPOSITION USED FOR FAULT SIMULATION

The steady state voltages to be evaluated in step (i) are nearly 1 p.u. The calculation procedure for the evaluation of the transient response to the injected voltage of step (ii) is described in the next section.

#### 4.3 EVALUATION OF TRANSIENT RESPONSE FOR THE INJECTED VOLTAGE

The general solution of the transformed transmission line equations for the transformed phase voltage and current vectors at any point,  $x$  units away from the source end is given by

$$V(x, \omega) = [\cosh \psi x] \underline{A} + [\sinh \psi x] \underline{B} \quad (4.1)$$

$$I(x, \omega) = -[Z]^{-1}[\psi] \{ [\cosh \psi x] \underline{B} + [\sinh \psi x] \underline{A} \} \quad (4.2)$$

where  $[\psi] = [Q][\gamma][Q]^{-1}$

$$[\cosh \psi x] = [Q][\cosh \gamma x][Q]^{-1}$$

$$[\sinh \psi x] = [Q][\sinh \gamma x][Q]^{-1}$$

$[\gamma]$  = the diagonal matrix, whose diagonal elements are the square roots of the eigenvalues of the matrix  $[P] = [Z][Y]$

$[Q]$  = the eigenvector matrix (modal transformation matrix), which makes  $[Q]^{-1}[P][Q]$  diagonal

and  $\underline{A}$  and  $\underline{B}$  are arbitrary constant vectors, which have to be evaluated by forcing the terminal conditions of the line.

Referring to Figure 4.1, let the fault be located at a distance  $X$  units from the left end. The line section to

the left of the fault point F is considered first. The terminal conditions at the left end of the line are as follows:

(i) As the two circuits are paralleled at this end, the transformed voltages of the connected phases of each of the circuits at this end, obtained by substituting  $x = X$  in the general solution expression (4.1) should be equal.

(ii) The transformed phase currents through the terminating source impedances at this end are the sum of the transformed currents fed by the corresponding phases of both the circuits, calculated by substituting  $x = X$  in the general expression for current (4.2). Further, the transformed voltages and currents at this end of the line should satisfy the transformed voltage-current relationship of the terminating impedances.

These conditions can be put down mathematically in the following form:

$$\begin{aligned} \text{Let } [CH] &= [\cosh \psi X] \\ [SH] &= [\sinh \psi X] \\ [SC] &= -[Z]^{-1} [\psi][\cosh \psi X] \\ [SS] &= -[Z]^{-1} [\psi][\sinh \psi X] \end{aligned}$$

Then denoting the elements of the above matrices by lower case letters in double subscript notation

$$\begin{aligned}
 & \begin{bmatrix} ch_{11} & ch_{12} & \dots & ch_{16} \\ ch_{21} & ch_{22} & \dots & ch_{26} \\ ch_{31} & ch_{32} & \dots & ch_{36} \end{bmatrix} \underline{A} + \begin{bmatrix} sh_{11} & sh_{12} & \dots & sh_{16} \\ sh_{21} & sh_{22} & \dots & sh_{26} \\ sh_{31} & sh_{32} & \dots & sh_{36} \end{bmatrix} \underline{B} \\
 & = \begin{bmatrix} ch_{61} & ch_{62} & \dots & ch_{66} \\ ch_{51} & ch_{52} & \dots & ch_{56} \\ ch_{41} & ch_{42} & \dots & ch_{46} \end{bmatrix} \underline{A} + \begin{bmatrix} sh_{61} & sh_{62} & \dots & sh_{66} \\ sh_{51} & sh_{52} & \dots & sh_{56} \\ sh_{41} & sh_{42} & \dots & sh_{46} \end{bmatrix} \underline{B} \\
 & \hspace{15em} (4.3)
 \end{aligned}$$

$$\begin{aligned}
 & \left\{ \begin{bmatrix} (ss_{11}+ss_{61}) & \dots & (ss_{16}+ss_{66}) \\ (ss_{21}+ss_{51}) & \dots & (ss_{26}+ss_{56}) \\ (ss_{31}+ss_{41}) & \dots & (ss_{36}+ss_{46}) \end{bmatrix} \underline{A} \right. \\
 & + \left. \begin{bmatrix} (sc_{11}+sc_{61}) & \dots & (sc_{16}+sc_{66}) \\ (sc_{21}+sc_{51}) & \dots & (sc_{26}+sc_{56}) \\ (sc_{31}+sc_{41}) & \dots & (sc_{36}+sc_{46}) \end{bmatrix} \underline{B} \right\} (a+j\omega)L_s \\
 & = \begin{bmatrix} ch_{11} & ch_{12} & \dots & ch_{16} \\ ch_{21} & ch_{22} & \dots & ch_{26} \\ ch_{31} & ch_{32} & \dots & ch_{36} \end{bmatrix} \underline{A} + \begin{bmatrix} sh_{11} & sh_{12} & \dots & sh_{16} \\ sh_{21} & sh_{22} & \dots & sh_{26} \\ sh_{31} & sh_{32} & \dots & sh_{36} \end{bmatrix} \underline{B} \\
 & \hspace{15em} (4.4)
 \end{aligned}$$

where  $L_s$  is the source inductance.

From (4.3) and (4.4),  $\underline{B}$  and  $\underline{A}$  can be related by the expression,

$$\underline{B} = [T_X] \underline{A} \quad (4.5)$$

where  $[T_X] = [T_{X1}]^{-1}[T_{X2}]$

$$[T_{X1}] = \begin{bmatrix} [sh_{11} - (a+j\omega)L_s(sc_{11}+sc_{61})] & \dots & [sh_{16} - (a+j\omega)L_s(sc_{16}+sc_{66})] \\ [sh_{21} - (a+j\omega)L_s(sc_{21}+sc_{51})] & \dots & [sh_{26} - (a+j\omega)L_s(sc_{26}+sc_{56})] \\ [sh_{31} - (a+j\omega)L_s(sc_{31}+sc_{41})] & \dots & [sh_{36} - (a+j\omega)L_s(sc_{36}+sc_{46})] \\ (sh_{61}-sh_{11}) & \dots & (sh_{66}-sh_{16}) \\ (sh_{51}-sh_{21}) & \dots & (sh_{56}-sh_{26}) \\ (sh_{41}-sh_{31}) & \dots & (sh_{46}-sh_{36}) \end{bmatrix}$$

$$[T_{X2}] = \begin{bmatrix} [(a+j\omega)L_s(ss_{11}+ss_{61})-ch_{11}] & \dots & [(a+j\omega)L_s(ss_{16}+ss_{66})-ch_{16}] \\ [(a+j\omega)L_s(ss_{21}+ss_{51})-ch_{21}] & \dots & [(a+j\omega)L_s(ss_{26}+ss_{56})-ch_{26}] \\ [(a+j\omega)L_s(ss_{31}+ss_{41})-ch_{31}] & \dots & [(a+j\omega)L_s(ss_{36}+ss_{46})-ch_{36}] \\ (ch_{11}-ch_{61}) & \dots & (ch_{16}-ch_{66}) \\ (ch_{21}-ch_{51}) & \dots & (ch_{26}-ch_{56}) \\ (ch_{31}-ch_{41}) & \dots & (ch_{36}-ch_{46}) \end{bmatrix}$$

From the general solution expressions (4.1) and (4.2) and equation (4.5), the input admittance of the left section of the line in frequency domain, when viewed from the fault point is

$$[Y_X] = -[Z]^{-1}[\psi][T_X] \quad (4.6)$$



By adopting a similar procedure, the input admittance of the right section of the line in the frequency domain, viewed from the fault point can be proved to be

$$[Y_{l-X}] = -[Z]^{-1} [\psi][T_{l-X}] \quad (4.7)$$

where  $[T_{l-X}]$  is obtained by substituting  $(l - X)$  in the place of  $X$  in the expression for  $[T_X]$ .

The total input admittance of the line as viewed from the fault point is  $[Y] = [Y_X] + [Y_{l-X}]$ .

Now at the fault point, the transformed voltage on the faulted phase,  $V_F$  (the modified Fourier transform of the injected voltage source) is known and the injected currents on the sound phases are zero.

Forming these conditions, we get

$$[Y] \begin{bmatrix} V_F \\ V_b \\ V_c \\ V_{c'} \\ V_{b'} \\ V_{a'} \end{bmatrix} = \begin{bmatrix} I_a \\ 0 \\ 0 \\ 0 \\ 0 \\ 0 \end{bmatrix} \quad (4.8)$$

From the above equation, the transformed voltages on the sound phases at the fault point are given in terms of the known quantity  $V_F$  by the expression

$$\begin{bmatrix} V_b \\ V_c \\ V_{c'} \\ V_{b'} \\ V_{a'} \end{bmatrix} = -V_F \begin{bmatrix} y_{22} & y_{23} & \cdots & y_{26} \\ y_{32} & y_{33} & \cdots & y_{36} \\ y_{42} & y_{43} & \cdots & y_{46} \\ y_{52} & y_{53} & \cdots & y_{56} \\ y_{62} & y_{63} & \cdots & y_{66} \end{bmatrix}^{-1} \begin{bmatrix} y_{21} \\ y_{31} \\ y_{41} \\ y_{51} \\ y_{61} \end{bmatrix} \quad (4.9)$$

The transient response, given above in the frequency domain is then transformed back to the time domain by performing the numerical integration.

#### 4.4 VERIFICATION OF THE COMPUTER PROGRAM

To check the computer program, developed for the fault study, the single circuit line examples, studied by Boonyubol et al [25] is solved. The data of the example is given in Appendix C.

The voltage waveforms at the fault point on the sound phases are plotted in Figure 4.2. These results agree well with those of Boonyubol et al.

#### 4.5 SYSTEM USED FOR THE STUDY

A typical 400 KV double circuit transmission line of configuration [10], shown in Figure 4.3 is next analysed for the evaluation of fault initiating transient. The line is fed on both the ends by similar sources. In the example considered, both the source sides are represented purely by lumped impedances. The values of these source impedances are

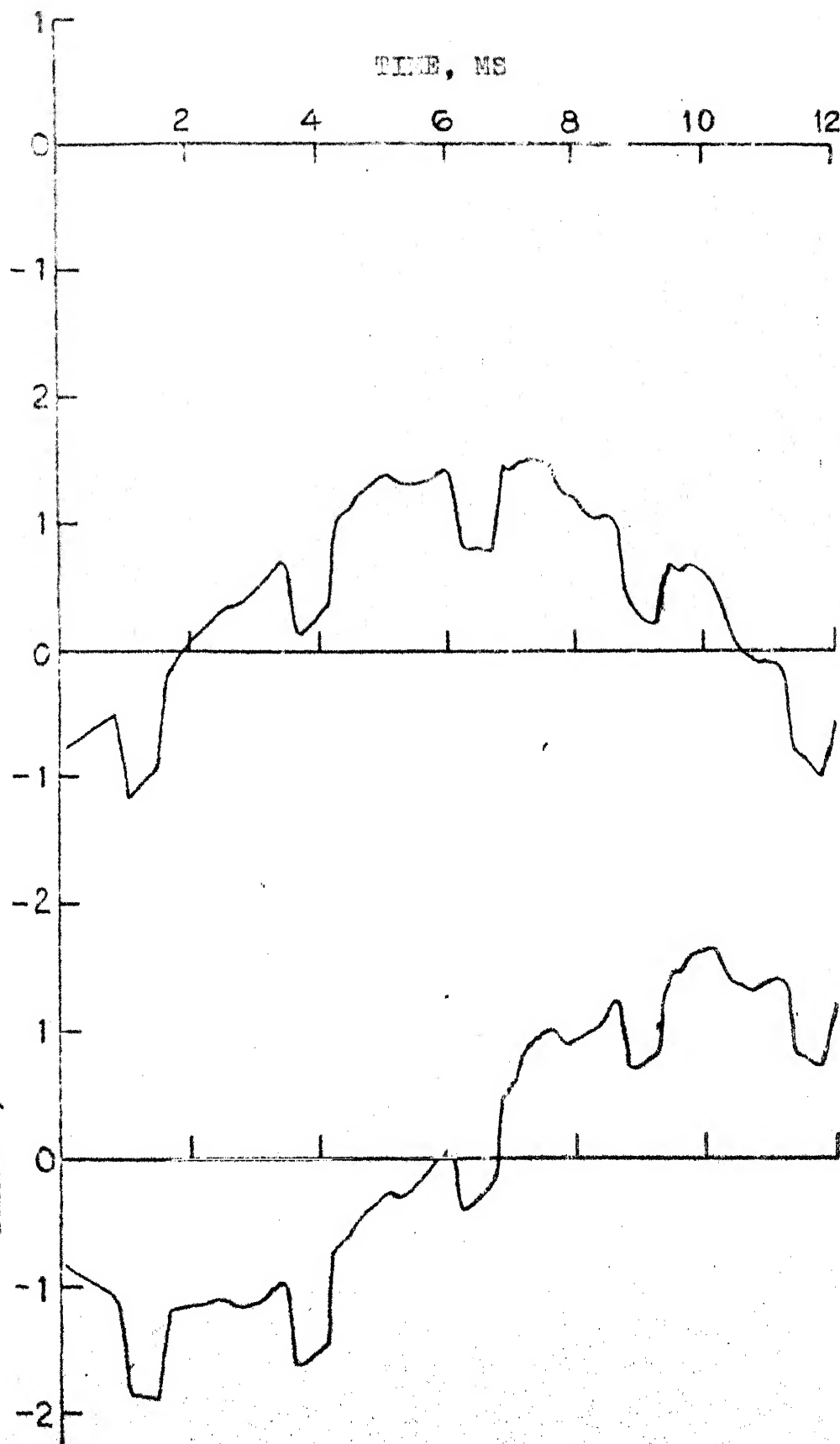
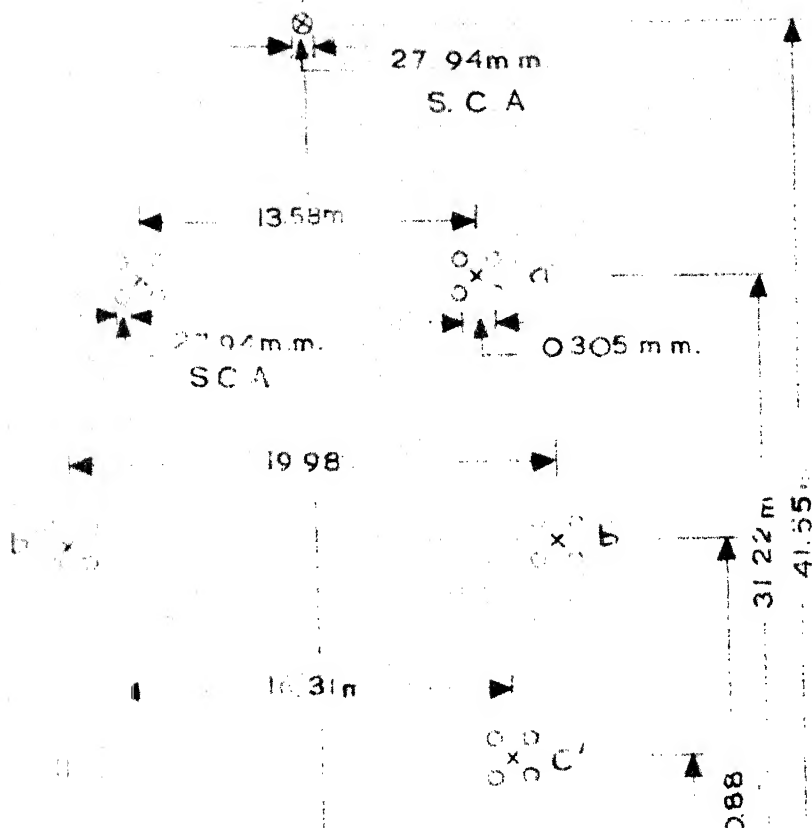


FIGURE 4.2: FAULT POINT VOLTAGE WAVEFORMS OF  
BOONYUBOL'S EXAMPLE - FAULT AT



derived from the system short circuit power and voltages at these buses. This simplified model for the source is somewhat approximate. However, here the aim is just to illustrate the application of the modified Fourier transform method of fault transient analysis for a double circuit line and hence source sides are not rigorously represented. For any particular system study, the source representation can be easily modified to suit particular requirements. For the present thesis, more complicated source representation is not considered to be necessary. However, there is no limitation for the applicability of the method for a detailed source side representation. The other lines terminating at the ends of the line under consideration can be represented quite accurately by equivalent shunt elements at these buses, the values of which are obtained by finding out the input admittance offered by these lines at these buses, taking into consideration the distributed nature of these lines and the terminal conditions existing at the remote ends of these lines.

The line parameters are calculated using the Carson's formulae. The effect of the presence of the ground wire is included by making the necessary correction to the line parameter matrices. The 50 Hz line parameters and other system data are given in Appendix D.

## 4.6 COMPUTATIONAL RESULTS

### 4.6.1 Fault Overvoltages on Single Circuit and Double Circuit Lines :

The transient due to initiation of a single line to ground fault on the double circuit line, as described in the last section, is studied. In this study, the line is assumed to be ideally transposed and the 50 Hz line parameters are used in the calculations. The fault is considered to be at the mid span on phase 'a'. It is assumed that the fault occurs at the instant when the voltage of phase 'a' at fault point is at positive peak. Next, the presence of the second circuit is ignored and the fault study is conducted for the single circuit line, keeping all the parameters the same. A comparison of the waveforms of the sound phase voltages at fault point for both the cases of single and double circuit lines is made in Figure 4.4. A maximum peak of -1.78 p.u. is observed to occur on phase- 'c' of the second circuit for the case of the double circuit line representation. For the single circuit line case, the maximum peak voltage of -1.98 p.u. occurs on phase 'c'. The voltage waveforms for the double circuit line case clearly exhibit more high frequency oscillations than those for the single circuit line case. This appears to be due to the fact that there are three distinct modes of propagation with three distinct velocities of wave propagation in the case of transposed double circuit lines; whereas for

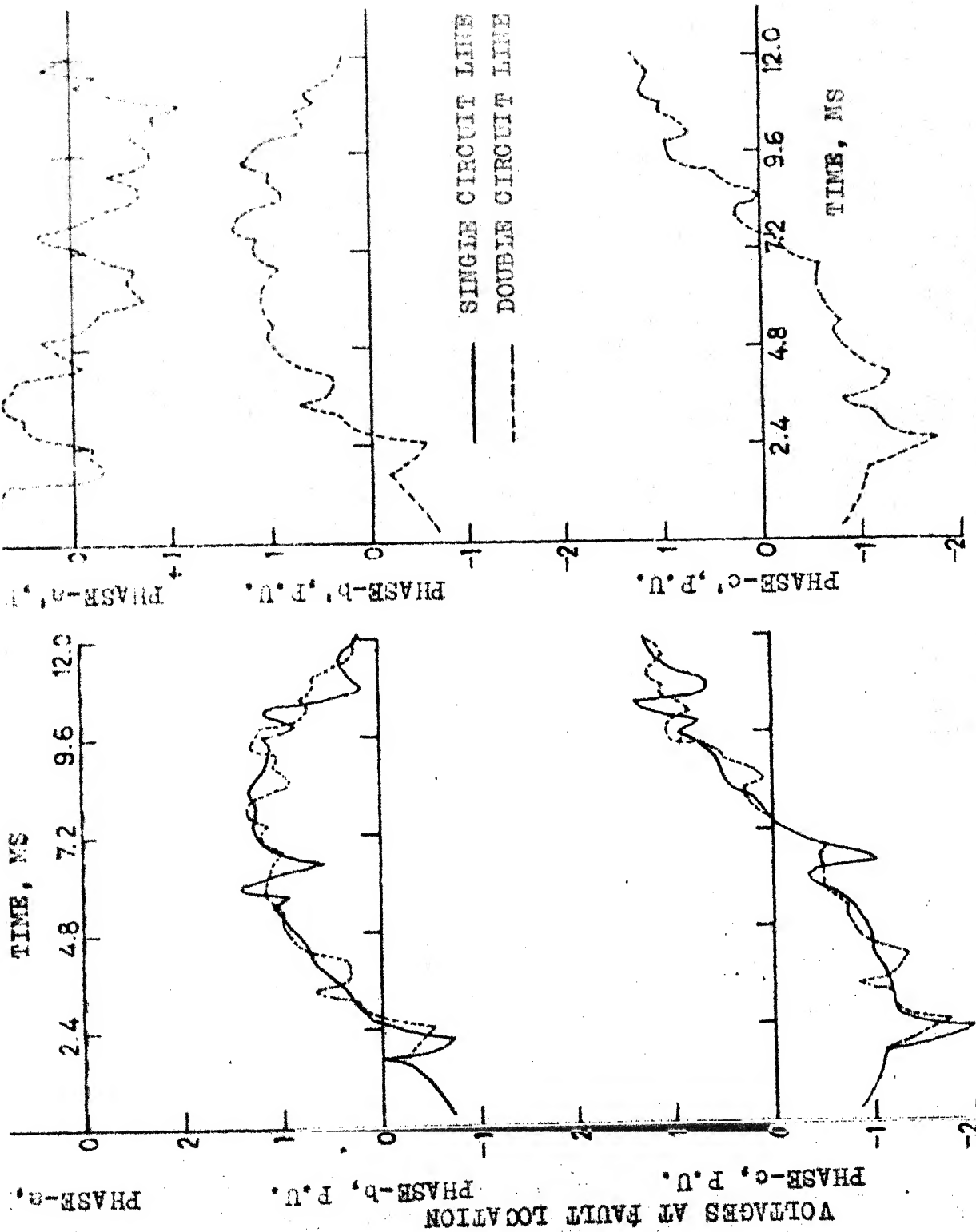


FIGURE 4.4: FAULT TRANSIENT ON TRANPOSED SINGLE CIRCUIT AND DOUBLE CIRCUIT LINES - FAULT AT MID SPAN ON

the case of a single circuit line, there are only two such distinct modes and velocities of propagation. Among these three modes for the double circuit line, two are ground modes, corresponding to the sum ( $[P_a] + [P_b]$ ) and the difference ( $[P_a] - [P_b]$ ) propagation coefficient matrices. The other one corresponds to the aerial mode of the sum and difference propagation coefficient matrices (vide Section 3.2).

#### 4.6.2 Transposed versus Untransposed Line:

The fault study is next conducted for the double circuit line, now assuming the line to be untransposed. For this case, the modal transformation is evaluated at each frequency of the numerical integration range. The line parameters are again assumed to be the 50 Hz values. The phase voltage waveforms at fault point (mid span) for the untransposed case are compared with those of the transposed case in Figure 4.5. It is to be noted that the maximum peak voltage in phase - c' is -1.97 p.u. for the untransposed configuration, whereas the maximum peak for the transposed configuration is -1.78 p.u.

#### 4.6.3 Effect of Incorporating Frequency Dependence of Line Parameters:

Next the continuous variation of line parameters with frequency is included in the calculation and the fault studies are repeated for both the transposed and the untransposed configurations of the line. The voltage



>

18

5

14.4

waveforms for the cases of transposed and untransposed lines are plotted in Figures 4.6 and 4.7 respectively. In each case the waveforms with and without incorporation of frequency dependence of line parameters are shown. The reduction in the maximum peak voltages when frequency dependence is included are about 11 percent and 13 percent for the transposed and untransposed cases respectively.

The maximum peak voltages, obtained in the various cases for mid span fault on the double circuit line are summarized in Table 4.1.

Table 4.1

Case	Max. peak voltage p.u.
Transposed line, without frequency dependence	-1.78
Transposed line, with frequency dependence	-1.585
Untransposed line, without frequency dependence	-1.97
Untransposed line, with frequency dependence	-1.72

#### 4.6.4 Overvoltages for Off-Centre Fault Locations:

So far in this chapter, the studies conducted have been for the mid span fault location. Next the case of the transposed line is considered and the study is repeated for different intermediate fault locations, ignoring the variation of line parameters with frequency. The sound phase voltage waveforms at fault point for the case of fault

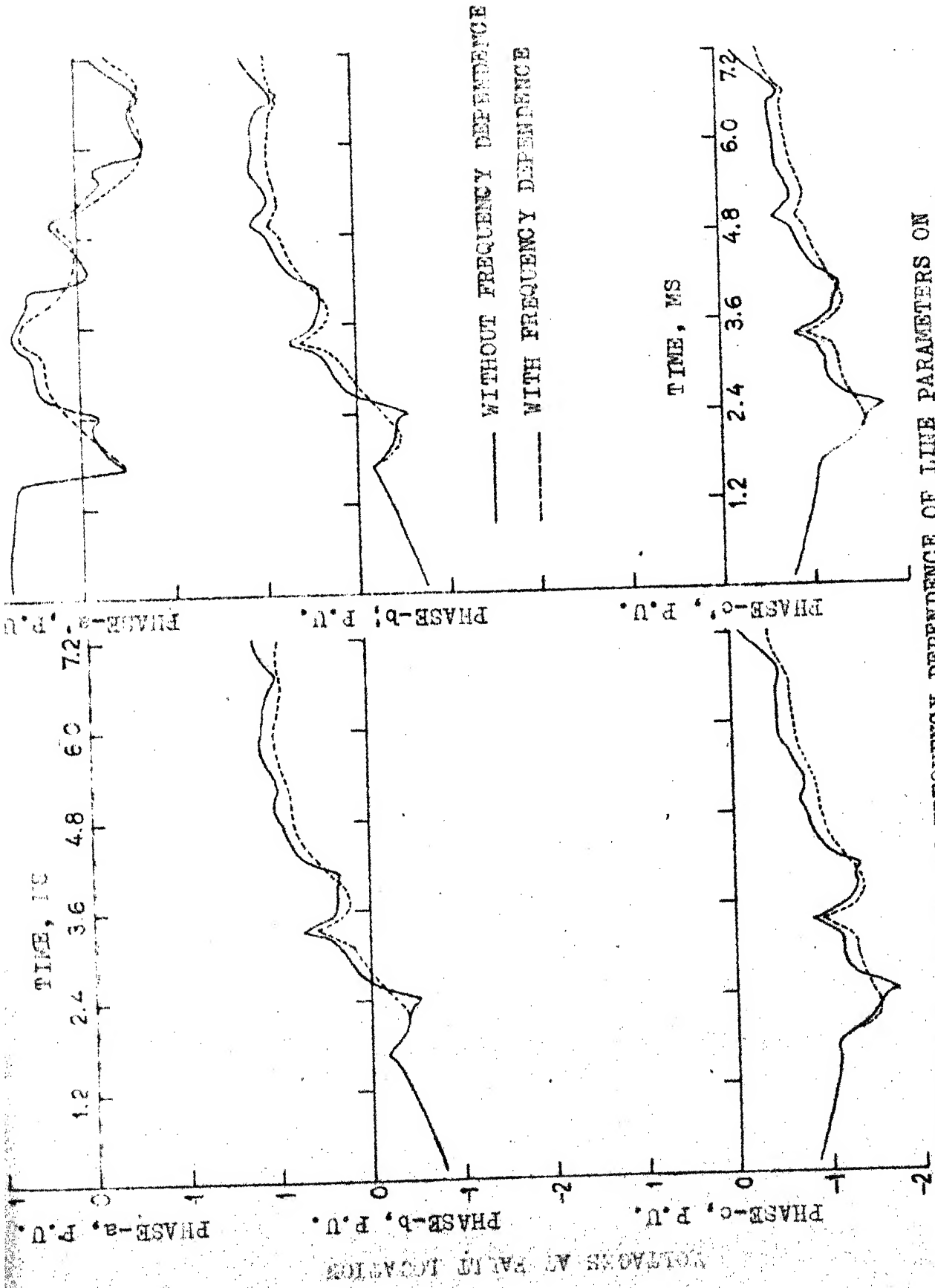


FIGURE 4.6: EFFECT OF FREQUENCY DEPENDENCE OF LINE PARAMETERS ON FAULT TRANSIENTS - TRANPOSED LINE - FAULT AT MID SPAN ON PHASE-a.

DEPT  
OF

1904

at a distance of 120 kms from one end of the line are plotted in Figure 4.8. The maximum peak voltages for various locations of fault points are given in Table 4.2. It is to be noted that the transients for fault locations symmetric with respect to the mid point of the line are identical because of the symmetrical nature of the system considered.

Table 4.2

Distance of the fault point from the line end in kms. (Total line length considered is 480 kms.)	Maximum peak voltage in p.u.
240	-1.78
180	-1.57
120	-1.55
60	-1.40
8	-1.36

The above off-centre fault location studies indicate that the maximum overvoltage occurs in the case of the mid span fault.

In all the above studies, the fault is assumed to occur only on the bottom most conductor (Figure 4.3) at the instant when the voltage of that phase at that point is passing through its positive peak. For the case of untransposed lines, if the fault occurs on one of the other two phase conductors, the fault transients and the associated maximum peaks will be

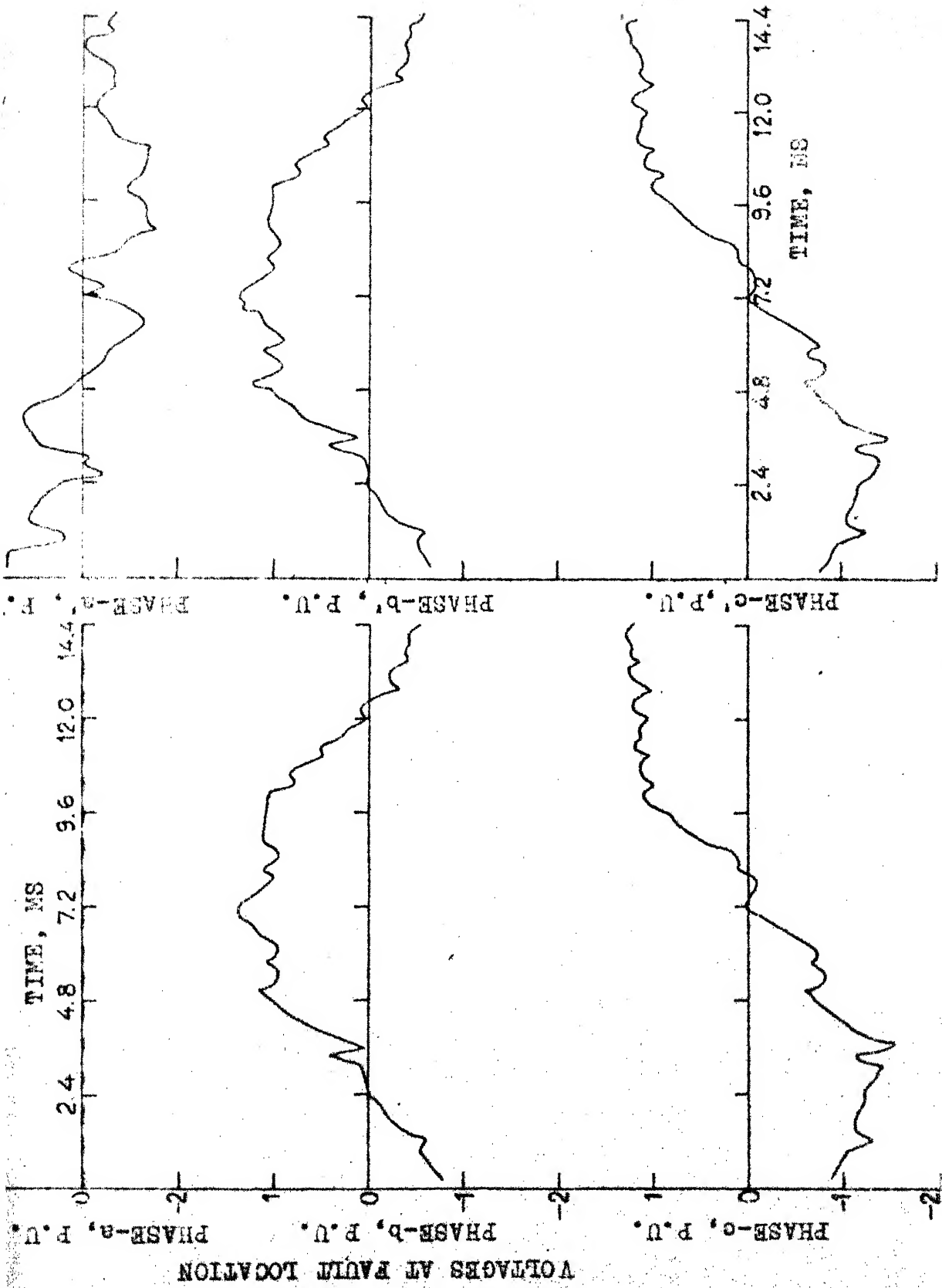


FIGURE 4.8: EFFECT OF CHANGE IN FAULT LOCATION TO QUARTER SPAN -  
TRANSCPOSED LINE - WITHOUT FREQUENCY DEPENDENCE.

different. However, there is no restriction on the applicability of the developed algorithm for studying the transients due to fault on the other phase conductors. As the aim of the thesis is to present a method of analysis using the modified Fourier transform method for double circuit lines, rather than any particular system study, consideration of various cases of data permutation have not been studied. It may be pointed out here that the case of considering the fault on the bottom-most conductor need not be the most serious from the point of view of determining the system insulation requirements. Such considerations are outside the scope of this thesis, but are essential in carrying out actual system studies using the method proposed in this thesis or using any other method of analysis. This comment also applies for other examples that are considered in subsequent chapters.

#### 4.7 CONCLUSIONS

The transient due to initiation of a single line to ground fault on a double circuit transmission line has been studied in this chapter. A mathematical analysis of the overvoltage transients, developed on the sound phases following the fault initiation at any intermediate point on the line has been presented. The double circuit line has been accurately modelled for the study, taking into account the mutual coupling between the two circuits. The study makes use of the modified Fourier transform method.

Both the cases of transposed and untransposed configurations of the line have been considered. As a frequency independent modal transformation exists for the case of the transposed double circuit line, as shown in Chapter 3, this case involves much less computational effort. In the case of the untransposed line, the evaluation of the modal transformation matrix at each frequency in the numerical integration range is required. The maximum peak voltage in the case of the untransposed line is observed to be nearly 10 percent higher than that of the transposed case.

The effect of frequency dependence of line parameters on the fault transient overvoltages for both the transposed and untransposed lines is investigated, using Carson's formulae for the calculation of line parameters. The inclusion of frequency dependence of line parameters is observed to reduce the maximum peak voltages by nearly 11 percent and 13 percent for the cases of transposed and untransposed lines respectively.

Finally the fault location is changed to various off-centre points along the line and the fault transients are studied. The mid span fault is found to give rise to the maximum peak overvoltage.



## CHAPTER 5

### ENERGISING TRANSIENT ON A DOUBLE CIRCUIT TRANSMISSION LINE

#### 5.1 INTRODUCTION

An EHV transmission line is subjected to high over-voltages because of energisation and re-energisation of the line. An accurate evaluation of these transients is essential for the economic design of the insulation. A double circuit line being a common element of any power system, a study of the transients due to its energisation is of importance. In the existing literature, the double circuit line transients have been analysed mainly using the transient network analyser [26]. In this chapter, the application of the modified Fourier transform method for analysing these transients and the results of these studies for both transposed and untransposed configurations of a typical line are presented.

#### 5.2 PROBLEM DESCRIPTION

In practice, the energisation of a double circuit line is done in two stages. First one circuit is energised and after an elapse of time, the second circuit is closed. There is bound to be a delay of a few seconds at least if not a few minutes between the closing of the first and second circuits of a double circuit line. During this delay

period, the transient arising in the first circuit due to its energisation would have died down and this circuit would be in steady state. Thus essentially two transients are involved in the study of the energisation phenomenon of a double circuit line, viz. (i) the transient due to the closing of the first circuit, while the second circuit is unenergised (ii) the transient due to the closing of the second circuit when the first circuit is already in steady state.

### 5.3 FIRST CIRCUIT ENERGISATION

In this section, a mathematical development of the analysis of transient due to the first circuit closure of a double circuit line, open at the receiving end is described.

As described in the earlier chapters, the general expressions for the transformed voltage and current vectors at any intermediate point on a double circuit transmission line at a distance  $x$  units away from the sending end are given by the expressions

$$\underline{V} = [\text{Cosh } \psi x] \underline{K} + [\text{Sinh } \psi x] \underline{M}$$

$$\underline{I} = -[Z]^{-1}[\psi] \{ [\text{Cosh } \psi x] \underline{M} + [\text{Sinh } \psi x] \underline{K} \}$$

where  $\underline{K}$  and  $\underline{M}$  are constant vectors, which are determined by the terminal conditions of the line and  $[\psi]$ ,  $[Z]$ ,  $[\text{Cosh } \psi x]$  and  $[\text{Sinh } \psi x]$  are the same as defined in the earlier chapters.

If the voltage transforms at the sending and receiving ends of the line ( $\underline{V}_S$  and  $\underline{V}_R$ ) are known, these conditions when forced on the general expressions determine the constant vectors  $\underline{K}$  and  $\underline{M}$  as follows:

$$\underline{K} = \underline{V}_S$$

$$\underline{M} = [\text{Cosech } \psi \ell] \underline{V}_R - [\text{Coth } \psi \ell] \underline{V}_S$$

where  $\ell$  is the length of the line.

Hence the sending and receiving end transformed currents can be expressed in terms of the transformed voltages at the two ends as

$$\begin{bmatrix} \underline{I}_S \\ \underline{I}_R \end{bmatrix} = \begin{bmatrix} [A] & [B] \\ [B] & [A] \end{bmatrix} \begin{bmatrix} \underline{V}_S \\ \underline{V}_R \end{bmatrix} \quad (5.1)$$

where  $[A] = [Z]^{-1}[\psi][\text{Coth } \psi \ell]$

and  $[B] = -[Z]^{-1}[\psi][\text{Cosech } \psi \ell]$ .

In the above expression  $\begin{bmatrix} [A] & [B] \\ [B] & [A] \end{bmatrix}$  can be interpreted as the short circuit admittance parameter matrix of the transmission line, treated as a two port network.

Now considering a double circuit line, which is connected to a voltage source with source resistance  $R_s$  and source inductance  $L_s$  at the sending end and whose receiving end is open (Figure 5.1.1), the voltage source with source impedance at the sending end can be replaced

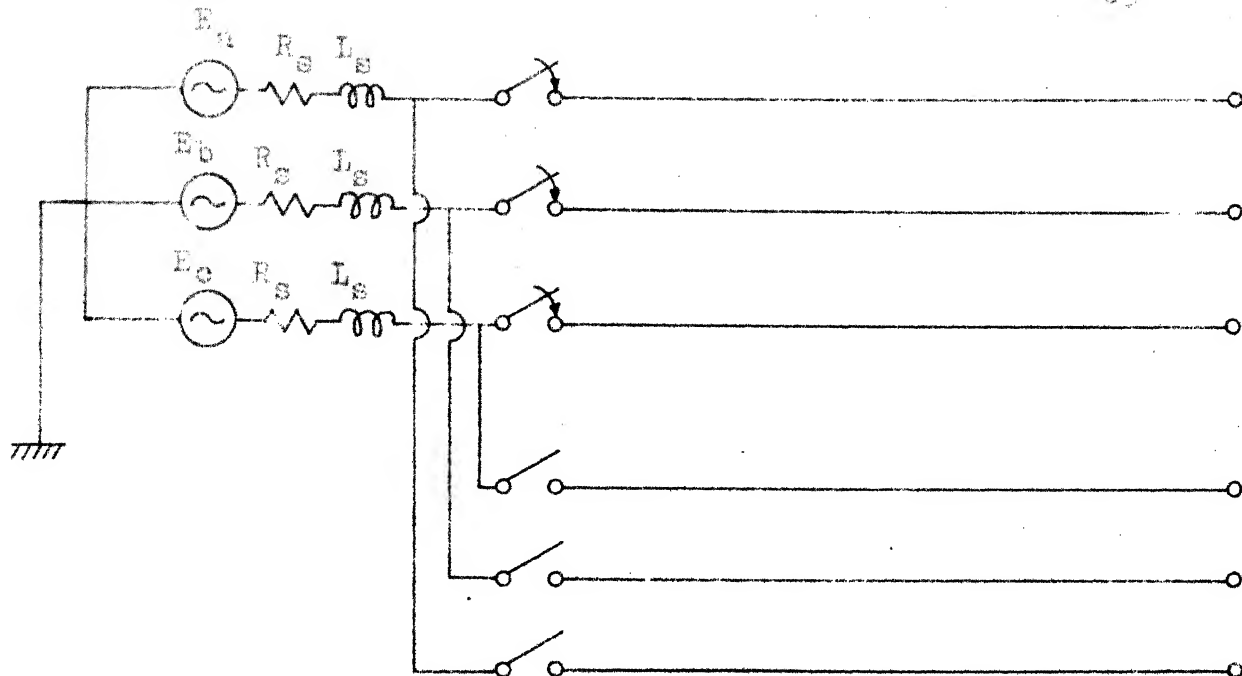


FIGURE 5.1.1: SYSTEM DIAGRAM WITH SOURCE REPRESENTATION

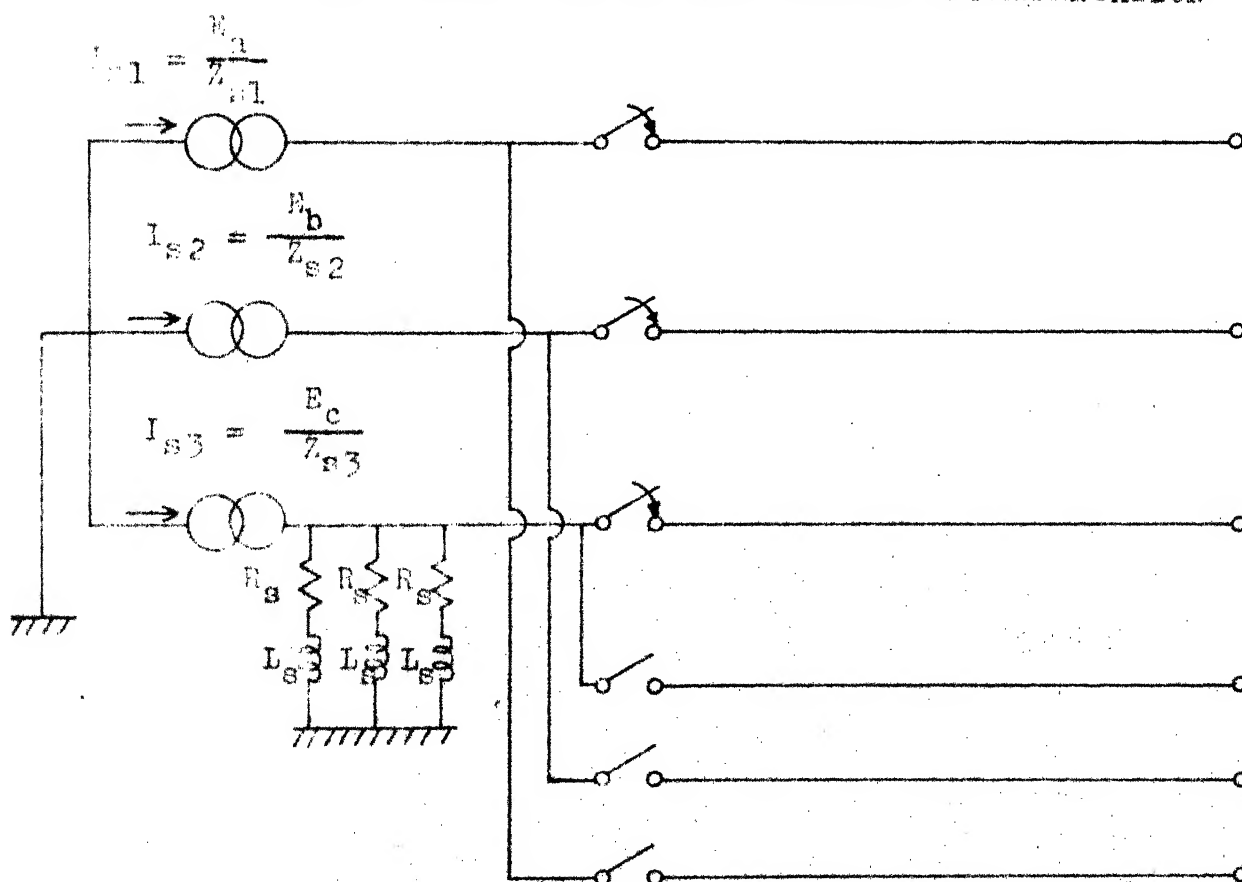


FIGURE 5.1.2: SYSTEM DIAGRAM WITH EQUIVALENT CURRENT SOURCE.

by an equivalent source with shunt admittance as shown in Figure 5.1.2.

As the second circuit of the double circuit line remains unenergised for the case under consideration, the forcing function is converted as a current source so that when the current injected to the second circuit phases at the sending end are taken as zero, the problem is directly simulated.

Now the double circuit line with the source admittance at the sending end can be viewed as a two port network and the incorporation of the shunt admittance at the sending end just introduces this additional admittance to the self admittance term of the sending end port of the short circuit admittance parameter matrix of the line. Therefore for this case, the two-port admittance equation takes the form

$$\begin{bmatrix} \underline{I}_s \\ \underline{0} \end{bmatrix} = \begin{bmatrix} ([A] + [Y_s]) & [B] \\ [B] & [A] \end{bmatrix} \begin{bmatrix} \underline{V}_s \\ \underline{V}_R \end{bmatrix} \quad (5.2)$$

where  $[A]$  and  $[B]$  are as defined in equation (5.1) except that they are now (6x6) matrices as we are dealing with the double circuit line.

Here  $\underline{0} = \begin{bmatrix} 0 \\ 0 \\ 0 \end{bmatrix}$

$$[Y_s] = \begin{bmatrix} 1/[R_s + (a + j\omega)L_s] & 0 & 0 & 0 & 0 & 0 \\ 0 & 1/[R_s + (a + j\omega)L_s] & 0 & 0 & 0 & 0 \\ 0 & 0 & 1/[R_s + (a + j\omega)L_s] & 0 & 0 & 0 \\ 0 & 0 & 0 & 0 & 0 & 0 \\ 0 & 0 & 0 & 0 & 0 & 0 \\ 0 & 0 & 0 & 0 & 0 & 0 \end{bmatrix}$$

$$\text{and } \underline{I}_s = \begin{bmatrix} E_a/[R_s + (a + j\omega)L_s] \\ E_b/[R_s + (a + j\omega)L_s] \\ E_c/[R_s + (a + j\omega)L_s] \\ 0 \\ 0 \\ 0 \end{bmatrix}$$

Equation (5.2) can be manipulated to write  $\underline{V}_R$  and  $\underline{V}_s$  in terms of  $\underline{I}_s$  as given below.

$$\underline{V}_R = \{ [B] - ([A] + [Y_s])[B]^{-1}[A] \}^{-1} \underline{I}_s$$

$$\underline{V}_s = \{ [A] + [Y_s] - [B][A]^{-1}[B] \}^{-1} \underline{I}_s$$

The calculation of matrices  $[\psi]$ ,  $[\text{Cosech } \psi l]$ ,  $[\text{coth } \psi l]$  and hence the calculation of matrices  $[A]$  and  $[B]$  differ for the transposed and untransposed configurations of the double circuit line. It has been shown in Chapter 3 that because of the special structure of the propagation coefficient

matrix for the case of the transposed double circuit line, a frequency independent constant modal transformation matrix exists for this case. This very much simplifies the calculation procedure for the transposed configuration. For handling the untransposed double circuit line, the eigenvalue eigenvector analysis of propagation coefficient matrix is to be performed at each frequency to arrive at the modal transformation matrix at that frequency. The frequency dependence of the line parameters can be directly incorporated in the analysis by using the appropriate line parameter values at each frequency, calculated using the Carson's formulae.

#### 5.4 COMPUTATIONAL RESULTS

The results of the study of single circuit energisation of a typical 400 KV double circuit line, open at the receiving end are presented in this section. The configuration and parameters of the line are the same as for the example considered in Chapter 4 (Appendix D) for fault studies. The length of the line is 240 kms and the source is taken as purely inductive of value 0.1 Henry/phase. The effect of the presence of the earth wire is included by making the necessary correction to the phase parameter matrices of the line. The earth resistivity is assumed to be 100 ohm-meter.

#### 5.4.1 Transposed Line Versus Untransposed Line:

The phase voltage waveforms at the open receiving end of the first circuit for the transposed and untransposed cases are compared in Figure 5.2. For both the cases, the energisation has been done when phase 'a' source voltage is at positive peak. From the plots, it is observed that a maximum peak voltage of -2.45 p.u. occurs on phase 'a' at 9.2 m.secs. for the case of transposed configuration. The maximum peak is 2.24 p.u. for the case of untransposed configuration and this occurs on phase 'c' at 12.8 m.secs. Because of the low order of magnitude of induced voltages on the unenergised second circuit, they have not been plotted.

#### 5.4.2 Single Circuit Versus Double Circuit Line Representations:

Next a set of energising studies are conducted, neglecting the presence of the second circuit with a view of comparing these results with those of double circuit representation.

For the case of transposed line, there is no appreciable difference in the waveshapes of receiving end voltages for the single circuit and double circuit representations. The reason for this appears to be that the induced charges on the three phases of the unenergised second circuit cancel with one another even during the transient period in the case of the transposed double circuit line.



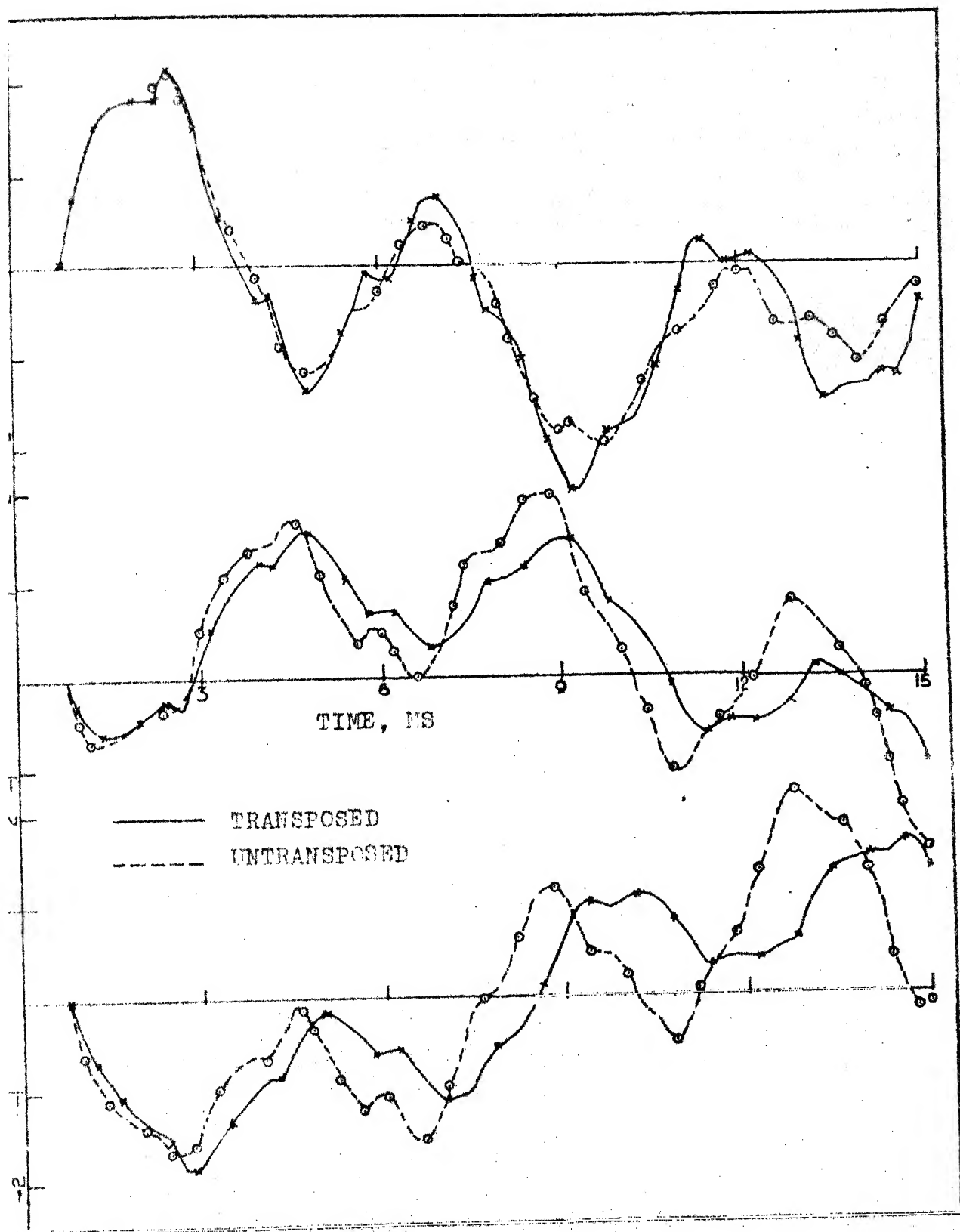


FIGURE 5.2: VOLTAGE TRANSIENTS AT RECEIVING END - FIRST CIRCUIT ENERCISATION - SECOND CIRCUIT OPEN.

The voltage waveforms at the open receiving end for the untransposed single and double circuit line representations are compared in Figure 5.3. From the plots, it can be observed that the maximum peak voltage of 2.22 p.u. occurs on phase 'c' at 13.26 m.secs. for the case of single circuit representation; whereas a maximum peak of 2.24 p.u. occurs on phase 'c' at 12.8 m.secs. for the case of double circuit representation.

## 5.5 SIMULATION OF SECOND CIRCUIT ENERGISATION

In this section, the analysis of the transient due to the closing of the second circuit, when the first circuit is in steady state, is described. Again the same example of a double circuit line, open at the receiving end and connected to a voltage source with source impedance at the sending end is considered and an algorithm for the analysis of the second circuit energising transient, using the modified Fourier transform method is developed.

The closing of the second circuit is simulated by voltage cancellation technique and superposition. The steps involved can be described with the help of Figures 5.4.1 and 5.4.2 as follows:

(i) First assuming that the second circuit continues to be unenergised, the response at any point of interest on the line (particularly the voltage at the open receiving end) and the voltages across the circuit breaker terminals

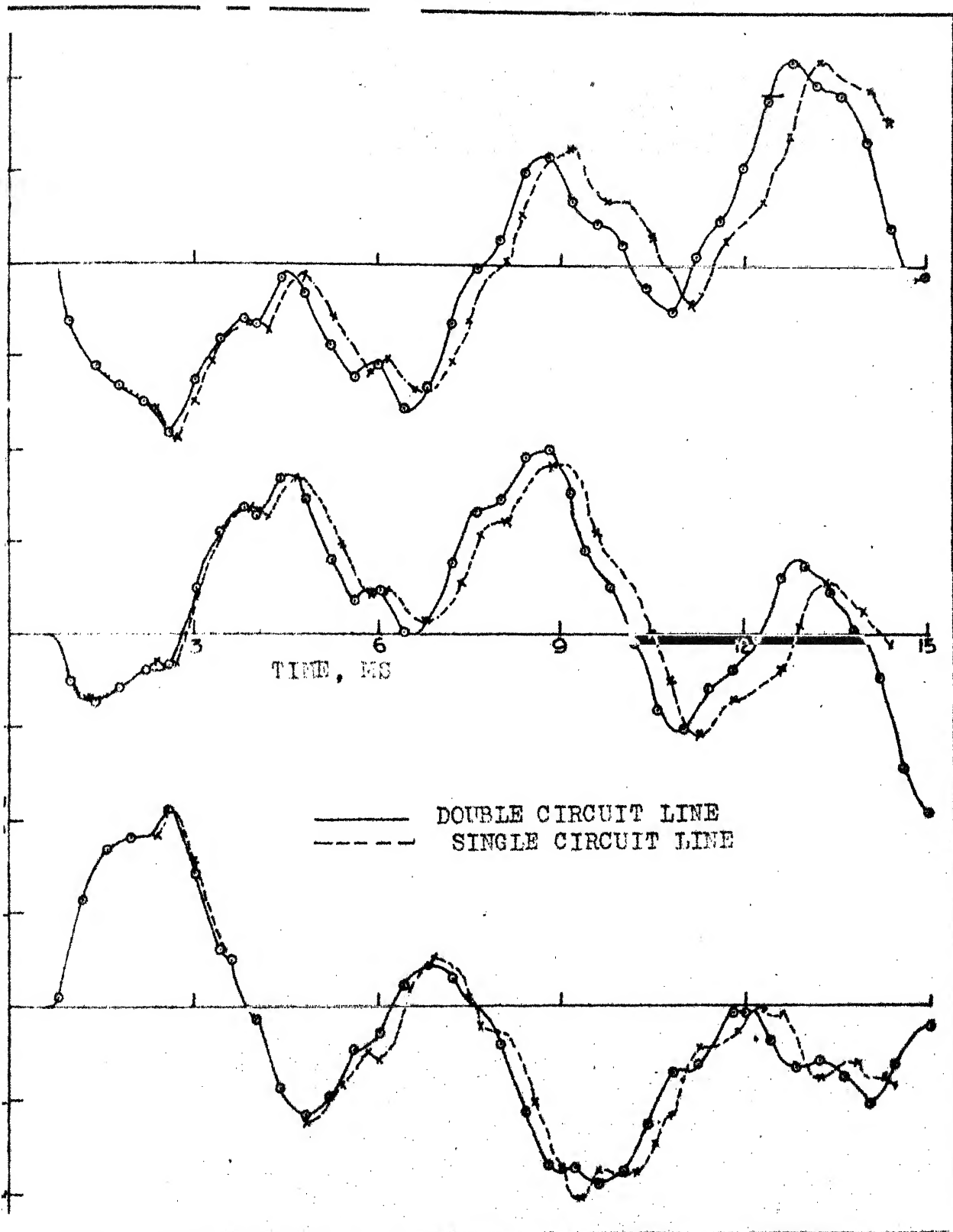
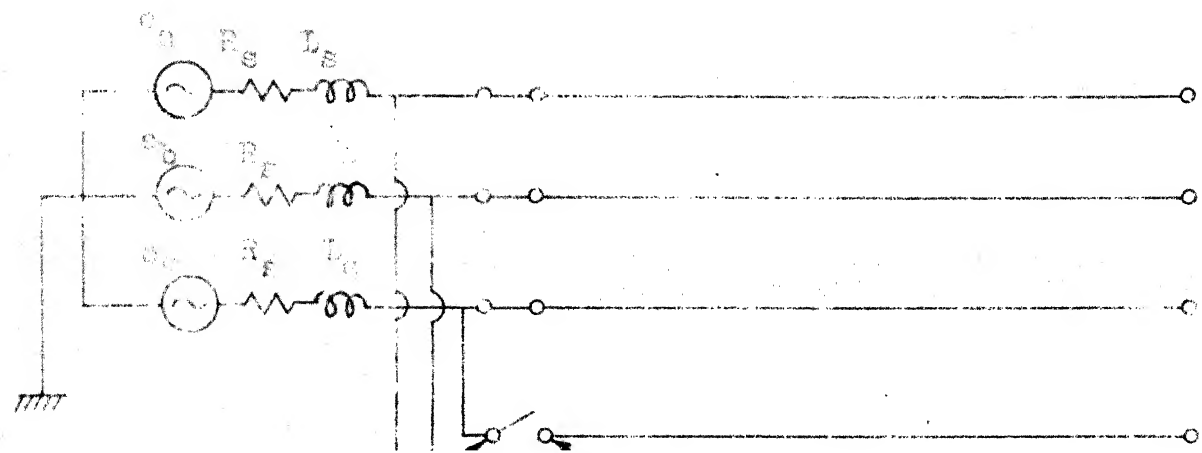


FIGURE 5.3: RECEIVING END VOLTAGE WAVEFORMS FOR UNTRANPOSED DOUBLE AND SINGLE CIRCUIT LINES - FIRST CIRCUIT ENERGISATION - SECOND CIRCUIT OPEN.



of all the three phases at the sending end of the second circuit are calculated. At this stage, as the first circuit is already in steady state, this step of the calculation is a steady state analysis.

(ii) The voltages across the breaker poles, calculated in step (i) are injected as cancellation voltages, with reversed polarity, across the same poles. The sending end terminals of the first circuit are short circuited to ground. The response at the above mentioned point of interest on the line is again calculated, now for these injected cancellation voltages alone.

(iii) Superimposing these two component responses, the total response is obtained.

Therefore, the procedure adopted for calculating the second circuit energising transient of a double circuit line essentially boils down to a steady state analysis, keeping the second circuit unenergised and finding the transient response of the line for a known set of sending end voltage conditions.

#### 5.5.1 Calculation of Steady State Response:

The method of calculating the steady state response at any point of interest on the line and the voltages across the circuit breaker poles at the sending end of the second circuit (step i of last section) is very similar to the

analysis of the transient subsequent to the closing of the first circuit when the second circuit is unenergised (described in Section 5.3). The only difference is that now the transmission line equations become full differential equations and the variables to be solved for are voltage phasors instead of instantaneous values of voltages because of the steady state nature of the analysis. It is to be noted that now all the variables involved are phasors at source frequency and no other frequency is involved in the calculations.

By adopting a similar solution procedure as in Section 5.3, the expressions for the sending end and receiving end voltage phasors in terms of sending end current phasors can be derived as follows:

$$\underline{V}_S = ([A] + [Y_S] - [B][A]^{-1}[B])^{-1} \underline{I}_S$$

$$\underline{V}_R = \{ [B] - ([A] + [Y_S])[B]^{-1}[A] \}^{-1} \underline{I}_S$$

where  $[A] = [Z]^{-1}[\psi][\text{Coth } \psi l]$

$$[B] = -[Z]^{-1}[\psi][\text{Cosech } \psi l]$$

$$l = \text{length of the line}$$

$$[Z] = [R] + j \omega_s [L]$$

$$[\psi] = [Q][\gamma][Q]^{-1}$$

$$[\gamma] = \text{diagonal matrix, whose diagonal elements are the square roots of the eigenvalues of the matrix product } [Z][Y]$$

$$[Y] = j\omega_s [C]$$

$\omega_s$  = angular velocity corresponding to source frequency

$[Q]$  = eigenvector matrix of the matrix product  $[Z][Y]$

$$[\text{Coth} \psi \ell] = [Q][\text{Coth} \gamma \ell][Q]^{-1}$$

$$[\text{Cosech} \psi \ell] = [Q][\text{Cosech} \gamma \ell][Q]^{-1}$$

$$[Y_s] = \begin{bmatrix} 1/(R_s + j\omega_s L_s) & 0 & 0 & 0 & 0 & 0 \\ 0 & 1/(R_s + j\omega_s L_s) & 0 & 0 & 0 & 0 \\ 0 & 0 & 1/(R_s + j\omega_s L_s) & 0 & 0 & 0 \\ 0 & 0 & 0 & 0 & 0 & 0 \\ 0 & 0 & 0 & 0 & 0 & 0 \\ 0 & 0 & 0 & 0 & 0 & 0 \end{bmatrix}$$

$R_s$  = resistance of the source/phase

$L_s$  = inductance of the source/phase

$[R]$  = resistance/unit length matrix of the line

$[L]$  = inductance/unit length matrix of the line

$[C]$  = capacitance/unit length matrix of the line,

$$\text{and } \underline{I}_s = \begin{bmatrix} 1/(R_s + j\omega_s L_s) \\ (-0.5 + j0.866)/(R_s + j\omega_s L_s) \\ (-0.5 - j0.866)/(R_s + j\omega_s L_s) \\ 0 \\ 0 \\ 0 \end{bmatrix}$$

If the double circuit line is transposed, the matrix  $[Q]$  takes a simple form as shown in Chapter 3. For the case of untransposed double circuit line, the eigenvalue eigenvector analysis is to be performed for the matrix product  $[Z][Y]$  to obtain the matrices  $[\gamma]$ ,  $[Q]$  and  $[Q]^{-1}$ .

When the above analysis is performed for the double circuit line example under study in this chapter, the steady state induced voltages on the unenergised second circuit at the sending and receiving ends are calculated to be as follows:

Transposed case:

At receiving end - Phase-a'  $(-0.83 \times 10^{-6} - j0.11 \times 10^{-5})$  p.u.  
 Phase-b'  $(0.19 \times 10^{-7} - j0.72 \times 10^{-5})$  p.u.  
 Phase-c'  $(-0.97 \times 10^{-7} + j0.19 \times 10^{-5})$  p.u.  
 At sending end - Phase-a'  $(-0.28 \times 10^{-5} + j0.77 \times 10^{-6})$  p.u.  
 Phase-b'  $(0.68 \times 10^{-6} - j0.29 \times 10^{-5})$  p.u.  
 Phase-c'  $(-0.22 \times 10^{-5} + j0.80 \times 10^{-5})$  p.u.

Untransposed case:

At receiving end - Phase-a'  $(0.016 + j0.68 \times 10^{-3})$  p.u.  
 Phase-b'  $(-0.025 - j0.025)$  p.u.  
 Phase-c'  $(-0.082 - j0.079)$  p.u.  
 At sending end - Phase-a'  $(0.011 + j0.40 \times 10^{-5})$  p.u.  
 Phase-b'  $(-0.029 - j0.025)$  p.u.  
 Phase-c'  $(-0.083 - j0.077)$  p.u.



The steady state voltages on the first circuit at the sending and receiving ends are calculated to be 1.03 p.u. and 1.07 p.u. respectively.

From the above analysis, it can be observed that the order of magnitude of the induced voltages on the second circuit is small when compared to the corresponding first circuit voltages. Hence it can be assumed that no voltages are induced on the second circuit conductors during this step of the calculation. In that case, the voltages across the sending end breaker poles of the second circuit can be taken as the steady state voltages at the sending end of the connected phases of the first circuit in step (i) of Section 5.5. However, if more accuracy is required, the induced voltages on the second circuit can be taken into account while calculating the voltages across the breaker poles of the second circuit at the sending end for the case of the untransposed line.

#### 5.5.2 Calculation of Transient Response for the Injected Voltages:

The step (ii) of this calculation involves evaluation of transient response of the transmission line for known sending end voltage conditions (viz. the first circuit terminals connected to ground and the injected voltages connected to the second circuit) with the receiving end terminals kept open.

These conditions, when substituted in the general solution expressions for transformed voltage and current vectors at any point on the transmission line lead to the evaluation of the constant vectors  $\underline{K}$  and  $\underline{M}$  as given below:

$$\underline{K} = \underline{V}_s$$

$$[\text{Cosh}\psi\ell] \underline{M} + [\text{Sinh}\psi\ell] \underline{V}_s = 0$$

i.e. 
$$\underline{M} = -[\text{Tanh}\psi\ell] \underline{V}_s$$

Therefore the transformed receiving end voltage vector becomes

$$\begin{aligned} \underline{V}_R &= [\text{Cosh}\psi\ell] \underline{V}_s - [\text{Sinh}\psi\ell][\text{Tanh}\psi\ell] \underline{V}_s \\ &= [\text{Sech}\psi\ell] \underline{V}_s \end{aligned}$$

where  $[\text{Sech}\psi\ell] = [Q][\text{Sech}\gamma\ell][Q]^{-1}$

and  $[\gamma]$  and  $[Q]$  are the eigenvalue and eigenvector matrices of the propagation coefficient matrix of the line respectively.

The inverse transformation of the transient response to the time domain is done by performing the numerical integration as described earlier in Section 2.2.

## 5.6 COMPUTATIONAL RESULTS

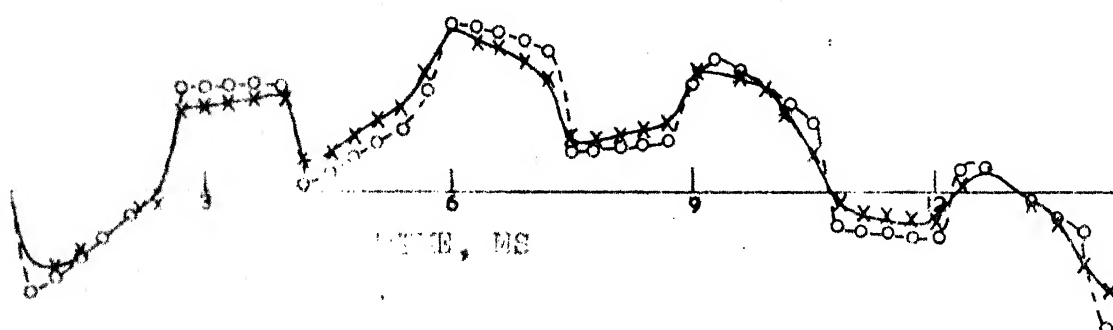
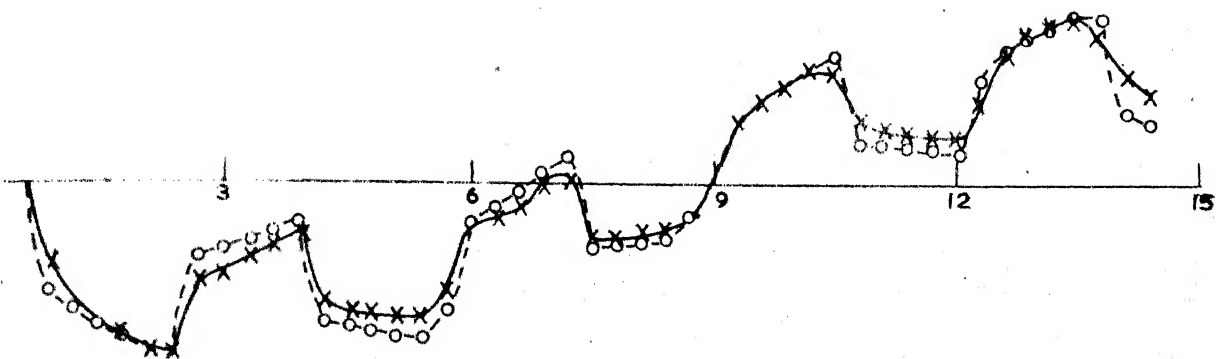
The same 400 KV double circuit line example, considered earlier in Section 5.4 of this chapter, is taken up to study the transient due to second circuit closure and the results are discussed below.

### 5.6.1 Transposed Versus Untransposed Configurations:

The above study is done for both the cases of transposed and untransposed configurations of the line. Again the existence of the frequency independent modal transformation matrix for the transposed double circuit line makes the computation for this case much easier when compared to the untransposed case. The comparison of the voltage waveforms at the open receiving end of the second circuit for the transposed and untransposed cases is done in Figure 5.5. For both the cases the closing of the circuit breakers is assumed to be at the instant when the source voltage of phase-a' is at positive peak. It is observed from the plots that a maximum peak voltage of 2.02 p.u. occurs on phase-a' at 1.02 m.secs. for the case of transposed line, whereas a maximum peak of 2.23 p.u. occurs on phase-a' at 0.9 m.secs. for the case of untransposed line. The receiving end voltages on first circuit subsequent to the closure of the second circuit are not plotted because of the lower magnitudes of these voltages in comparison with those of the second circuit phases.

### 5.6.2 Single Versus Double Circuit Line Representations:

Next a balanced three phase voltage of 1.03 p.u. (the steady state phase voltages at the sending end terminals of the first circuit before the closure of the second circuit) is applied to the second circuit and the resulting transient overvoltages at the open receiving end



\* — UNTRANPOSED  
 o — TRANPOSED



16

ECULT

are computed, neglecting the presence of the first circuit. This is done to compare the transients for the single and double circuit representations of the line.

For the case of transposed configuration of the line, there is no appreciable difference in the open receiving end voltage waveforms for single and double circuit representations since the induced voltages on the second circuit due to the currents in the three phases of the first circuit balance one another. However, it is observed later in Section 7.7.1 that once the method is extended for handling the nonsimultaneous closing of the poles of the breakers, even for the transposed configuration of the line, the double circuit representation gives rise to a difference in voltage waveforms as compared to the single circuit representation.

For the case of the untransposed line, a considerable difference in the waveshapes of the receiving end voltage waveforms is observed even for simultaneous closing of the breaker poles of the second circuit. A maximum peak over-voltage of magnitude  $-2.5$  p.u. is developed on phase-a' at 12 m.secs. for double circuit representation. On the other hand, a maximum peak of  $2.02$  p.u. occurs on phase-a' at 1.26 m.secs. for the case of single circuit representation. Apart from the difference in peak values, the voltage waveforms (Figure 5.6) for the single and double circuit representations

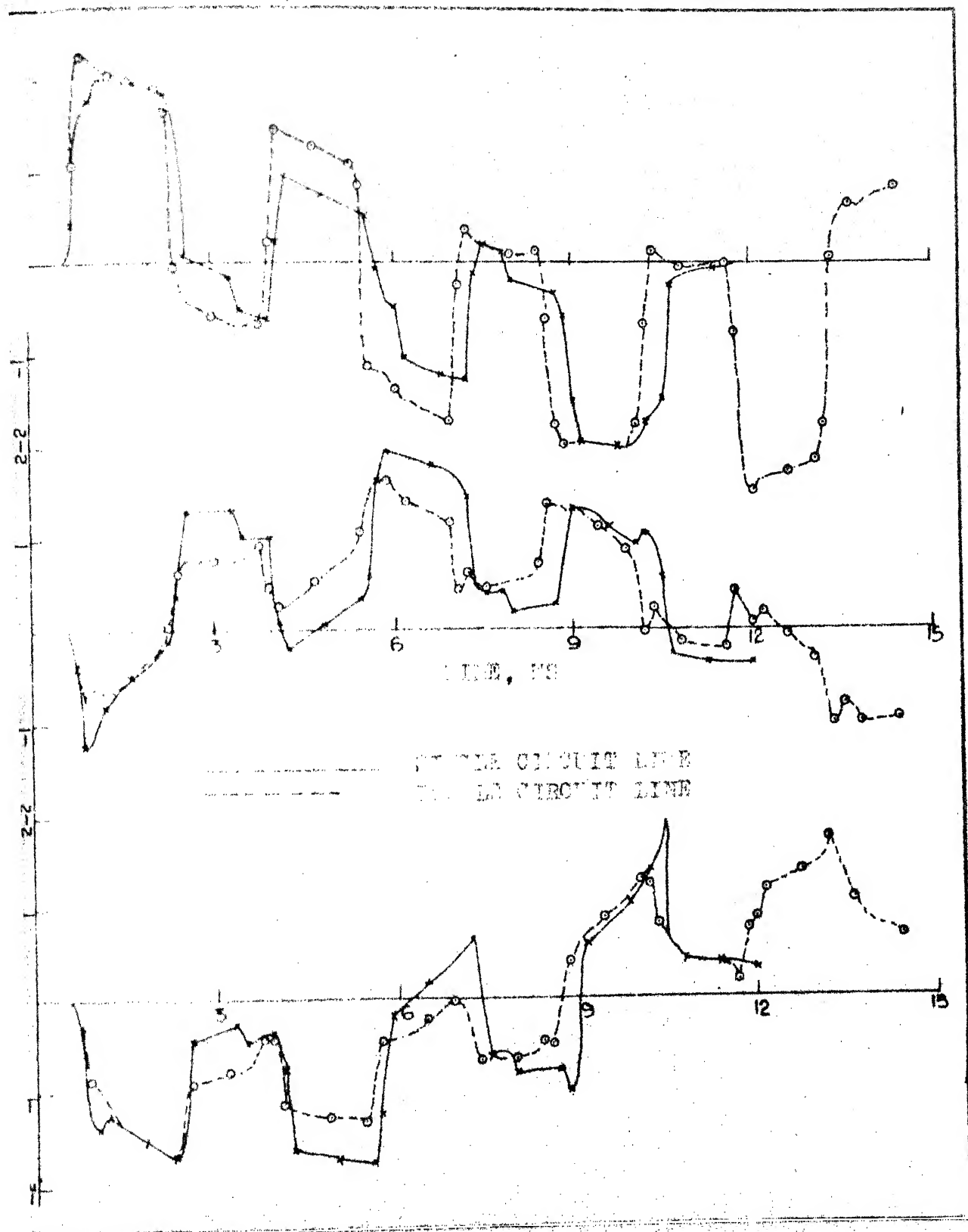


FIGURE 5.6: RECEIVING END VOLTAGE WAVEFORMS FOR UNTRANSDPOSED  
DOUBLE AND SINGLE CIRCUIT LINES - SECOND CIRCUIT  
ENERGISATION - FIRST CIRCUIT IN STEADY STATE.

differ widely in shape also. This seems to be due to the fact that for the case of untransposed double circuit lines, there are six distinct modes and velocities of propagation; whereas for untransposed single circuit lines, there are only three such distinct modes and velocities of propagation.

## 5.7 EFFECT OF INCORPORATION OF FREQUENCY DEPENDENCE OF LINE PARAMETERS

Next the continuous variation of line parameter values with frequency is incorporated in the program and the voltage transients are computed for the various cases. However, it has been observed that in all these cases, the effect of incorporation of frequency dependence of the line parameters on the voltage waveforms is not substantial. This appears to be due to the absence of the zero sequence ground currents in all these cases because of the simultaneous closing of the circuit breaker poles and only zero sequence components of the resistance and inductance of the line vary considerably with frequency. It is observed later in Section 7.7.2 that when nonsimultaneous closing of the circuit breaker poles is incorporated in the program, the frequency dependence of line parameters affects the transient voltage waveforms considerably.

## 5.8 CONCLUSIONS

The modified Fourier transform method has been applied to analyse the energising transients of a double circuit line in this chapter. Algorithms have been

developed for computing the transient due to the closing of the first circuit with the second circuit unenergised and that caused by the closing of the second circuit when the first circuit is in steady state. An example of a typical 400 KV double circuit line has been used to evaluate the transients for both transposed and untransposed configurations of the line. The energising transients for the double circuit representation of the line have been compared with the transients caused by the energisation of the corresponding single circuit line (neglecting the presence of the other circuit). The effect of the inclusion of frequency dependence of line parameters on the energising transients is observed to be insignificant for the case of simultaneous closing of the circuit breaker poles.



## CHAPTER 6

### EXTENSION OF URAM AND MILLER'S METHOD FOR DOUBLE CIRCUIT LINE ENERGISATION TRANSIENT ANALYSIS

#### 6.1 INTRODUCTION

In this chapter, the theory of the Uram and Miller's method [4,5] of calculating the switching transients on transmission lines is extended for the case of double circuit lines. The existence of a constant modal transformation matrix for the case of transposed double circuit lines, as shown in Chapter 3 makes this possible. The example, tried in Chapter 5 (using the modified Fourier transform method) is taken up and the two transients, involved in the energisation of a double circuit line, viz., the transient due to the closing of the first circuit when the second circuit is unenergised and that due to the closing of the second circuit, when the first circuit is in steady state are studied. The results obtained by both the methods are compared. As the Uram and Miller's method is a time domain method, the frequency dependence of the line parameters cannot be directly incorporated in this method. The untransposed lines also cannot be handled by this method. However, it takes relatively less computer time.

## 6.2 EXTENSION OF URAM AND MILLER'S METHOD FOR DOUBLE CIRCUIT LINE TRANSIENTS

A brief outline of the Uram and Miller's method of solving electrical transients on transmission lines is given in Appendix E. In this section the theory is extended for the case of double circuit lines.

The energisation of a double circuit line is to be studied in two stages. One transient is due to the closing of the first circuit, with the second circuit unenergised. The other possibility is that one circuit may be operating in steady state and the second circuit may be energised. The evaluation of both these transients is essential to arrive at the insulation level of the line and other equipments.

It has been shown in Chapter 3 that a frequency independent constant modal transformation matrix exists for a transposed double circuit line. This makes the extension of the theory of Uram and Miller's method (described in Appendix E) possible for studying both the transients, involved in the case of a double circuit line.

The equations (E.10), (E.11), (E.12) and (E.13) developed for the sending and receiving end voltage and current vectors in the Appendix E hold good for the double circuit line also. But now, the line parameters and hence  $[Z]$  and  $[Y]$  become  $6 \times 6$  matrices. The vectors  $\underline{k}_1(t)$ ,  $\underline{k}_2(t)$ ,  $\underline{a}(t)$  and  $\underline{b}(t)$  are all of order 6.

The modal transformation matrix  $[T]$  takes the form

$$[T] = \begin{bmatrix} [Q] & -[Q] \\ [Q] & [Q] \end{bmatrix}$$

where

$$[Q] = \begin{bmatrix} 1 & 1 & 0 \\ 1 & 0 & 1 \\ 1 & -1 & -1 \end{bmatrix}$$

is the modal transformation matrix for a single circuit three phase line as described in Section 3.2.1.

As described in Chapter 3, the line parameter matrices of the transposed double circuit line have the following special structures:

$$[R] = \begin{bmatrix} [R_a] & [R_b] \\ [R_b] & [R_a] \end{bmatrix} ; [L] = \begin{bmatrix} [L_a] & [L_b] \\ [L_b] & [L_a] \end{bmatrix} ;$$

$$[C] = \begin{bmatrix} [C_a] & [C_b] \\ [C_b] & [C_a] \end{bmatrix}$$

In the above matrices, each of the submatrices,  $[R_a]$ ,  $[L_a]$  and  $[C_a]$  is a  $3 \times 3$  matrix, the diagonal elements of which are equal and the off-diagonal elements of which are also equal. Each of the submatrices  $[R_b]$ ,  $[L_b]$  and  $[C_b]$  is a  $3 \times 3$  matrix, the elements of which are all equal.

It has been shown in Chapter 3 that the double circuit line problem can be reduced to two decoupled single circuit lines problem and the line parameter matrices of these two equivalent single circuits are  $([R_a]+[R_b]), ([L_a]+[L_b]), ([C_a]+[C_b])$  and  $([R_a]-[R_b]), ([L_a]-[L_b]), ([C_a]-[C_b])$ .

Denoting  $[R_a]+[R_b]$  by  $[R_s]$ ,  $[L_a]+[L_b]$  by  $[L_s]$ ,  
 $[C_a]+[C_b]$  by  $[C_s]$ ,  $[R_a]-[R_b]$  by  $[R_d]$ ,  
 $[L_a]-[L_b]$  by  $[L_d]$ ,  $[C_a]-[C_b]$  by  $[C_d]$ ,

the diagonal elements of  $[R_s], [L_s], [C_s]$  by  $R_{sd}, L_{sd}, C_{sd}$  respectively; the off-diagonal elements of  $[R_s], [L_s], [C_s]$  by  $R_{sod}, L_{sod}, C_{sod}$  respectively; the diagonal elements of  $[R_d], [L_d], [C_d]$  by  $R_{dd}, L_{dd}, C_{dd}$  respectively and the off-diagonal elements of  $[R_d], [L_d], [C_d]$  by  $R_{dod}, L_{dod}, C_{dod}$  respectively, the matrix  $[\Omega]$  in equations (E.11) and (E.13) (Appendix E) can be written for a transposed double circuit line as

$$[\Omega] = \begin{bmatrix} [\Omega_s] & [0] \\ [0] & [\Omega_d] \end{bmatrix}$$

where  $[\Omega_s] = \begin{bmatrix} (L_{s0}/C_{s0})^{\frac{1}{2}} & 0 & 0 \\ 0 & (L_{s1}/C_{s1})^{\frac{1}{2}} & 0 \\ 0 & 0 & (L_{s1}/C_{s1})^{\frac{1}{2}} \end{bmatrix}$

$$[Z_d] = \begin{bmatrix} (L_{d0}/C_{d0})^{\frac{1}{2}} & 0 & 0 \\ 0 & (L_{d1}/C_{d1})^{\frac{1}{2}} & 0 \\ 0 & 0 & (L_{d1}/C_{d1})^{\frac{1}{2}} \end{bmatrix}$$

$$[O] = \begin{bmatrix} 0 & 0 & 0 \\ 0 & 0 & 0 \\ 0 & 0 & 0 \end{bmatrix}$$

$$R_{s0} = R_{sd} + 2R_{sod} ; R_{s1} = R_{sd} - R_{sod}$$

$$R_{d0} = R_{dd} + 2R_{dod} ; R_{d1} = R_{dd} - R_{dod}$$

$$L_{s0} = L_{sd} + 2L_{sod} ; L_{s1} = L_{sd} - L_{sod}$$

$$L_{d0} = L_{dd} + 2L_{dod} ; L_{d1} = L_{dd} - L_{dod}$$

$$C_{s0} = C_{sd} + 2C_{sod} ; C_{s1} = C_{sd} - C_{sod}$$

$$C_{d0} = C_{dd} + 2C_{dod} \text{ and } C_{d1} = C_{dd} - C_{dod}$$

Here it can be observed that  $R_{d1} = R_{s1} ; L_{d1} = L_{s1} ; C_{d1} = C_{s1}$  showing that there are only 3 distinct modes of propagation in the case of transposed double circuit lines.

### 6.3 FIRST CIRCUIT ENERGISATION TRANSIENT

The first step in the Uram and Miller's method is to express the vectors  $\underline{k}_1$  and  $\underline{b}$ , in terms of the delayed functions  $\underline{a}$  and  $\underline{k}_2$  by forcing the boundary conditions, existing at the ends of the line.

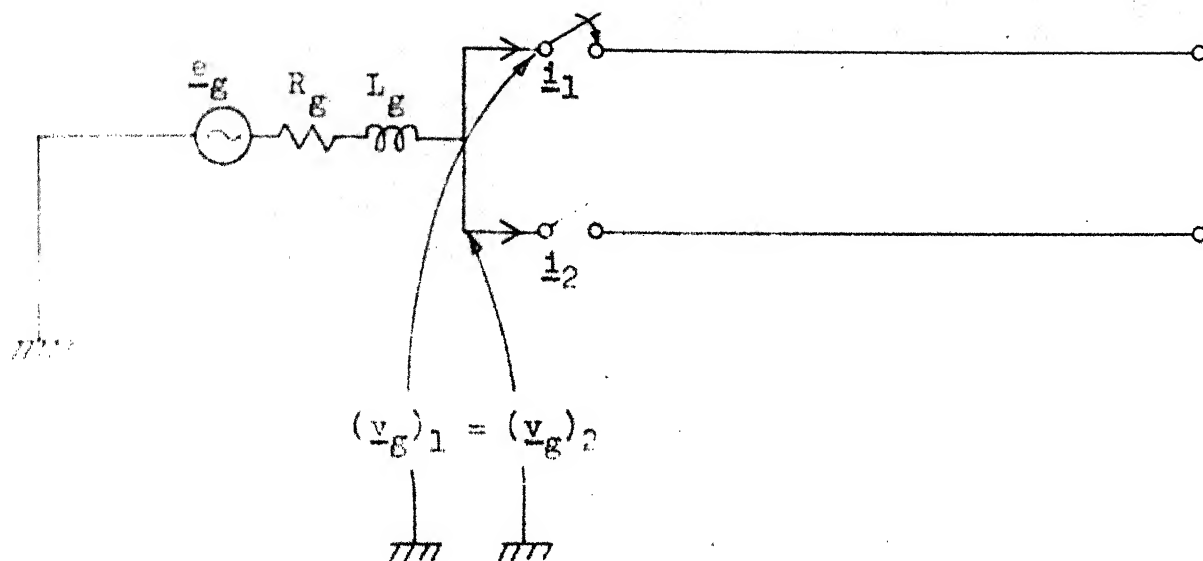


FIGURE 6.1: SINGLE LINE DIAGRAM - FIRST CIRCUIT  
ENERGISATION - SECOND CIRCUIT OPEN.

Referring to Figure 6.1, which is a single line diagram for the first circuit energisation study of a double circuit line, open at the receiving end, the expression for the sending end current [Equation (E.11)] can be written as

$$\begin{bmatrix} \underline{i}_1 \\ \underline{i}_2 \end{bmatrix} = \begin{bmatrix} [Q] & -[Q] \\ [Q] & [Q] \end{bmatrix} \begin{bmatrix} [\Omega_s]^{-1} & [0] \\ [0] & [\Omega_d]^{-1} \end{bmatrix} \begin{bmatrix} (\underline{k}_1)_1 & -(\underline{k}_2)_1 \\ (\underline{k}_1)_2 & -(\underline{k}_2)_2 \end{bmatrix} \quad (6.1)$$

where  $\underline{k}_1$  and  $\underline{k}_2$  are partitioned as

$$\underline{k}_1 = \begin{bmatrix} (\underline{k}_1)_1 \\ (\underline{k}_1)_2 \end{bmatrix} \quad \text{and} \quad \underline{k}_2 = \begin{bmatrix} (\underline{k}_2)_1 \\ (\underline{k}_2)_2 \end{bmatrix}$$

The expression for the sending end voltage [equation (E.10)] can be written as

$$\begin{bmatrix} (\underline{v}_g)_1 \\ (\underline{v}_g)_2 \end{bmatrix} = \begin{bmatrix} [Q] & -[Q] \\ [Q] & [Q] \end{bmatrix} \begin{bmatrix} (\underline{k}_1)_1 + (\underline{k}_2)_1 \\ (\underline{k}_1)_2 + (\underline{k}_2)_2 \end{bmatrix} \quad (6.2)$$

As the second circuit is unenergised, forcing the condition  $\underline{i}_2 = \underline{0}$  in equation (6.1) yields

$$[\Omega_s]^{-1} \{ (\underline{k}_1)_1 - (\underline{k}_2)_1 \} + [\Omega_d]^{-1} \{ (\underline{k}_1)_2 - (\underline{k}_2)_2 \} = \underline{0}$$

$$\text{i.e. } (\underline{k}_1)_2 = (\underline{k}_2)_2 + [\Omega_d][\Omega_s]^{-1} \{ (\underline{k}_2)_1 - (\underline{k}_1)_1 \} \quad (6.3)$$

The other sending end terminal condition is determined by the source impedance. This can be written as

$$\begin{aligned} & \underline{E}_g - R_g [Q] \{ [\Omega_s]^{-1} [(\underline{k}_1)_1 - (\underline{k}_2)_1] - [\Omega_d]^{-1} [(\underline{k}_1)_2 - (\underline{k}_2)_2] \} \\ & - L_g [Q] \{ [\Omega_s]^{-1} \left[ \frac{d(\underline{k}_1)_1}{dt} - \frac{d(\underline{k}_2)_1}{dt} \right] - [\Omega_d]^{-1} \left[ \frac{d(\underline{k}_1)_2}{dt} - \frac{d(\underline{k}_2)_2}{dt} \right] \} \\ & = [Q] \{ (\underline{k}_1)_1 + (\underline{k}_2)_1 - (\underline{k}_1)_2 - (\underline{k}_2)_2 \} \end{aligned}$$

Expressing  $(\underline{k}_1)_2$  in terms of  $(\underline{k}_1)_1$  as per equation (6.3), the above equation can be manipulated to the form

$$\begin{aligned} \frac{d(\underline{k}_1)_1}{dt} &= \frac{1}{2L_g} [\Omega_s] [Q]^{-1} \underline{E}_g - \left[ \frac{R_g}{L_g} + \frac{1}{2L_g} \{ [\Omega_d] + [\Omega_s] \} \right] (\underline{k}_1)_1 \\ &+ \left[ \frac{R_g}{L_g} + \frac{1}{2L_g} \{ [\Omega_d] - [\Omega_s] \} \right] (\underline{k}_2)_1 + \frac{1}{L_g} [\Omega_s] (\underline{k}_2)_2 + \frac{d(\underline{k}_2)_1}{dt} \end{aligned} \quad (6.4)$$

By forcing the condition that the line is open at the receiving end, we get the relationship,

$$\underline{b} = \underline{a} \quad (6.5)$$

The delay functions  $\underline{a}$  and  $\underline{k}_2$  are related to the functions  $\underline{k}_1$  and  $\underline{b}$  as follows:

$$a_1 = e^{-(R_{s0}/2) \sqrt{(C_{s0}/L_{s0})} \ell} [k_{11}(t - \tau_{s0})]_1$$

$$a_2 = e^{-(R_{s1}/2) \sqrt{(C_{s1}/L_{s1})} \ell} [k_{12}(t - \tau_{s1})]_1$$



$$\begin{aligned}
a_3 &= e^{-(R_{s1}/2) \sqrt{(C_{s1}/L_{s1})} \ell} [k_{13}(t - \tau_{s1})]_1 \\
a_4 &= e^{-(R_{d0}/2) \sqrt{(C_{d0}/L_{d0})} \ell} [k_{11}(t - \tau_{d0})]_2 \\
a_5 &= e^{-(R_{s1}/2) \sqrt{(C_{s1}/L_{s1})} \ell} [k_{12}(t - \tau_{s1})]_2 \\
a_6 &= e^{-(R_{s1}/2) \sqrt{(C_{s1}/L_{s1})} \ell} [k_{13}(t - \tau_{s1})]_2
\end{aligned}
\tag{6.6}$$

where  $\tau_{s0} = \ell \sqrt{(L_{s0} C_{s0})}$  ;  $\tau_{s1} = \ell \sqrt{(L_{s1} C_{s1})}$  and

$$\tau_{d0} = \ell \sqrt{(L_{d0} C_{d0})}.$$

$$\begin{aligned}
(k_{21})_1 &= e^{-(R_{s0}/2) \sqrt{(C_{s0}/L_{s0})} \ell} b_1(t - \tau_{s0}) \\
(k_{22})_1 &= e^{-(R_{s1}/2) \sqrt{(C_{s1}/L_{s1})} \ell} b_2(t - \tau_{s1}) \\
(k_{23})_1 &= e^{-(R_{s1}/2) \sqrt{(C_{s1}/L_{s1})} \ell} b_3(t - \tau_{s1}) \\
(k_{21})_2 &= e^{-(R_{d0}/2) \sqrt{(C_{d0}/L_{d0})} \ell} b_4(t - \tau_{d0}) \\
(k_{22})_2 &= e^{-(R_{s1}/2) \sqrt{(C_{s1}/L_{s1})} \ell} b_5(t - \tau_{s1}) \\
(k_{23})_2 &= e^{-(R_{s1}/2) \sqrt{(C_{s1}/L_{s1})} \ell} b_6(t - \tau_{s1})
\end{aligned}
\tag{6.7}$$

With the help of equations (6.3) - (6.7) an incremental solution for the four vectors  $\underline{k}_1$ ,  $\underline{k}_2$ ,  $\underline{a}$  and  $\underline{b}$

at each instant of time and hence the response at any point of interest on the transmission line can be evaluated. As equation (6.4) is a differential equation, a numerical solution of this equation becomes necessary to arrive at the values of  $(k_1)_1$  at each instant.

#### 6.4 SECOND CIRCUIT ENERGISATION

An algorithm for studying the transient due to the energisation of the second circuit, when the first circuit is in steady state is developed in this Section. The voltage cancellation technique and the principle of superposition are used for simulating the circuit breaker closing operation. The principle of superposition is applicable for this part of the analysis as the system considered is linear.

The steps involved can be described with the help of Figures 6.2.1 and 6.2.2 as follows:

(i) First assuming that the second circuit continues to be unenergised, the response at any point of interest on the line (particularly the voltage at the open receiving end) and the voltages across the circuit breaker terminals at the sending end of the second circuit are calculated. As the first circuit is in steady state, this step of the calculation is a steady state analysis.

(ii) The voltages across the breaker poles, calculated in step (i) are injected across the poles with reversed polarity as cancellation voltages and the sending end

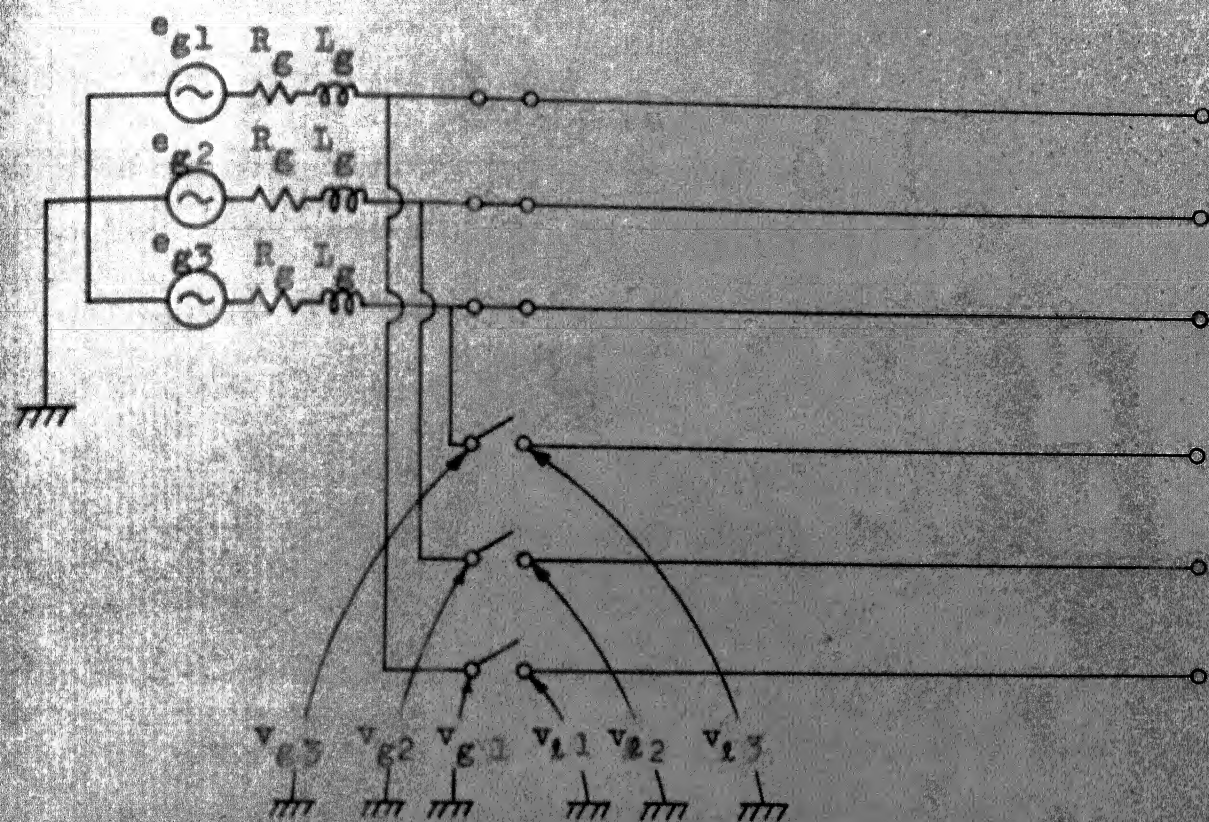


FIGURE 6.2.1

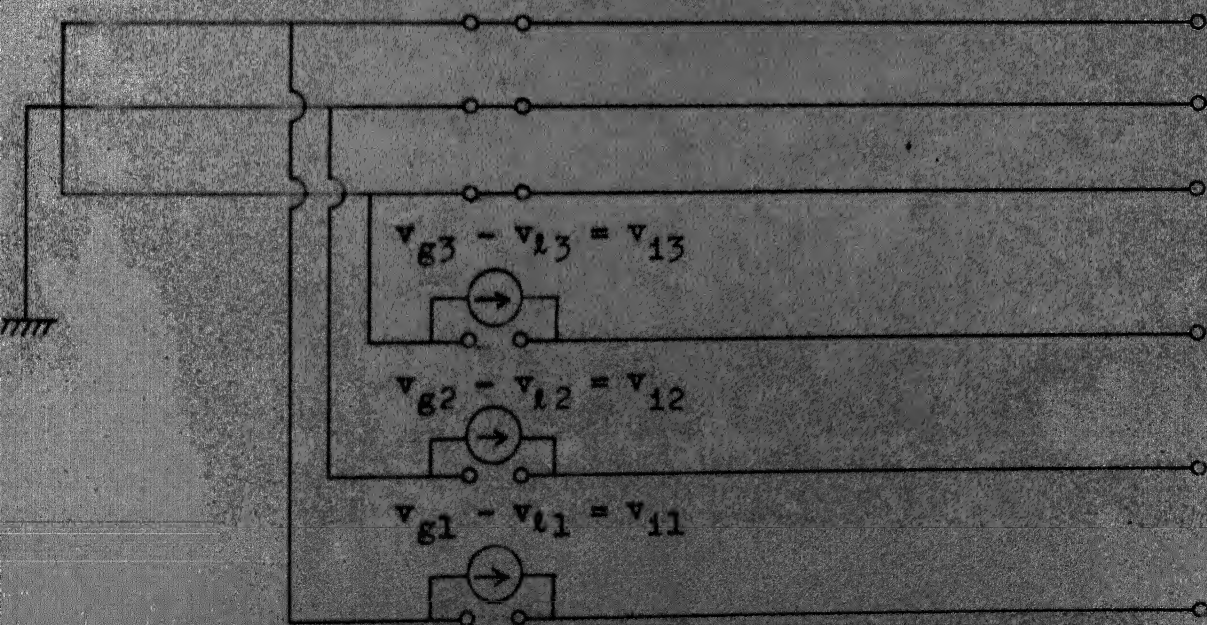


FIGURE 6.2.2

PRINCIPLE OF SUPERPOSITION USED FOR SIMULATION OF  
SECOND CIRCUIT ENERGISATION - FIRST CIRCUIT IN  
STEADY STATE.

terminals of the first circuit are grounded. Now with these cancellation voltages alone present, the response at the above mentioned point of interest is again calculated.

(iii) Superimposing these two component responses, the total response is obtained.

The algorithm for finding the response to the injected voltage (step ii) by Uram and Miller's method is developed as follows:

Referring to Figure 6.2.2, the terminal conditions at the sending end are that the voltages of the first circuit are zero and those of the second circuit are  $v_{i1}$ ,  $v_{i2}$  and  $v_{i3}$ .

Forcing these conditions and using the same notation, as used for the first circuit energisation case, equation (6.2) becomes

$$\begin{bmatrix} [Q] & -[Q] \\ [Q] & [Q] \end{bmatrix} \begin{bmatrix} (\underline{k}_1)_1 + (\underline{k}_2)_1 \\ (\underline{k}_1)_2 + (\underline{k}_2)_2 \end{bmatrix} = \begin{bmatrix} \underline{0} \\ \underline{v}_i \end{bmatrix} \quad (6.8)$$

$$\text{where } \underline{0} = \begin{bmatrix} 0 \\ 0 \\ 0 \end{bmatrix} \quad \text{and} \quad \underline{v}_i = \begin{bmatrix} v_{i1} \\ v_{i2} \\ v_{i3} \end{bmatrix}$$

$$\text{i.e. } [Q] \{ (\underline{k}_1)_1 + (\underline{k}_2)_1 + (\underline{k}_1)_2 + (\underline{k}_2)_2 \} = \underline{v}_i \quad (6.9)$$

$$\text{and } (\underline{k}_1)_1 = (\underline{k}_1)_2 - (\underline{k}_2)_1 + (\underline{k}_2)_2 \quad (6.10)$$

Substituting for  $(\underline{k}_1)_1$  in equation (6.9) by equation (6.10), we get

$$(\underline{k}_1)_2 = \frac{1}{2}[Q]^{-1} \underline{v}_1 - (\underline{k}_2)_2 \quad (6.11)$$

Substituting (6.11) in (6.10), we get

$$(\underline{k}_1)_1 = \frac{1}{2}[Q]^{-1} \underline{v}_1 - (\underline{k}_2)_1 \quad (6.12)$$

As the receiving end is open, from equation (E.13), we get

$$\underline{b} = \underline{a} \quad (6.13)$$

The functions  $(\underline{k}_1)_2$ ,  $(\underline{k}_1)_1$  and  $\underline{b}$  have been expressed in terms of delayed functions and known quantities  $[Q]$ ,  $\underline{v}_1$  by equations (6.11) - (6.13) respectively.

The delay functions  $\underline{a}$  and  $\underline{k}_2$  are related to the functions  $\underline{k}_1$  and  $\underline{b}$  by the sets of equations (6.6) and (6.7). Hence with the help of equations (6.6), (6.7), (6.11), (6.12) and (6.13), an incremental solution for the desired response for the injected voltage can be calculated.

## 6.5 COMPUTATIONAL RESULTS

The same example, tried in Chapter 5, using the modified Fourier transform method is taken up and the Uram and Miller's method is used for evaluating both the first and the second circuit energising transients on the double circuit line. The modal components of the parameters for this line are given below.

$$R_{s0} = 0.321396 \, \Omega/\text{mile} ; \quad L_{s0} = 0.00686016 \, \text{H}/\text{mile} ;$$

$$C_{s0} = 0.934644 \times 10^{-8} \, \text{f}/\text{mile}$$

$$R_{s1} = R_{d1} = 0.030330 \, \Omega/\text{mile} ; \quad L_{s1} = L_{d1} = 0.00142587 \, \text{H}/\text{mile}$$

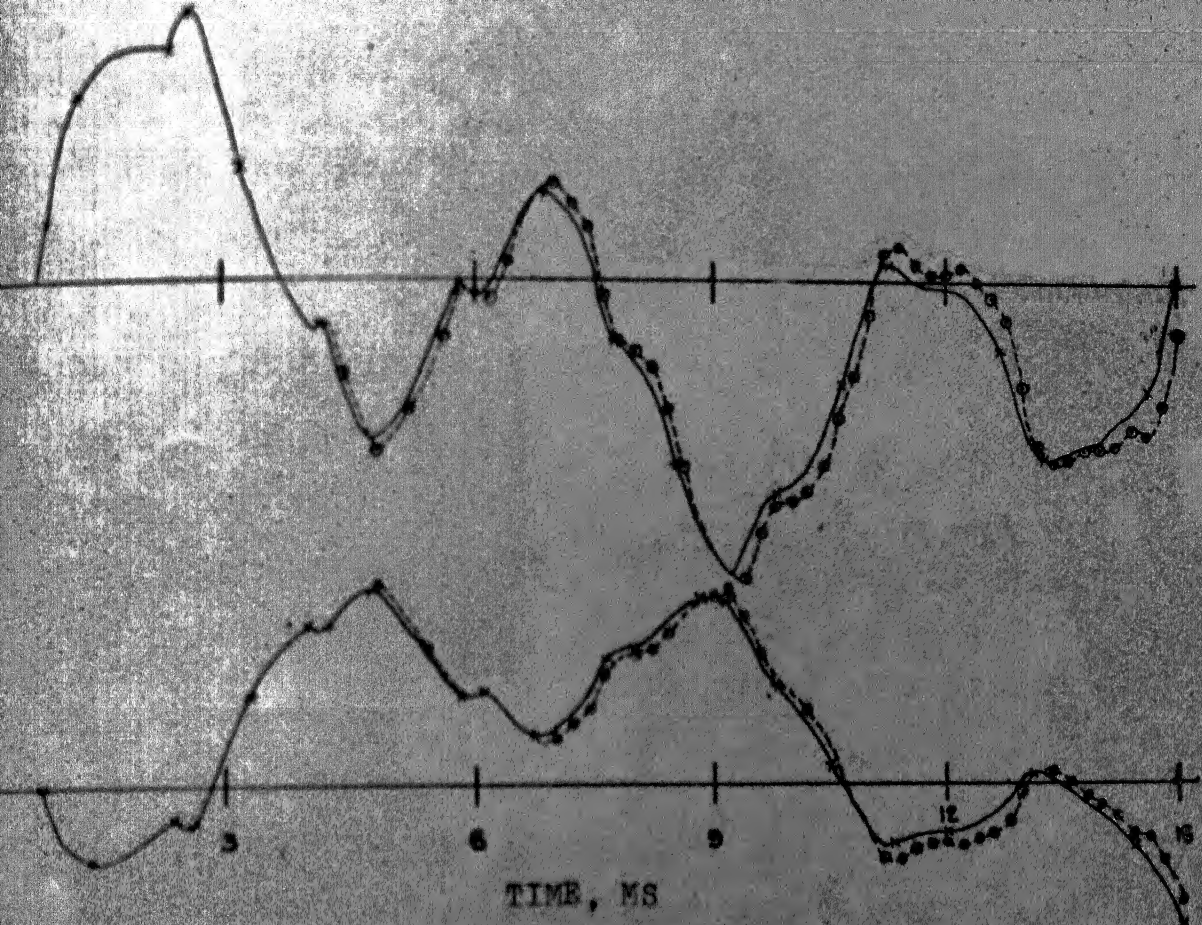
$$C_{s1} = C_{d1} = 2.085753 \times 10^{-8} \, \text{f}/\text{mile} ; \quad R_{d0} = 0.03 \, \Omega/\text{mile}$$

$$L_{d0} = 0.00187236 \, \text{H}/\text{mile} ; \quad C_{d0} = 1.620324 \times 10^{-8} \, \text{f}/\text{mile}.$$

The phase voltage waveforms at the receiving end of the first circuit, subsequent to the closing of the first circuit are plotted in Figure 6.3. The breakers of all the three phases are assumed to close simultaneously at the instant when the source voltage of phase 'a' is at positive peak. A maximum peak of 2.32 p.u. is observed to occur on phase 'a' at 9.2 m.secs. for this case. The corresponding voltage waveforms, obtained using the modified Fourier transform method are also plotted in the same figure. It can be observed that there is a close matching between the waveforms obtained by both the methods.

Next for the same line, the transient due to the closing of the second circuit, when the first circuit is in steady state (described in Section 6.4) is studied. The steady state analysis of Section 5.5.2 holds good here also and hence in step (ii) of Section 6.4, it can be assumed that no voltages are induced on the second circuit conductors. Hence, the voltages across the breaker poles of the second circuit (which is the injected voltage source) can be taken





x---x URAM AND MILLER'S METHOD  
 o---o MODIFIED FOURIER TRANSFORM METHOD

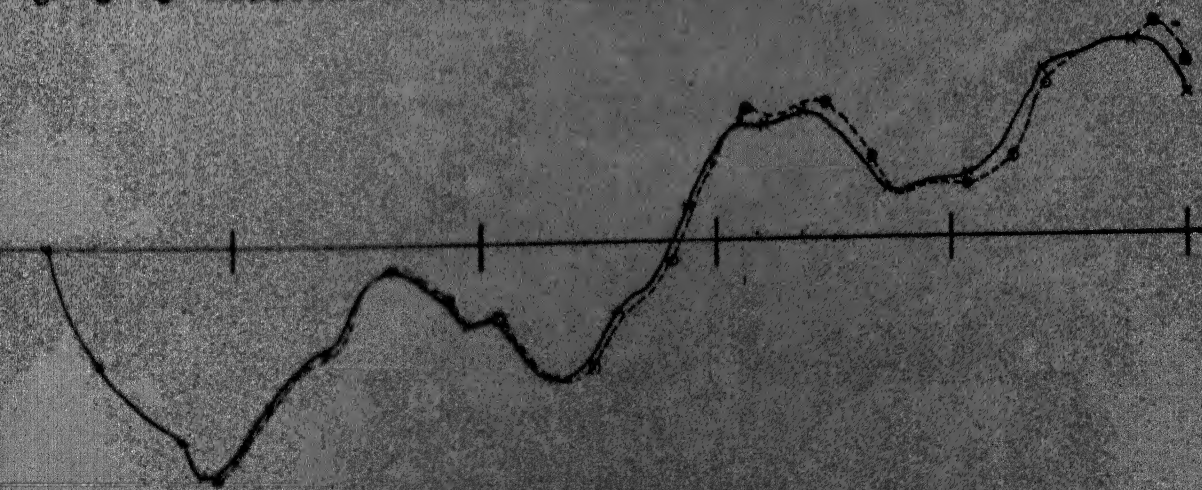


FIGURE 6.3: COMPARISON OF VOLTAGE WAVEFORMS AT RECEIVING END  
 BY URAM AND MILLER AND MODIFIED FOURIER TRANSFORM  
 METHODS - FIRST CIRCUIT ENERGISATION - SECOND  
 CIRCUIT OPEN.

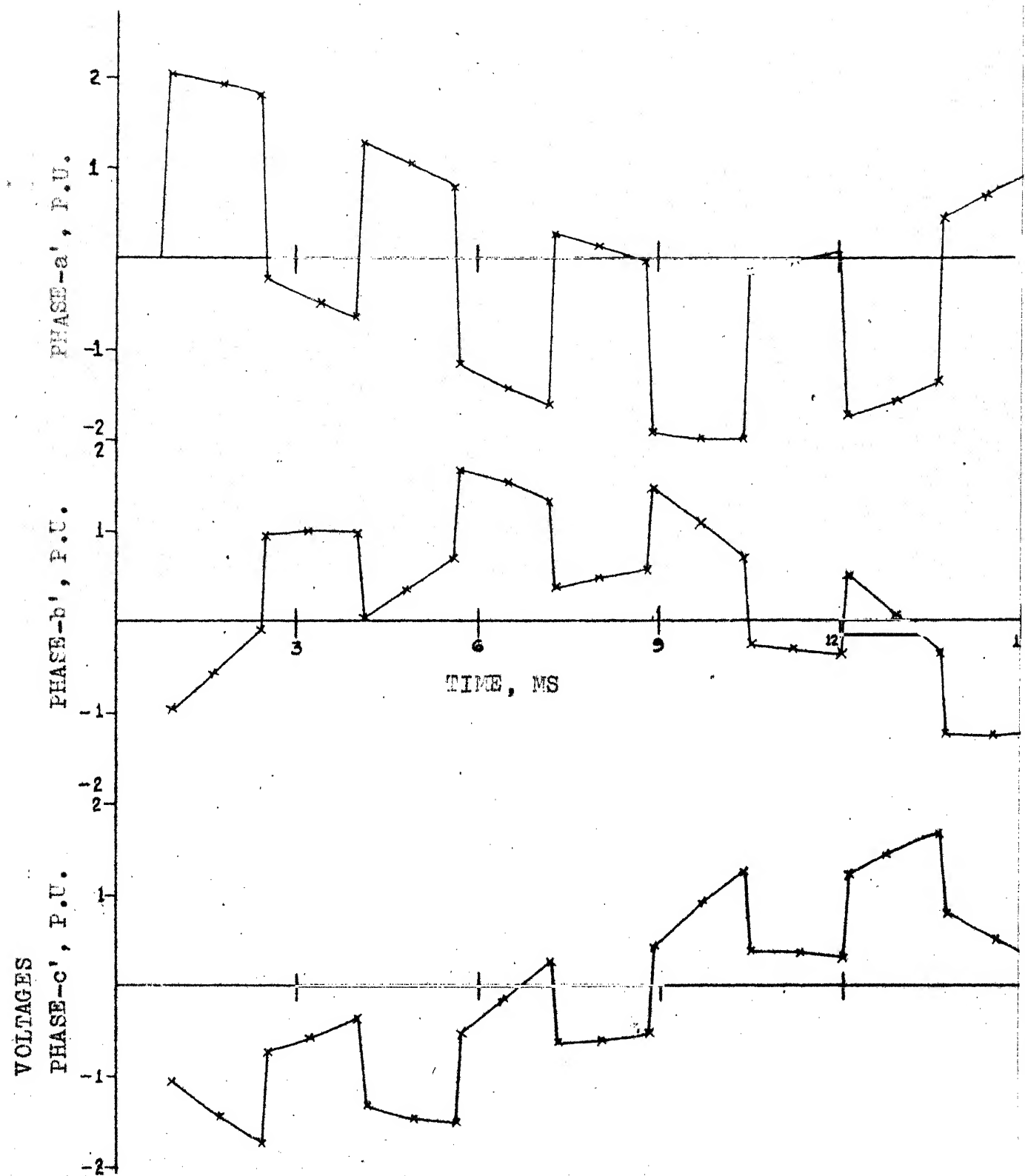


FIGURE 6.4: VOLTAGE WAVEFORMS AT RECEI  
ENERGISATION - FIRST CIRCU



as the steady state voltages at the sending end of the connected phases of the first circuit. Again the breaker poles of all the three phases of the second circuit are assumed to close simultaneously at the instant, when the phase-a' voltage is at positive peak. The phase voltage waveforms at the receiving end of the second circuit, subsequent to the closing of the second circuit are plotted in Figure 6.4. A maximum peak of 2.02 p.u. is observed to occur for this case at 0.9 m.secs. on phase-a'. These waveforms are almost coinciding with the corresponding ones, obtained using the modified Fourier transform method in Chapter 5.

## 6.6 CONCLUSIONS

The extension of the theory of Uram and Miller's method for solving the energisation transients on a transposed double circuit line has been presented in this chapter. The same line, tried in Chapter 5 using the modified Fourier transform method, has been taken up and the transient due to the energisation of the first circuit alone, with the second circuit remaining unenergised and the transient due to the energisation of the second circuit, when the first circuit is operating in steady state, have been studied. The voltage waveforms at the open receiving end of the line, obtained using both the Uram and Miller's and the modified Fourier transform methods have been compared. The results by both

the methods have been found to be closely matching. As the Uram and Miller's method is a time domain method, the frequency dependence of line parameters cannot be directly incorporated in this method. The untransposed lines also cannot be handled by this method. However, this method takes relatively less computer time.

## CHAPTER 7

### ENERGISATION TRANSIENT DUE TO SEQUENTIAL CLOSING OF CIRCUIT BREAKER POLES

#### 7.1 INTRODUCTION

In reality, during the energisation of a transmission line, the poles of the circuit breaker do not close simultaneously. However, such an assumption is generally made only to simplify the analysis and to get an idea of the magnitude of the switching overvoltages involved. The difference in time in the closing of different poles of a circuit breaker is small, but this time is comparable to the time period of the electrical transients in the overvoltages that develop. This has been seen in earlier chapters to be of the order of a few m.secs. Therefore, for an accurate analysis, the non-simultaneous or sequential closing of the circuit breaker poles has to be incorporated in the program. The sequential closing of the breaker poles is bound to give rise to a higher order of overvoltages. There are basically two approaches in the existing literature for the incorporation of sequential closing feature in the Fourier transform method of studying the energisation transient on a transmission line. Wedepohl and Mohamed [27] have proposed a method of solving the problem by numerically evaluating the Fourier transform of the induced voltages on the unenergised phases, known at discrete intervals of time. On the other hand, the method proposed

by Battison et al [28] solves the problem by using a convolution integral approach for taking into account the sequential pole closure. In this chapter, the method proposed by Wedepohl and Mohamed is extended for the case of a double circuit line. After presenting the relevant theory for this extension, the double circuit line example, with receiving end open, of Chapters 5 and 6 is considered. The transient, arising due to the sequential closure of the circuit breaker poles of the second circuit, when the first circuit is operating in steady state, is evaluated. The transient voltage waveforms obtained by the double circuit modelling is compared with those obtained by ignoring the presence of the first circuit. Also the effect of the continuous variation of line parameter values with frequency on the energisation transient for both transposed and untransposed lines is investigated.

## 7.2 INCORPORATION OF SEQUENTIAL CLOSING OF CIRCUIT BREAKER POLES IN FOURIER TRANSFORM METHOD

The sequential closing of the circuit breaker poles involves changes in the terminal conditions at the sending end of a transmission line at the closing instant of each breaker pole. As the Fourier transform method is a frequency domain method and because the change in system conditions due to sequential closing occurs at different instants of time, an indirect solution of the problem becomes essential.

To start with, when only the first phase of the line is getting closed, the conditions to be forced at the sending end are that the currents on the other two unenergised phases are zero. Further, the voltage and current on the first phase at the sending end are determined by the source voltage and the impedance, present on this phase at this end. After a short time of the order of a few m.secs., the second pole gets closed, leaving only the third phase unenergised. At this stage, the current through the third phase is zero and the voltages and currents in the first and second phases at the sending end are determined by the source voltages and impedances present on these phases at the sending end. After the elapse of a few more m.secs., the third pole gets closed and from this instant onwards, the voltages and currents on all the three phases are determined by the source voltages and impedances at the sending end. During the interval between the first and second pole closure, voltages are induced on the floating second and third phase conductors. In the Fourier transform method, these induced voltages at the sending end should be first calculated as functions of time and then the modified Fourier transform of these functions so calculated at discrete interval of time should be numerically evaluated to be fed as input in frequency domain. Similarly during the interval between the second and third pole closure, voltage is induced on the floating third phase conductor because of the mutual effect between

this phase and the other two energised phases. The modified Fourier transform of this function in this time interval, augmented by the induced voltage on this phase during the interval between the first and second pole closure is to be numerically computed and fed as input voltage in frequency domain to this phase.

The steps involved in the solution of the sequential closing transient can be summarized as follows:

(i) The first pole closes (say at zero time) and the sending end boundary conditions at this stage are a known voltage on the first phase and zero currents on the other two phase conductors. Using the modified Fourier transform method, the system response at the point of interest is computed as a function of time. In particular, the induced voltages at the sending end on the two unenergised phase conductors are also computed.

(ii) After a time interval  $T_1$ , the second pole closes and the new boundary conditions at the sending end are known voltages on the first two phases and zero current on the third phase. The transformed voltages to be fed as input on the second phase includes the modified Fourier transform of the induced voltage on this conductor in the interval  $0 < \text{time} < T_1$  (evaluated numerically) in addition to the transform of the source voltage, connected to this phase for time  $> T_1$  (for which an analytical expression can be obtained). For these terminal conditions, the response

at the point of interest can be computed as a function of time. In particular, the induced voltage on the floating third phase conductor is also to be computed. These responses are valid right from zero time. But the response, so obtained will be a mere repetition of the corresponding response, obtained in the first step in the interval  $0 < t < T_1$ . However, if it is computed again here, it can be utilized to get an idea of the error, introduced by the numerical integration and the numerical evaluation of the transform of the induced voltages involved in this step.

(iii) After an elapse of time, finally the third pole closes at time  $T_2$ . Now the transformed voltages on all the three phases at the sending end are known and hence the response at the point of interest for time  $> T_2$  can be computed. Here the transformed voltages, to be fed at the sending end as input, includes in addition to the analytically known transformed voltages on all the three phases, the numerically evaluated transforms of the induced voltage on second phase in the interval  $0 < \text{time} < T_1$  and that of the induced voltage on the third phase in the interval  $0 < \text{time} < T_2$ . Again the computing of the response right from zero instant helps in giving an idea of the error, introduced by the numerical processes involved.

### 7.3 DEVELOPMENT OF ALGORITHM FOR HANDLING SEQUENTIAL CLOSING

As described in the last section, the incorporation of sequential closing essentially involves finding the transient response of the line for three different sending end terminal conditions. The change in terminal conditions occurs at the closing instant of each pole. The terminal conditions are zero currents on unenergised phases and known voltages on the energised phases behind source reactances, which can be converted to equivalent current sources with appropriate shunt admittances. Hence, once a set of equations are formed for computing the transient response of the line for known sending end currents, it can be used repeatedly thrice with the suitable currents injected at each of the pole closing instants, to get the complete response.

It has been derived in Section 5.3 that when a transmission line is viewed as a two port network, the transformed currents and voltages at the terminals are related by the expression,

$$\begin{bmatrix} \underline{I}_S \\ \underline{I}_R \end{bmatrix} = \begin{bmatrix} [A] & [B] \\ [B] & [A] \end{bmatrix} \begin{bmatrix} \underline{V}_S \\ \underline{V}_R \end{bmatrix} \quad (7.1)$$

where  $[A] = [Z]^{-1}[\psi][\text{Coth}\psi\ell]$

$$[B] = -[Z]^{-1}[\psi][\text{Cosech}\psi\ell]$$

$$[Z] = [R] + (a + j\omega)[L]$$



$$[Y] = (a+j\omega)[C]$$

$$[\psi] = [Q][\gamma][Q]^{-1}$$

$$[\text{Coth } \psi \ell] = [Q][\text{Coth } \gamma \ell][Q]^{-1}$$

$$[\text{Cosech } \psi \ell] = [Q][\text{Cosech } \gamma \ell][Q]^{-1}$$

and  $[\gamma]$  is the diagonal matrix, whose diagonal elements are square roots of the eigen values of the matrix product  $[Z][Y]$ .

When the open receiving end condition is forced into equation (7.1),  $\underline{V}_R$  and  $\underline{V}_S$  can be expressed in terms of  $\underline{I}_S$  as follows:

$$\underline{V}_S = ([A] - [B][A]^{-1}[B])^{-1} \underline{I}_S \quad (7.2)$$

$$\underline{V}_R = ([B] - [A][B]^{-1}[A])^{-1} \underline{I}_S \quad (7.3)$$

When there is a shunt admittance  $[Y_S]$  at the sending end, equations (7.2) and (7.3) take the form

$$\underline{V}_S = \{ [A] + [Y_S] - [B][A]^{-1}[B] \}^{-1} \underline{I}_S \quad (7.4)$$

$$\underline{V}_R = \{ [B] - ([A] + [Y_S])[B]^{-1}[A] \}^{-1} \underline{I}_S \quad (7.5)$$

where now  $\underline{I}_S$  includes the current drawn by the shunt admittance in addition to the current drawn by the line.

In the equations (7.4) and (7.5), the quantities  $[Y_S]$  and  $\underline{I}_S$  vary according to whether the different phase poles of the breaker at the sending end is open or closed.

Initially, in the interval  $0 < t < T_1$ , when only the first pole is closed,  $[Y_s]$  and  $\underline{I}_s$  are given by the expressions

$$[Y_s] = \begin{bmatrix} 1/[R_s + (a+j\omega)L_s] & 0 & 0 \\ 0 & 0 & 0 \\ 0 & 0 & 0 \end{bmatrix}$$

$$\underline{I}_s = \begin{bmatrix} E_{s1}/[R_s + (a+j\omega)L_s] \\ 0 \\ 0 \end{bmatrix}$$

where  $E_{s1}$  is the modified Fourier transform of the first phase source voltage and  $R_s, L_s$  are the source resistance and inductance per phase respectively.

In the interval  $T_1 < t < T_2$ , the first and second poles are closed and now

$$[Y_s] = \begin{bmatrix} 1/[R_s + (a+j\omega)L_s] & 0 & 0 \\ 0 & 1/[R_s + (a+j\omega)L_s] & 0 \\ 0 & 0 & 0 \end{bmatrix}$$

$$\underline{I}_s = \begin{bmatrix} E_{s1}/[R_s + (a+j\omega)L_s] \\ (E_{s2} + V_{s2})/[R_s + (a+j\omega)L_s] \\ 0 \end{bmatrix}$$

where  $E_{s2}$  is the modified Fourier transform of the source voltage of this phase (which becomes the line side voltage also on this phase from time  $T_1$  onwards) [i.e. the modified Fourier transform of  $e_{s2}(t-T_1) u(t-T_1)$ ] and  $V_{s2}$  is the

numerically evaluated modified Fourier transform of the induced voltage on the second phase conductor at the sending end in the interval  $0 < t < T_1$ .

From the instant  $T_2$  onwards, all the three poles are closed and hence

$$[Y_S] = \begin{bmatrix} 1/[R_S + (a + j\omega)L_S] & 0 & 0 \\ 0 & 1/[R_S + (a + j\omega)L_S] & 0 \\ 0 & 0 & 1/[R_S + (a + j\omega)L_S] \end{bmatrix}$$

$$\underline{I}_S = \begin{bmatrix} E_{s1}/[R_S + (a + j\omega)L_S] \\ (E_{s2} + V_{s2})/[R_S + (a + j\omega)L_S] \\ (E_{s3} + V_{s3})/[R_S + (a + j\omega)L_S] \end{bmatrix}$$

where  $E_{s3}$  is the modified Fourier transform of the source voltage of this phase (which becomes the line side voltage on this phase from time  $T_2$  onwards) [i.e. the modified Fourier transform of  $e_{s3}(t - T_2) u(t - T_2)$ ] and  $V_{s3}$  is the numerically evaluated modified Fourier transform of the induced voltage on the third phase conductor at the sending end in the interval  $0 < t < T_2$ .

The appropriate values of  $[Y_S]$  and  $\underline{I}_S$ , when used in expressions (7.4) and (7.5) in the appropriate intervals of time, facilitates calculation of the desired transient overvoltage response in frequency domain and it can be converted to time domain by computing numerically the inverse transformation integral.

Here it can be observed that the numerical integration of the transformed response to time domain can be limited to the extent of calculating the induced voltages at the sending end on the second and third phase floating conductors in the interval  $0 < t < T_1$ , subsequent to the first pole closing and calculating the induced voltage at the sending end on the third phase conductor alone in the interval  $T_1 < t < T_2$ , subsequent to second pole closing. The transforming back of the receiving end voltages to time domain may be done just once at the end.

The method of calculating numerically the modified Fourier transform of the induced voltages on unenergised conductors, known at discrete interval of time is given in the following section.

A flow chart of the program for computing the energisation transient on a single circuit transmission line with sequential closing of circuit breaker poles by modified Fourier transform method is presented in Appendix F.

#### 7.4 NUMERICAL EVALUATION OF THE MODIFIED FOURIER TRANSFORM

For numerically evaluating the modified Fourier transform of a known function  $f(t)$ , it can be divided into  $N$  strips of equal width, the interval of the strip being sufficiently small, such that the variation of the function within any of these intervals can be approximated by a

straight line. Then the modified Fourier transform of the function  $f(t)$  can be obtained by summing up the modified Fourier transforms of all these individual strips. A typical strip of the function and how it can be split up into components of step and ramp functions are shown in Figures 7.1.1 and 7.1.2. This strip can be split into two component step functions (one of magnitude  $f_{n-1}$ , starting at instant  $(n-1)\Delta t$ , the other of magnitude  $-f_n$ , starting after a delay  $\Delta t$  at the instant  $n\Delta t$ ) and two ramp components (one of slope  $\frac{\Delta f_n}{\Delta t}$ , starting at instant  $(n-1)\Delta t$  and the other of slope  $-\frac{\Delta f_n}{\Delta t}$ , starting after a delay  $\Delta t$  at the instant  $n\Delta t$ ).

When the modified Fourier transforms of the two component steps of all such strips are summed up, the transform of all such steps in the entire range of time is obtained as

$$F_s(\omega) = \frac{1}{(a+j\omega)} [f_0 - f_N e^{-(a+j\omega)N\Delta t}] \quad (7.6)$$

The sum of the modified Fourier transforms of all component ramps can be given by

$$F_r(\omega) = - \frac{1}{\Delta t(a+j\omega)^2} \sum_{n=1}^N \Delta f_n [e^{-(a+j\omega)(n-1)\Delta t} - e^{-(a+j\omega)n\Delta t}] \quad (7.7)$$

An economy in the computation of  $F_r(\omega)$  can be effected by expanding and grouping the consecutive terms

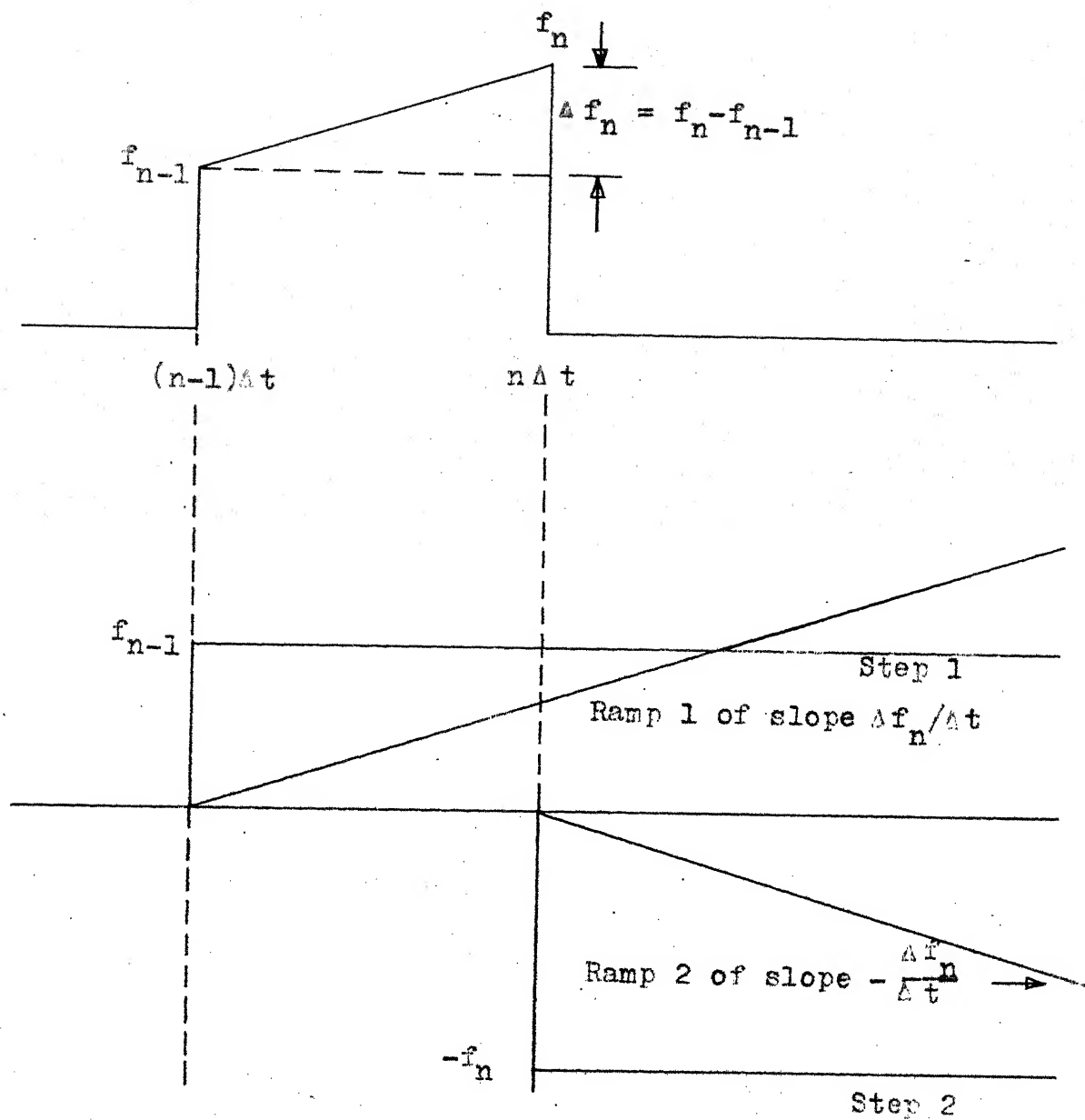


FIGURE 7.1: NUMERICAL EVALUATION OF FOURIER TRANSFORM OF A FUNCTION.

of (7.7) together. By this manipulation, equation (7.7) can be reduced to the form

$$F_r(\omega) = \frac{1}{\Delta t(a+j\omega)^2} [f_1 - f_0 - (f_N - f_{N-1}) e^{-(a+j\omega)N\Delta t} \\ + \sum_{n=1}^{N-1} (f_{n+1} - 2f_n + f_{n-1}) e^{-(a+j\omega)n\Delta t}]$$

Hence the modified Fourier transform of the function  $f(t)$  in the whole range of time can be written as

$$F(\omega) = \frac{1}{(a+j\omega)} [f_0 \{1 - \frac{1}{\Delta t(a+j\omega)}\} + \frac{f_1}{\Delta t(a+j\omega)} \\ + \{ \frac{f_{N-1}}{\Delta t(a+j\omega)} - f_N (1 + \frac{1}{\Delta t(a+j\omega)}) \} e^{-(a+j\omega)N\Delta t} \\ + \frac{1}{\Delta t(a+j\omega)} \sum_{n=1}^{N-1} (f_{n+1} - 2f_n + f_{n-1}) e^{-(a+j\omega)n\Delta t}]$$

## 7.5 SINGLE CIRCUIT LINE EXAMPLES

### 7.5.1 Verification of Computer Program:

To check the computer program, developed using the modified Fourier transform method, incorporating the sequential closing of circuit breaker poles, the transient voltage at the receiving end of a typical 400 KV single circuit line, computed by this method is compared with the results, obtained for the same example by Uram and Miller's method.

This transmission line of Uttar Pradesh State Electricity Board is 400 kms. long and connects Lucknow with Obra. It has got two shunt reactors, one each at sending and receiving ends. The energisation study is done for energisation at Obra end. Figure 7.2 gives the system set up. The system data are given in Appendix G.

The phase sequence of closing of the circuit breaker poles is assumed for the study to be RBY and the switching instants of B phase and Y phase are taken as 3.3 m.secs. and 6.7 m.secs. respectively (taking the instant of closing of R phase as zero time). This set of switching instants are such that each pole gets closed when the source voltage of that phase is at peak value.

The phase voltage waveforms at the receiving end, obtained using both the methods are compared in Figure 7.3. There is a close matching between the waveforms, obtained by the two methods. A maximum peak of -3.01 p.u. in the case of the modified Fourier transform method and -2.88 p.u. in the case of the Uram and Miller's method are observed to occur, in both the cases on phase R at 9 m.secs.

This particular example contains reactors at both the ends of the line additionally as compared to the system, considered in Section 7.3, while developing the necessary theory for incorporating sequential closing feature in the modified Fourier transform method. When



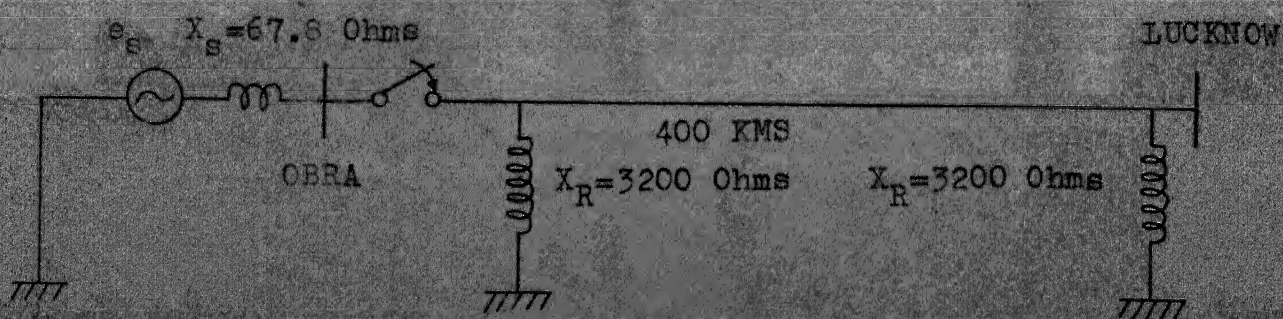


FIGURE 7.2: SYSTEM DIAGRAM OF THE EXAMPLE

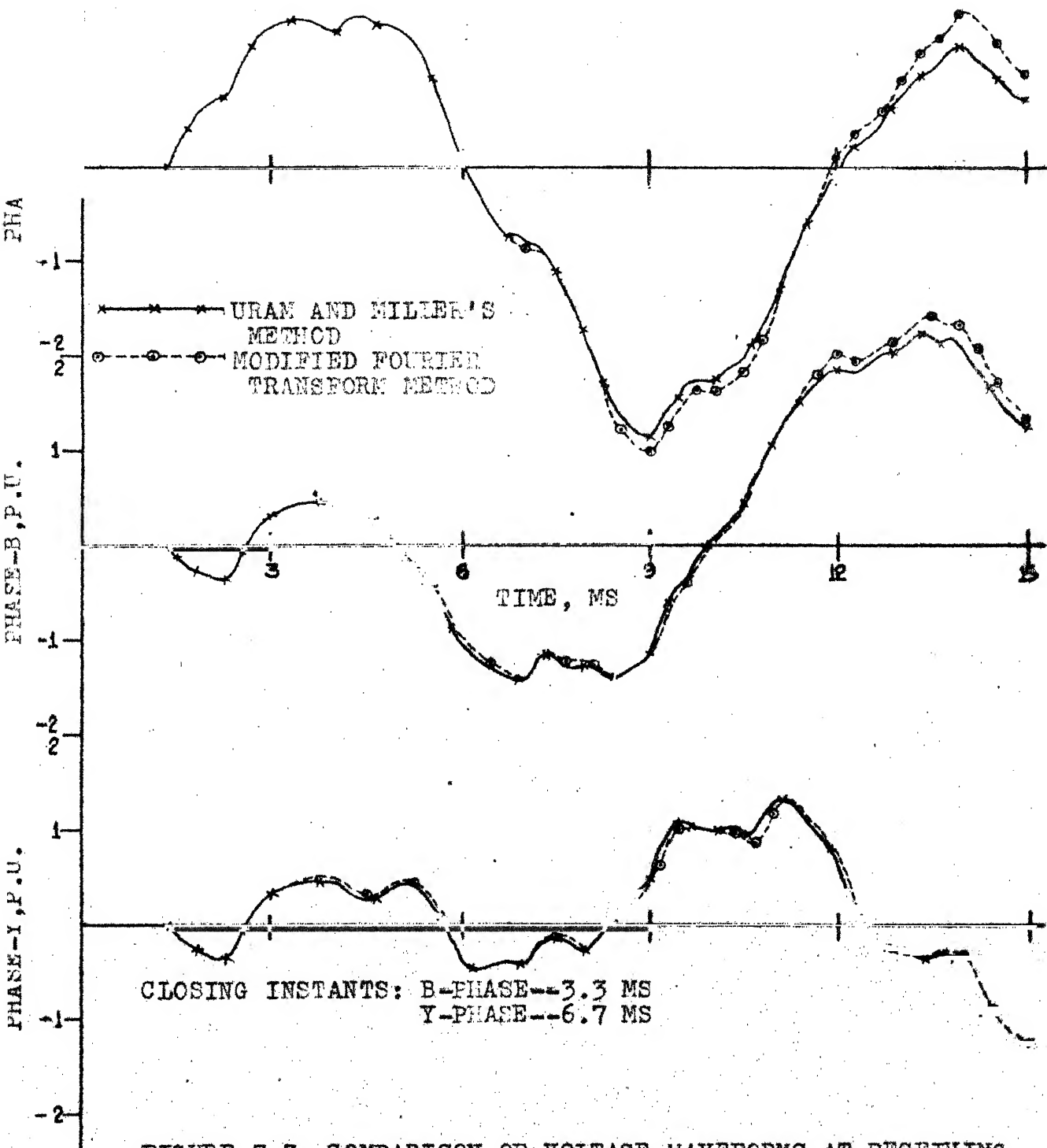


FIGURE 7.3: COMPARISON OF VOLTAGE WAVEFORMS AT RECEIVING END BY URAM AND MILLER AND MODIFIED FOURIER TRANSFORM METHODS - UPSEB SINGLE CIRCUIT LINE SEQUENTIAL ENERGISATION.

these reactors are introduced, the equations of Section 7.3 get modified as given in the following para.

The matrix  $\begin{bmatrix} [A] & [B] \\ [B] & [A] \end{bmatrix}$  in equation (7.1) can be interpreted as the short circuit admittance parameters of the transmission line. The introduction of the shunt admittances  $[Y_{sh}]$  at both the ports just adds these admittance values to the self admittance terms of the short circuit admittance parameter matrix, for obtaining the overall short circuit parameters of the system.

Hence equations (7.4) and (7.5), with the reactors introduced, read as follows:

$$\underline{V}_S = \{ [A] + [Y_{sh}] + [Y_S] - [B]([A] + [Y_{sh}])^{-1}[B] \}^{-1} \underline{I}_S \quad (7.8)$$

$$\underline{V}_R = \{ [B] - ([A] + [Y_{sh}] + [Y_S])[B]^{-1}([A] + [Y_{sh}]) \}^{-1} \underline{I}_S \quad (7.9)$$

$$\text{where } [Y_{sh}] = \begin{bmatrix} 1/(a+j\omega)L_{sh} & 0 & 0 \\ 0 & 1/(a+j\omega)L_{sh} & 0 \\ 0 & 0 & 1/(a+j\omega)L_{sh} \end{bmatrix}$$

and  $L_{sh}$  is the inductance of the shunt reactor.

### 7.5.2 Effect of Incorporating Frequency Dependence of Line Parameters:

In order to investigate the effect of frequency dependence of line parameters on the transient overvoltage, produced by the sequential closing of circuit breaker poles,

a single circuit of the double circuit line example, studied in Chapters 4,5 and 6 is considered. This line is 150 miles long and has a source inductance of 0.1 H. The continuous variation of the line parameter values with frequency are calculated, using the Carson's formulae and are used in the calculations. The switching instants are assumed to be 0, 3.3 and 6.7 m.secs. The phase sequence of pole closing is assumed to be RBY, so that each pole gets closed when the source voltage of that phase is at peak value. The comparison of the transient voltage waveforms at the open receiving end with and without frequency dependence of line parameters is done in Figure 7.4. From the waveforms it can be observed that the maximum peak overvoltage value gets reduced considerably and the oscillations in the voltage waveforms get smoothened, when the frequency dependence of line parameters is considered. A maximum peak of 2.72 p.u. occurs on phase Y at 9.3 m.secs. for the case without frequency dependence of line parameters; whereas a maximum peak of -2.36 p.u. occurs on phase B at 5.9 m.secs. for the case with frequency dependence of line parameters, included. The line is assumed to be uniformly transposed for both the cases.

## 7.6 ENERGISATION TRANSIENT ON A DOUBLE CIRCUIT LINE

In this section, the necessary theory for studying the transient on a double circuit line, due to the sequential closing of the circuit breaker poles of the second circuit,

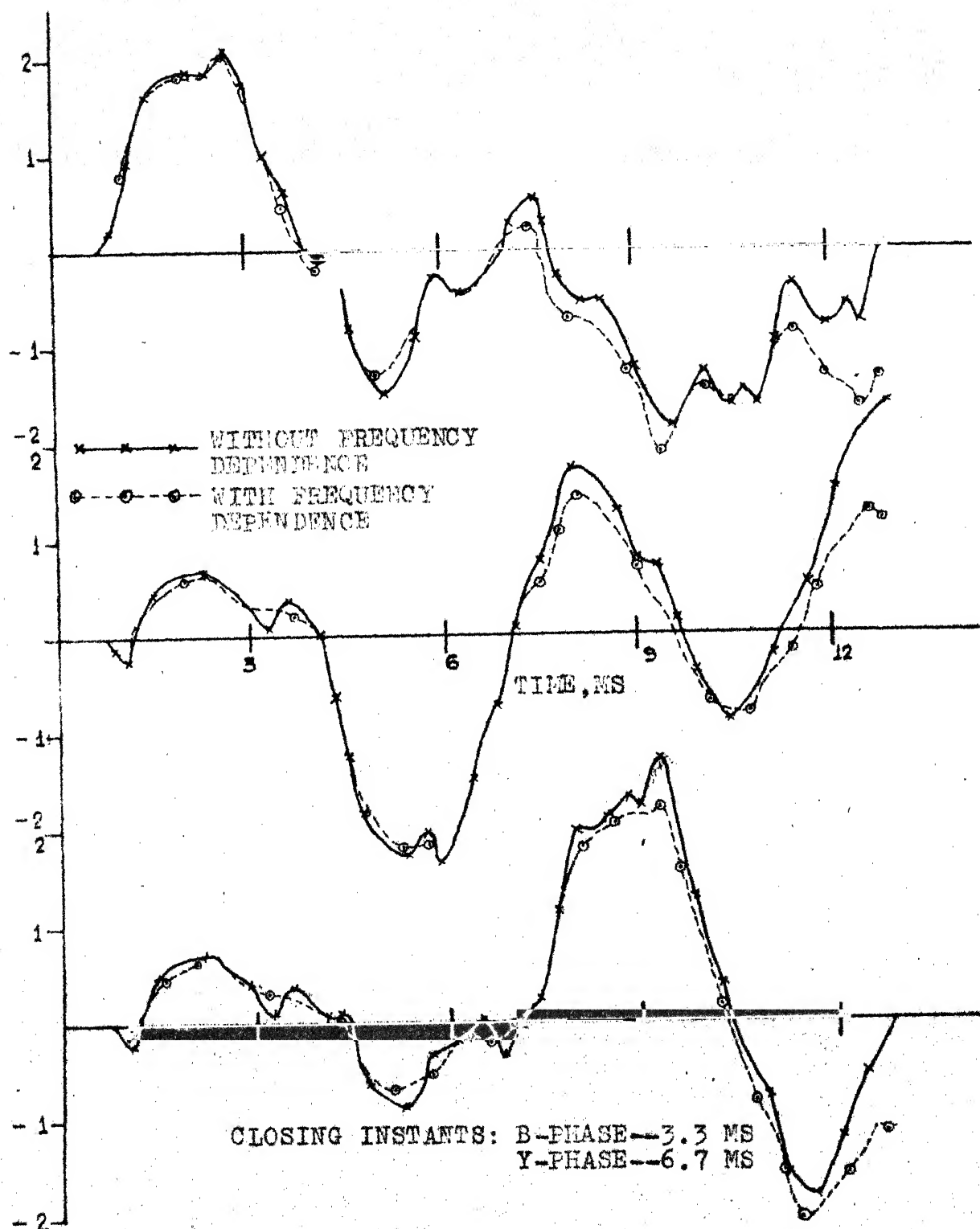


FIGURE 7.4: EFFECT OF FREQUENCY DEPENDENCE OF LINE PARAMETERS ON SEQUENTIAL ENERGISATION TRANSIENTS OF A TRANSPOSED SINGLE CIRCUIT LINE.

when the first circuit is operating in steady state, is developed. Section 5.5 describes the method of calculating the transient due to the closing of the second circuit but for the simultaneous closing of the breaker poles only. For the energisation study, introducing the sequential closing feature also, the principle of superposition can be used, as shown in Section 5.5. But additionally here, the effect of induced voltages on the floating conductors prior to their energisation has to be considered. As described in Section 5.5, the procedure for calculating the second circuit energisation transient of a double circuit line involves

- (i) a steady state analysis, assuming the second circuit to remain unenergised and
- (ii) the determination of the transient response of the line for a known set of sending end voltage conditions.

It has been shown in Section 5.5.1 that for the case of a transposed double circuit line, the induced voltages on the unenergised conductors, obtained in the above mentioned steady state analysis (step i) will be negligible. Hence the voltages to be injected at the sending end on the second circuit conductors, for which the transient response has to be calculated (in step ii) are the steady state values of voltages of the connected phases at the sending end of the first circuit. The voltages on the first circuit conductors at the sending end for the calculation of the above transient response are zero.

The procedure for the calculation of this transient response at the point of interest (in this case the voltage at the receiving end) on the double circuit line may be described by referring to Figure 7.5.

The general expressions for transformed voltage and current vectors at any point on a transmission line, subsequent to a switching operation, using the same notation as used early in this chapter, are given by

$$\underline{V} = [\text{Cosh} \psi x] \underline{K} + [\text{Sinh} \psi x] \underline{M} \quad (7.10)$$

$$\underline{I} = -[Z]^{-1} [\psi] \{ [\text{Cosh} \psi x] \underline{M} + [\text{Sinh} \psi x] \underline{K} \} \quad (7.11)$$

where  $\underline{K}$  and  $\underline{M}$  are constants, determined by the boundary conditions, existing at the ends of the line.

In the interval  $0 < t < T_1$ , only the first phase of the second circuit is closed. Hence in this interval, the voltage on the first phase alone gets the value of the injected voltage and the other conditions, to be forced at the sending end are zero currents on the two unenergised conductors of the second circuit, in addition to the zero voltage conditions on the first circuit conductors.

By forcing the known voltage conditions at the sending end, the first four components of  $\underline{K}$  in equation (7.10) are determined as follows:

$$K_1 = 0 \quad ; \quad K_2 = 0 \quad ; \quad K_3 = 0 \quad (7.12)$$

$K_4 = E_{s1}$ , the modified Fourier transform of the voltage injected to the first phase of the second circuit.

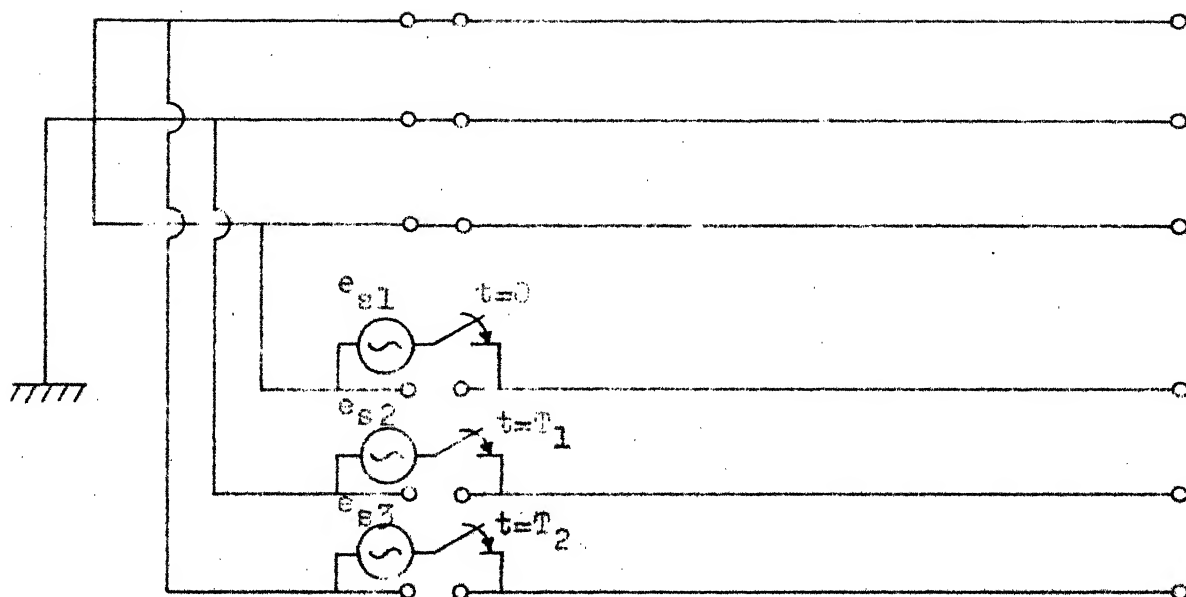


FIGURE 7.5: SYSTEM DIAGRAM FOR CALCULATION OF TRANSIENT RESPONSE FOR INJECTED VOLTAGE - SEQUENTIAL CLOSING.



Denoting the elements of matrices by double subscripted lower case letters and the matrix  $[Z]^{-1}[\psi]$  by  $[U]$ , forcing of the zero current conditions on the two unenergised phases of the second circuit, make equation (7.11) take the form

$$- \begin{bmatrix} u(5,1) & u(5,2) & \dots & u(5,6) \\ u(6,1) & u(6,2) & \dots & u(6,6) \end{bmatrix} \begin{bmatrix} M_1 \\ M_2 \\ \vdots \\ M_6 \end{bmatrix} = \begin{bmatrix} 0 \\ 0 \end{bmatrix} \quad (7.13)$$

The open receiving end condition gives rise to another equation

$$\underline{M} = -[\text{Tanh} \psi l] \underline{K} \quad (7.14)$$

Replacing  $\underline{M}$  in (7.13) by (7.14), we get

$$\begin{bmatrix} u(5,1) & u(5,2) & \dots & u(5,6) \\ u(6,1) & u(6,2) & \dots & u(6,6) \end{bmatrix} [\text{Tanh} \psi l] \underline{K} = \begin{bmatrix} 0 \\ 0 \end{bmatrix} \quad (7.15)$$

Denoting

$$\begin{bmatrix} u(5,1) & u(5,2) & \dots & u(5,6) \\ u(6,1) & u(6,2) & \dots & u(6,6) \end{bmatrix} [\text{Tanh} \psi l] \text{ by } [UT]$$

and substituting for known components of  $\underline{K}$  by equation (7.12), (7.15) becomes

$$\begin{bmatrix} ut(1,1) & ut(1,2) & \dots & ut(1,6) \\ ut(2,1) & ut(2,2) & \dots & ut(2,6) \end{bmatrix} \begin{bmatrix} 0 \\ E_{s1} \\ K_4 \\ K_5 \end{bmatrix} = \begin{bmatrix} 0 \\ 0 \end{bmatrix} \quad (7.16)$$

where  $\underline{Q} = \begin{bmatrix} 0 \\ 0 \\ 0 \end{bmatrix}$

From (7.16),  $K_4$  and  $K_5$  can be expressed in terms of known quantities as follows:

$$\begin{bmatrix} K_4 \\ K_5 \end{bmatrix} = - \begin{bmatrix} \underline{ut}(1,5) & \underline{ut}(1,6) \\ \underline{ut}(2,5) & \underline{ut}(2,6) \end{bmatrix}^{-1} \begin{bmatrix} \underline{ut}(1,4) \\ \underline{ut}(2,4) \end{bmatrix} E_{sl} \quad (7.17)$$

$K_4$  and  $K_5$  are nothing but the transforms of the induced voltages at the sending end on the second and third phases of the second circuit.

These transforms of the induced voltages on the floating conductors are to be transferred to time domain by performing the numerical integration. For continuing the calculations, when the second and the third poles get closed, a numerically evaluated modified Fourier transform of these induced voltages on these floating conductors during the interval when they are open should be added to the analytically known transforms of the second and third phase injected voltages of the second circuit, which come into the calculations from instants  $T_1$  and  $T_2$  respectively.

At the instant  $T_1$ , the second pole gets closed and now the conditions to be forced at the sending end are known voltages on first and second phase conductors and zero current on the third unenergised phase conductor of the

second circuit, in addition to zero voltage conditions on the three phases of the first circuit.

The known transformed voltages at the sending end determine the first five components of the vector  $\underline{K}$  now as follows:

$$\begin{aligned} K_1 &= 0 ; \quad K_2 = 0 ; \quad K_3 = 0 ; \quad K_4 = E_{s1} \\ K_5 &= E_{s2} + V_{s2} \end{aligned} \quad (7.18)$$

where  $E_{s2}$  is the analytically known modified Fourier transform of the injected voltage on the second phase of the second circuit (which starts from instant  $T_1$ ) and  $V_{s2}$  is the numerically evaluated modified Fourier transform of the induced voltage on the second phase of the second circuit in the interval  $0 < t < T_1$ .

The zero current condition on the third phase of the second circuit gives rise to the equation

$$[ut(1,1) \quad ut(1,2) \quad \dots \quad ut(1,6)] \begin{bmatrix} \underline{0} \\ E_{s1} \\ (E_{s2} + V_{s2}) \\ K_6 \end{bmatrix} = 0 \quad (7.19)$$

where  $[UT]$  is the same as used earlier and

$$\underline{0} = \begin{bmatrix} 0 \\ 0 \\ 0 \end{bmatrix}$$

From equation (7.19), the unknown  $K_6$  can be expressed in terms of known quantities as follows:

$$K_6 = -[ut(1,4) E_{s1} + ut(1,5)(E_{s2} + V_{s2})]/ut(1,6) \quad (7.20)$$

$K_6$  so obtained is the transform of the induced voltage on the third phase of the second circuit, valid in the time interval  $0 < t < T_2$ . The addition of the numerically evaluated modified Fourier transform of this induced voltage in this interval to the analytically known transform of the third phase injected voltage is essential for carrying on the transient calculations after the instant  $T_2$ .

At instant  $T_2$ , the third pole closes and now the transformed voltages on all the phases at the sending end, valid in the entire time range are known.

Hence for the open receiving end condition, an expression for the transformed voltage at the receiving end can be derived using the general expressions (7.10) and (7.11) as follows:

$$\underline{V}_R = [\text{Sech}\psi l] \underline{V}_S$$

where  $\underline{V}_S$  is the known transformed voltage vector at the sending end.

A numerical integration of this transformed voltage  $\underline{V}_R$  to time domain gives the desired transient response.

This transient response, when added to the steady state response, calculated assuming the second circuit to be unenergised, yields the total response.

## 7.7 COMPUTATIONAL RESULTS

### 7.7.1 Double Circuit Versus Single Circuit Lines:

The same double circuit line example, considered in Chapters 5 and 6 is taken up and the transient overvoltage at the open receiving end, resulting from the sequential closing of circuit breaker poles is evaluated by the procedure described in the last section. Next the presence of the first circuit is ignored and the receiving end transient voltage, resulting due to the injection of the steady state voltage, calculated at the sending end of the first circuit in the steady state analysis, is computed. The line is assumed to be transposed and the closing instants of the phases are taken to be 0, 3.3 and 6.7 m.secs. for both the cases. The phase sequence of breaker pole closing is assumed to be R'B'Y'. The 50 Hz parameters of the line are used in the calculations. The open receiving end voltage waveforms for the single and double circuit representations are compared in Figure 7.6. A maximum peak of 2.505 p.u. is observed to occur on phase Y' at 8.3 m.secs. for the case of double circuit representation; whereas the maximum peak for the case of single circuit representation is -2.9 p.u. on phase B' at 4.8 m.secs. Noticing the wide variation in the voltage

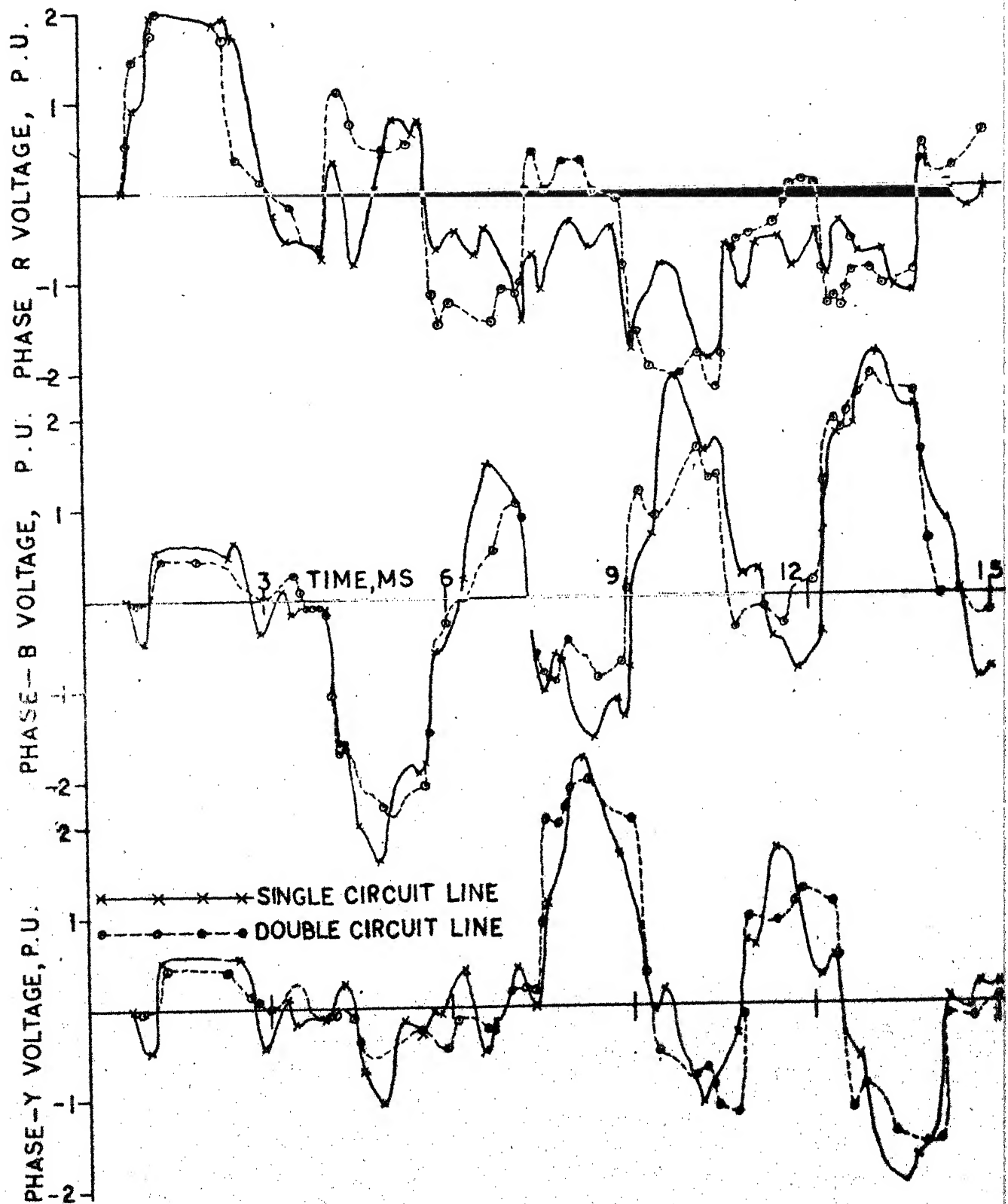


FIGURE 7.6: COMPARISON OF VOLTAGE WAVEFORMS AT RECEIVING END FOLLOWING SEQUENTIAL CLOSING FOR TRANSPOSED SINGLE AND DOUBLE CIRCUIT LINES.

waveforms and in the maximum peak values (about 16 percent difference) of both the cases, it may be concluded that the double circuit modelling is essential for the energisation transient study.

#### 7.7.2 Transposed Versus Untransposed Double Circuit Lines:

Next the energisation transient of the same example for the untransposed configuration of the line is evaluated. The eigenvalue, eigenvector analysis at each frequency in the integration range is performed for the double circuit line to arrive at the modal transformation matrix for using in these calculations. The voltage waveforms at the open receiving end for the transposed and untransposed configurations of the line are compared in Figure 7.7. Considerable difference in waveshapes is observed for the two configurations as there are six distinct modes and velocities of propagation for the case of untransposed line, whereas for the transposed line there are only three such distinct modes and velocities of propagation. A maximum peak voltage of 2.505 p.u. is observed to occur on phase Y' at 8.3 m.secs. for the transposed line. The maximum peak for the untransposed line is -2.46 p.u. and it occurs on phase B' at 4.95 m.secs.

#### 7.7.3 Effect of Frequency Dependence of Line Parameters:

The effect of continuous variation of line parameter values with frequency on the transient overvoltage waveforms

PHASE-F VOLTAGE, P.U.

PHASE-B VOLTAGE, P.U.

PHASE-Y VOLTAGE, P.U.

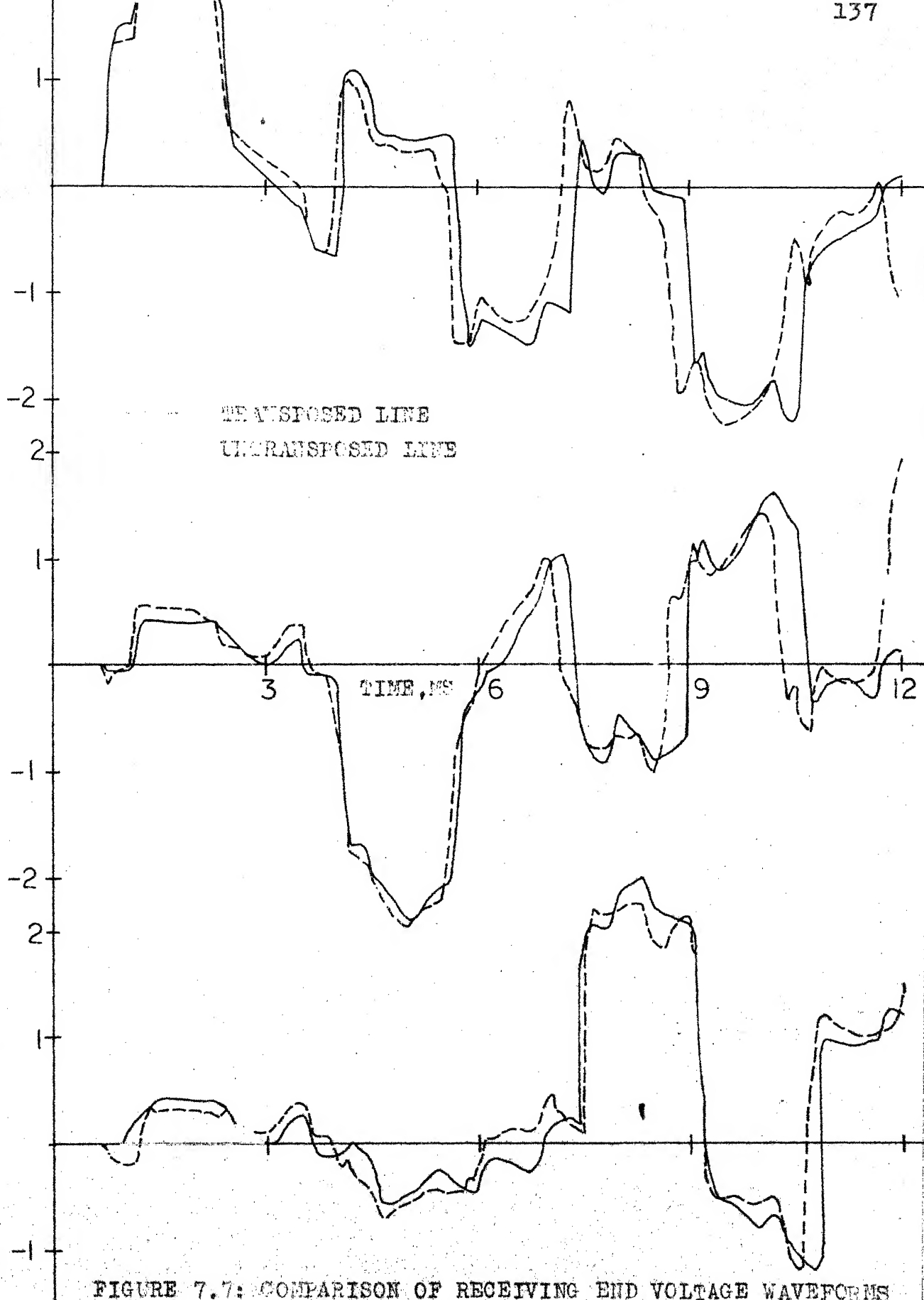


FIGURE 7.7: COMPARISON OF RECEIVING END VOLTAGE WAVEFORMS FOLLOWING SEQUENTIAL CLOSING FOR TRANSPOSED AND UNTRANSPOSED LINES.



due to sequential closing of transposed and untransposed double circuit lines is next examined. The line parameters, calculated at each frequency using Carson's formulae are used in the calculations. The resulting transient voltage waveforms at the open receiving end for the same example, with and without frequency dependence of line parameters incorporated for transposed and untransposed lines are compared in Figures 7.8 and 7.9 respectively. Again the closing instants of the phases are assumed to be 0, 3.3, 6.7 m.secs. The phase sequence of closing is taken as R'B'Y'. For the transposed configuration of the line, without considering the frequency dependence of line parameters, the maximum peak overvoltage (2.505 p.u.) occurs on phase Y' at 8.3 m.secs. When the frequency dependence of line parameters is considered the maximum peak value reduces to 2.21 p.u. (about 14 percent reduction) and this occurs at 8.1 m.secs. on phase Y'. The corresponding peak values for the untransposed configuration of the line without and with frequency dependence of line parameters, incorporated, are -2.46 p.u. (on phase B' at 4.95 m.secs.) and -2.28 p.u. (on phase B' at 4.95 m.secs.) respectively. There is also a smoothening of oscillations in the waveforms when frequency dependence of line parameters is included for both the configurations of the line.

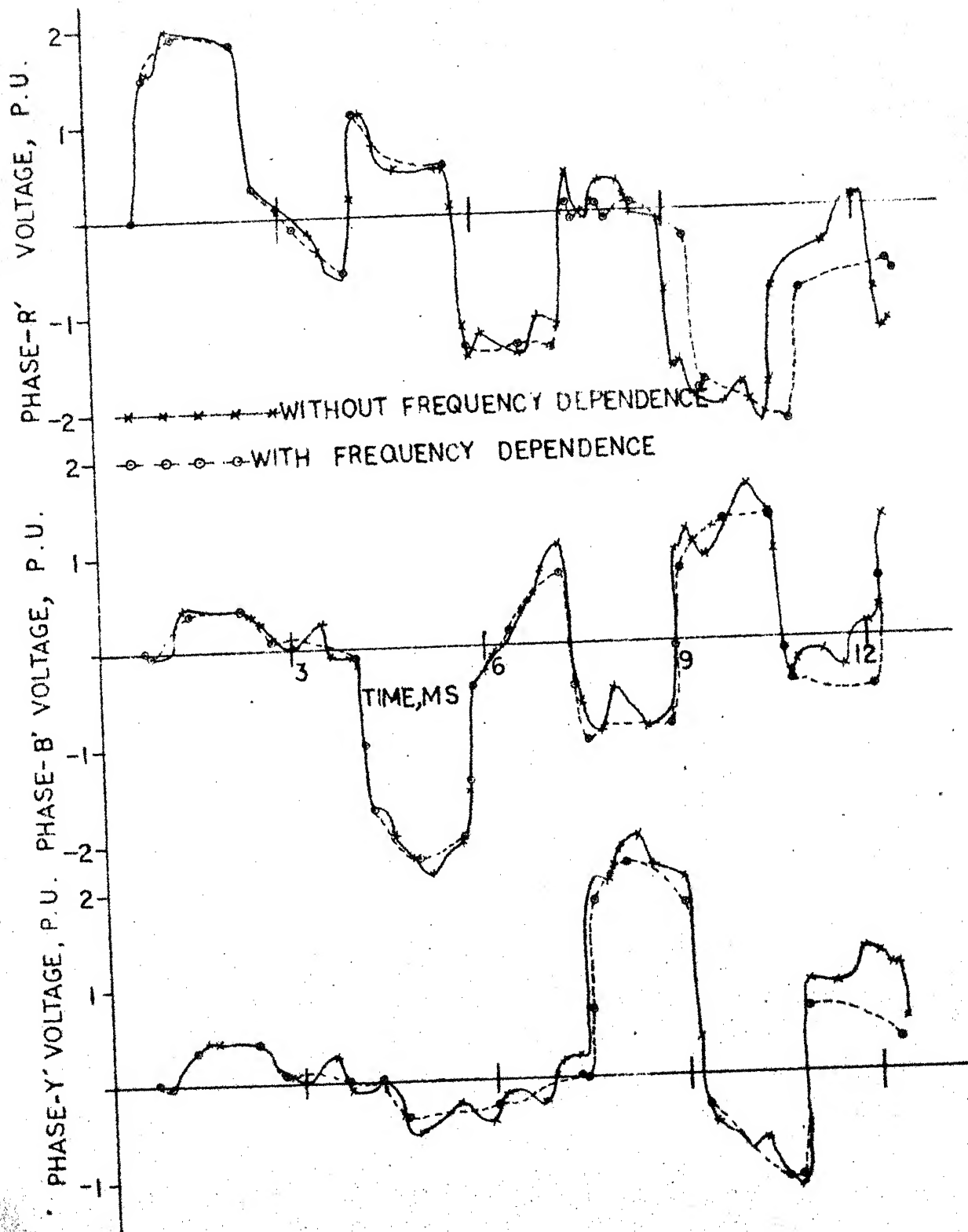


FIGURE 7.8: EFFECT OF FREQUENCY DEPENDENCE OF LINE PARAMETERS ON VOLTAGE TRANSIENTS DUE TO SEQUENTIAL CLOSING FOR TRANSPOSED DOUBLE CIRCUIT LINE.

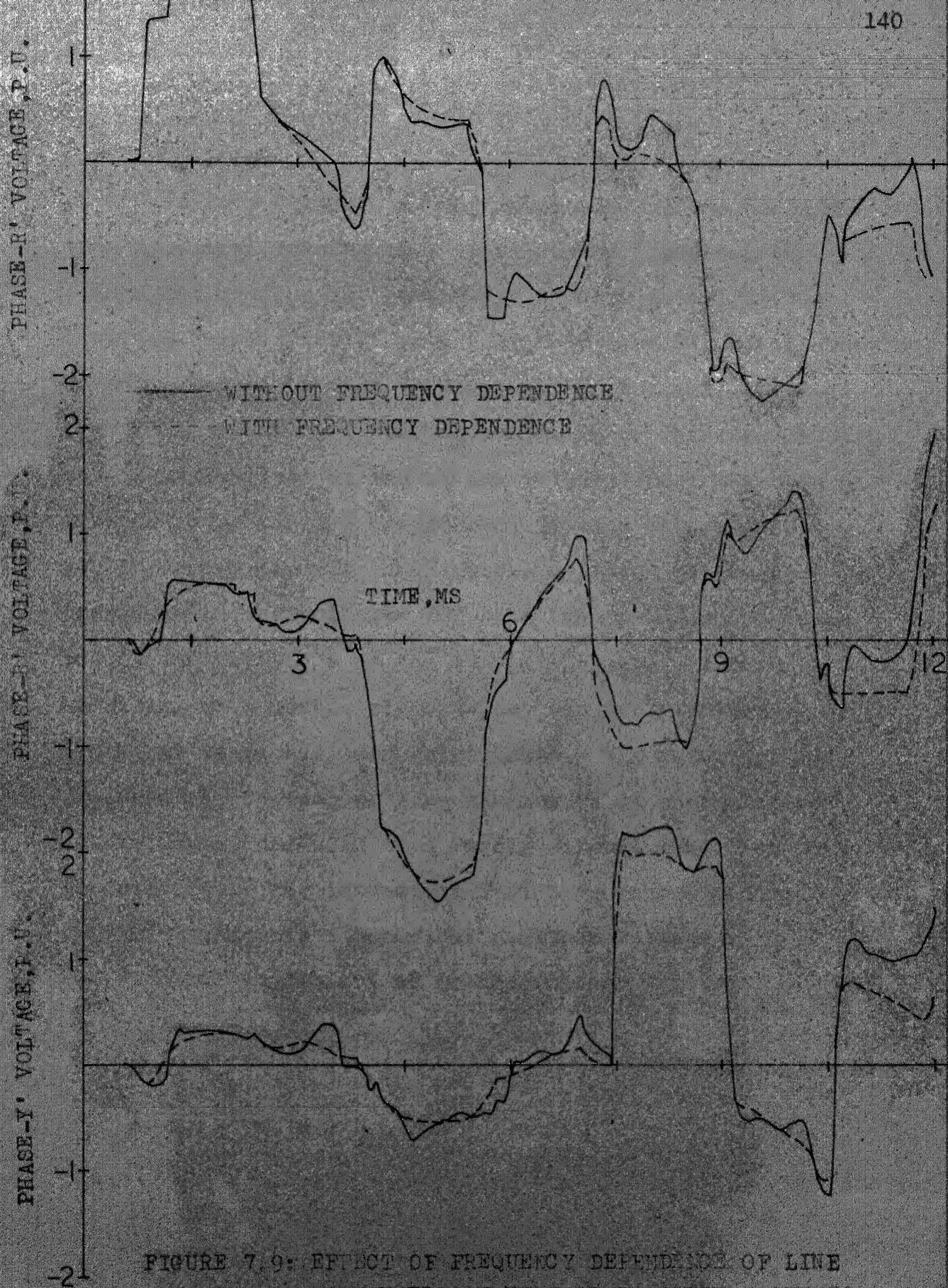


FIGURE 7.9: EFFECT OF FREQUENCY DEPENDENCE OF LINE PARAMETERS ON VOLTAGE TRANSIENTS DUE TO SEQUENTIAL CLOSING FOR UNTRANSPOSED DOUBLE CIRCUIT LINE.

## 7.8 CONCLUSIONS

In this chapter, a program to compute the energisation transient arising on a transmission line, due to sequential closing of the circuit breaker poles, by the modified Fourier transform method, has been described. The method, first developed by Wedepohl and Mohamed, using numerically evaluated Fourier transform of induced voltages on the unenergised phases in the calculations, has been extended here for the double circuit line case. A typical 400 KV double circuit line example has been studied for energisation overvoltages for both transposed and untransposed configurations of the line. The need for the modelling of a double circuit line for energisation transient study has been established. The effect of frequency dependence of line parameters on energisation overvoltages, produced on a double circuit line, has been investigated. The introduction of frequency dependence of line parameters reduces the peak overvoltage and smoothens the oscillations in the voltage waveforms.

## CHAPTER 8

### SUMMARY AND CONCLUSIONS

#### 8.1 CONCLUSIONS

8.1.1 : The study of electrical transients on EHV power systems has gained great importance, particularly in view of the increasing operating voltage of the transmission systems. The cost of insulation forms a major portion of the total cost of a transmission system. Especially as the system voltage increases to EHV level, the insulation cost of the line increases at a very rapid rate. While doing these planning studies, if the models of the transmission line and other equipments that are employed in the transient calculations are not very accurate, it is necessary to use a high factor of safety to take care of the likelihood of the consequent margin of error in the calculated values. This ultimately reflects in higher cost of insulation. If this factor of safety and insulation costs are to be reduced, it can be done only if the calculated results predict the system performance with a high degree of accuracy. To achieve this, it is necessary to employ accurate models for all the components of a **system** while doing the required studies.

Double circuit lines are common features of any power system. However, digital calculation of transients on double circuit lines have not been reported. Nevertheless a few TNA studies for double circuit lines have been reported

as acknowledged in Section 5.1. An accurate mathematical model of a double circuit line suitable for studying the electrical transients arising on it has been proposed in this thesis. Further, this model is made use of to study the energisation and fault transients on a typical 400 KV double circuit line. This illustrates the use of the above method and also shows that it is essential to represent the double circuit lines adequately in any transient studies.

There are various methods of calculating the over-voltage transients that are available in the literature. These methods and their special features are discussed in Chapter 1. Among these, the modified Fourier transform method is regarded as one of the more accurate methods, because it considers all the line parameters to be distributed, can incorporate the effect of frequency dependence of line parameters with ease and can also handle untransposed lines. Therefore the proposed model in this thesis largely refers to the modified Fourier transform method. In one of the chapters, it has also been applied to Uram and Miller's method. Similarly, it can be extended to other methods, if desired.

8.1.2: A mathematical model of a double circuit line, suitable for transient overvoltage studies has been developed in Chapter 3. It has been shown in Section 3.2.1

that there exists a constant modal transformation matrix for the case of a transposed double circuit line, whose conductors are situated at a mirror symmetric position with respect to a vertical plane. This transformation holds good at each frequency in the numerical integration range. Thus, for calculations of switching overvoltages involving transposed double circuit lines considerable saving in computation time can be achieved. On the other hand, in the case of untransposed double circuit lines, the eigenvalue, eigenvector analyses of two  $3 \times 3$  matrices are to be performed, at each frequency, to arrive at the modal transformation matrix.

8.1.3: The transient overvoltages, arising on the sound phases of a double circuit line due to the initiation of a single line to ground fault on one of the circuits, have been studied in Chapter 4. Necessity for the study of the transients due to the initiation and clearing of fault in a system arises when effective methods are adopted for controlling the overvoltages, caused by energisation and re-energisation of the line. At present, as there are very effective methods, such as multistep resistance closing, controlling the closing instants of the individual poles of the circuit breaker etc. available to limit the energisation and re-energisation overvoltages, the fault initiation and clearing transients may dominate the scene. These fault transients have been studied by various



authors in the past for single circuit lines using various digital methods. However, an accurate analysis of these fault transients on double circuit lines has not been reported. Moreover, in all the above studies, the lines were assumed to be transposed and the frequency dependence of line parameters have not been taken into account since they used lattice diagram or Laplace transform approach. In this thesis the modified Fourier transform method has been employed for these studies. Further, this has also been extended to the double circuit line model that has been proposed. A typical 400 KV double circuit line example has been considered. The transient voltage waveforms on the sound phases, following a single line to ground fault at mid span on the line, have been computed for both the transposed and untransposed configurations of the line. As shown in Figure 4.5, the maximum peak voltage in the case of untransposed line is observed to be nearly 10 percent higher than that of the transposed case.

In the above set up the presence of the second circuit is ignored for calculation of the same transients, thus representing a single circuit line. In this case fault is considered on one of the phases and the resulting transients on the remaining sound phases are evaluated. The voltage waveforms on the sound phases at the fault point for the double and single circuit representations have been shown



in Figure 4.4. The voltage waveforms for the case of the double circuit line clearly exhibit more high frequency oscillations than those for the case of the single circuit line. This seems to be due to the fact that there are three distinct modes of propagation with three distinct velocities of propagation in the case of transposed double circuit line; whereas for the case of a transposed single circuit line, there are only two such distinct modes and velocities of propagation. A maximum peak of  $-1.78$  p.u. is observed to occur on phase-c' of the second circuit for the double circuit line representation. For the single circuit line, the maximum peak of  $-1.98$  p.u. (10 percent more) occurs on phase-c. This order of difference between the peak voltages for the single and double circuit representations shows that it is important to represent the double circuit line adequately. The effect of frequency dependence of line parameters on the fault transient overvoltages for both the transposed and untransposed configurations of the transmission line has also been investigated as shown in Section 4.6.3. The inclusion of the frequency dependence of line parameters is observed to reduce the maximum peak voltage by nearly 11 percent and 13 percent (see Figures 4.6 and 4.7) for the cases of transposed and untransposed lines respectively. There is also a smoothening of oscillations in the transient voltage waveforms when frequency dependence is included in

the calculations. The fault transients have been evaluated for various off-centre fault locations as shown in Table 4.2. The mid span fault is found to give rise to the maximum peak overvoltage.

8.1.4: The modified Fourier transform method has been applied to analyse the energising transients on double circuit lines in Chapter 5. Algorithms have been developed to study the transients due to the closing of the first circuit with the second circuit unenergised, as well as for the transients due to the closing of the second circuit when the first circuit is operating in steady state. Here all the three poles of the circuit breaker are assumed to close simultaneously during energisation. A typical 400 KV double circuit line, open at the receiving end has been considered and both the above mentioned energising transients at the receiving end have been calculated. The energising transient for the double circuit line representation has been compared with the transient caused by the energisation of the corresponding single circuit line (ignoring the presence of the other circuit). For the untransposed configuration of the line, a difference of 20 percent in the peak transient voltages is observed for the single and double circuit representations (Figure 5.6). Apart from such a considerable difference in peak overvoltages, the voltage waveforms for these two representations also differ widely in shape. This may be attributed to the reason that in the case of

untransposed double circuit lines there are six distinct modes and velocities of propagation; whereas there are only three such distinct modes and velocities of propagation in the case of untransposed single circuit lines.

The effect of inclusion of the frequency dependence of line parameters is observed to be insignificant for the case of the simultaneous closing of the breaker poles. This appears to be due to the absence of the zero sequence currents for simultaneous closing of the circuit breaker poles and only the zero sequence components of the resistance and inductance of the line (ground return path taken into account) vary considerably with frequency.

8.1.5: In Chapter 6, the Uram and Miller's method has been extended to study the energising transients on double circuit lines. Uram and Miller's method is a time domain method, in which by making some assumptions, an incremental solution of the transmission line equations is made possible. The existence of a frequency independent modal transformation matrix is necessary for the application of this method. Such a transformation is shown to exist for the transposed double circuit line in Section 3.2.1. The same double circuit line example as in Chapter 5 has been considered. The transients at the open receiving end, following the energisation of the first circuit with the second circuit unenergised as well as that due to the closing of the second circuit when the first circuit is

operating in steady state have been computed. The results obtained by this method are found to be closely matching with those obtained using the modified Fourier transform method. This serves as an important check on the validity and accuracy of the method proposed here as well as the two computer programs developed for this purpose. The Uram and Miller's method takes much less computer time but can handle only transposed lines and cannot take into account the frequency dependence of line parameters directly.

8.1.6: So far in all the studies all the three poles of a circuit breaker are assumed to operate simultaneously. However, in reality, there may be a difference of a few m.secs. in the operation of different poles of the circuit breaker. The incorporation of the nonsimultaneous closing feature of the circuit breaker poles in the modified Fourier transform method of calculating energisation transients has been described in Chapter 7. The method has been extended to evaluate the transient arising due to sequential energisation of the second circuit of a double circuit line when the first circuit is operating in steady state. The same 400 KV double circuit line example as of Chapters 5 and 6 has been studied. When the sequential closing of the breaker poles is incorporated in the study, for the transposed configuration of the line, the peak voltage is 16 percent lower in the case of a double circuit line as compared to that of the corresponding single circuit line (Figure 7.6).

It may be noted here that there was no difference in the peak values for transposed single and double circuit lines when the breaker poles are assumed to close simultaneously (see Section 5.6.2). The need for the modelling of the double circuit line has been established by comparing the transient arising on the second circuit obtained by ignoring the presence of the first circuit with that obtained by the double circuit representation.

The transient voltages at the receiving end following sequential closing for the transposed and untransposed configurations of the double circuit lines have been studied. A considerable difference in wave-shapes has been observed for the two configurations as shown in Figure 7.7.

The effect of inclusion of frequency dependence of line parameters on the transient overvoltages arising on the double circuit line following sequential closing has also been investigated. The introduction of the frequency dependence of line parameters is observed to reduce peak overvoltages by 14 percent and 8 percent for the transposed and untransposed configurations of the line respectively for the example considered. There is also a smoothening of oscillations in the voltage waveforms.

In this thesis, the transient arising due to re-energisation of a double circuit line on trapped charges

has not been considered. However, the method is general enough and this aspect may be studied in future. In the various examples considered in this thesis the source sides have been represented by lumped impedances. The values of these source impedances have been derived from the system short circuit levels. This simplified model for the source is somewhat approximate. However, here the aim is just to illustrate the application of the modified Fourier transform method for transient analysis on double circuit lines and hence source sides have not been rigorously represented. However, there is no limitation for the applicability of the method proposed here for a detailed source representation. The other lines terminating at the ends of the line under consideration, can be represented quite accurately by shunt elements at these buses, the values of which can be obtained by finding out the equivalent admittances offered by these lines at these buses, taking into consideration the distributed nature of these lines and the terminal conditions existing at the remote ends of these lines.

In addition to the above the following suggestions are made for future extension of this work.

1. Computation of transient arising due to the re-energisation of a double circuit line on trapped charge.

2. Fault clearing overvoltages and transient recovery voltages evaluation for a system consisting of double circuit lines.
3. Development of a general purpose program, using modified Fourier transform method to accommodate general source side network.
4. Studies of transients in systems, consisting of non-linearities such as transformer saturation, lightning arresters etc. using modified Fourier transform method for the line.
5. Studies of overvoltage transients on double circuit lines with series capacitor compensation.

## 8.2 SUMMARY

We have seen that in the case of a typical 400 KV line, considerable difference in calculated results is obtained when the line is represented by a single circuit or a double circuit model. In particular, the following results are very significant.

1. The maximum peak overvoltage arising on sound phases following a single line to ground fault for the transposed double circuit representation is -1.78 p.u. The corresponding maximum peak for the transposed single circuit representation is -1.98 p.u.
2. For the transposed configuration of the double circuit line, maximum peak voltage due to fault initiation is -1.78 p.u. For the untransposed configuration, the corresponding maximum peak is -1.97 p.u.

3. When frequency dependence of line parameters is considered, the maximum peak voltage due to fault initiation reduces by 11 percent and 13 percent for the transposed and untransposed configurations of the double circuit line respectively.
4. The maximum peak voltage due to simultaneous breaker pole closing of the first circuit of a transposed double circuit line is -2.45 p.u. and occurs on phase-a at 9.2 m.secs. The corresponding maximum peak for the untransposed double circuit line is 2.24 p.u. and this occurs on phase-c at 12.8 m.secs.
5. The maximum peak voltage due to simultaneous breaker pole closing of the second circuit of the transposed double circuit line is 2.02 p.u. and occurs on phase a' at 1.02 m.secs. The corresponding maximum peak for the case of untransposed double circuit line is 2.23 p.u. and occurs on phase a' at 0.9 m.secs.
6. With sequential closing of circuit breaker poles incorporated, the maximum peak voltage due to second circuit energisation for transposed double circuit line is 2.505 p.u. and occurs on phase Y' at 8.3 m.secs. The maximum peak value for the corresponding single circuit line is -2.9 p.u. and occurs on phase B' at 4.8 m.secs.
7. A maximum peak voltage of 2.505 p.u. is observed to occur on phase Y' at 8.3 m.secs. for sequential second



circuit energisation of the transposed double circuit line; whereas the corresponding maximum peak for untransposed double circuit line is -2.46 p.u. on phase B' at 4.95 m.secs.

8. Reduction in peak values of 14 percent and 8 percent is observed in the transients due to second circuit sequential energisation for transposed and untransposed double circuit lines respectively, when frequency dependence of line parameters is considered.

The order of magnitude of the error in the above cases is such that it appears vital to consider the following while doing any transient studies.

- a. Double circuit lines should be represented adequately.
- b. Transposition of the lines or otherwise, should be taken into account.
- c. Frequency dependence of line parameters can be ignored only when it is justified specifically.
- d. Non-simultaneous operation of the circuit breaker poles should be considered in these calculations.

In the opinion of the author, optimum costs of insulation of a transmission line can be achieved only when all the above factors are taken into account. These have been implemented in the computer programmes developed by the author and therefore the above suggestions are quite feasible. The validity of these suggestions is well borne out by the study of a typical 400 KV line that has been

carried out throughout. In particular power systems, the errors due to the various approximations may be even higher than those reported here. Therefore, the importance of accurate representation of the components of the system in transient calculations cannot be under emphasised. Methods to incorporate all the above suggestions have been successfully implemented in the procedures proposed in this thesis.

## LIST OF REFERENCES

1. L.V. Bewley, Travelling waves on transmission lines, (Book) Dover Publications (1963).
2. L.O. Barthold and G.K.Carter, 'Digital travelling wave solutions', AIEE Trans. on Power Apparatus and Systems, Vol.80, pp. 812-820, 1961.
3. J.P. Bickford and P.S.Doepal, 'Calculation of switching transients with particular reference to line energisation', Proc. IEE, Vol.114, No.4, pp. 465-477, April 1967.
4. R. Uram and R.W. Miller, 'Mathematical analysis and solution of transmission line transients I - Theory', IEEE Trans.on Power Apparatus and Systems, Vol.PAS-83, pp. 1116-1123, 1964.
5. R.Uram and W.E.Feero, 'Mathematical analysis and solution of transmission line transients II - Applications', IEEE Trans. on Power Apparatus and Systems, Vol.PAS-83, pp. 1123-1137, 1964.
6. S.J.Day, N. Mullineux and J.R. Reed, 'Developments in obtaining transient response using Fourier transform Pt.I - Gibb's phenomena and Fourier integral', Int. J. Elec.Engng. Educ.,Vol.3, pp. 501-506, 1965.
7. S.J.Day, N. Mullineux and J.R. Reed, 'Developments in obtaining transient response using Fourier transforms Pt.II - Use of modified Fourier transforms', Int. J. Elec. Engng. Educ., Vol.4, pp. 31-40, 1966.
8. S.J.Day, N. Mullineux and J. R. Reed, 'Developments in obtaining transient response, using Fourier transforms Pt.III - Global response', Int. J. Elec. Engng. Educ., Vol.6, pp. 259-265, 1968.
9. M.J.Battison, S.J.Day, K.G.Parton, N. Mullineux and J.R. Reed, 'Calculation of switching phenomena in power systems', Proc. IEE, Vol.114, No.4, pp. 478-486, April 1967.

10. L.M.Wedepohl and S.E.T. Mohamed, 'Multiconductor transmission lines theory of natural modes and Fourier integral applied to transient analysis', Proc. IEE, Vol.116, No.9, pp. 1553-1563, Sept. 1969.
11. H.W.Dommel, 'A method for solving transient response phenomena in multiphase systems', PSCC Proceedings, Pt.3, 2nd Power Systems Computations Conference, report 5.8, 1966.
12. H.W.Dommel, 'Digital computer solution of electromagnetic transients in single and multiphase networks', IEEE Trans. on Power Apparatus and Systems, Vol.PAS-88, pp. 388-400, April 1969.
13. P.L. Arlett and R. Murray - Shelley, 'The use of graphical method for solution of transients on simple symmetrical 3 phase systems', Int. J. Elec.Engng. Educ., Vol.5, pp. 377-388, 1967.
14. P.L. Arlett and R. Murray - Shelley, 'The study of over-voltages transients in large systems', PSCC Proceedings, Pt.3, 2nd Power Systems Computation Conference, report 5.6, 1966.
15. E.W.Stafford, D.J.Evans and N.G. Hingorani, 'Calculation of travelling waves on transmission lines by finite differences', Proc. IEE, Vol.112, pp. 941-947, 1965.
16. R. Raghavan, 'Digital calculation of transient phenomena in EHV power systems', Ph.D. thesis, I.I.T. Kanpur, August 1971.
17. R. Raghavan and V.R.Sastry, 'Digital Calculation of Transient phenomena in EHV systems', IEEE Trans. on Power Apparatus and Systems, Vol.PAS-90, Sept./Oct. 1971.
18. Electrical Transmission and Distribution Reference Book - Westinghouse Electric Corporation, 1950.
19. D.H.Welle, R.A. Hedin, L.A. Burkhard, C.H. Thomas, A.E.Kilgour and W.R.Lund, 'Parallel EHV untransposed transmission lines, studied for overvoltages due to switching surges and resonance', IEEE Trans. on Power Apparatus and Systems, Vol.PAS-91, pp. 190-194, 1972.

20. L.M. Wedepohl, 'Application of matrix methods to the solution of travelling wave phenomena in polyphase systems', Proc. IEE, Vol.110(2), pp. 2200-2212, 1963.
21. J. Grad and M.A. Brebner, 'Eigenvalues and eigenvectors of a general matrix', Communications of the ACM, Vol.11, pp. 820-825, 1968.
22. E.W. Kimbark and A.C. Legate, 'Fault surge versus switching surge - A study of transient overvoltages caused by line to ground faults', IEEE Trans. on Power Apparatus and Systems, Vol.PAS-87, pp. 1762-1769, 1968.
23. A. Clerici and A. Taschini, 'Overvoltages due to line energisation and re-energisation versus overvoltages caused by faults and fault clearing in EHV systems', IEEE Trans. on Power Apparatus and Systems, Vol.PAS-89, pp. 932-941, 1970.
24. R.G. Colclaser, C.L. Wagner and D.E. Buettner, 'Transient overvoltages caused by the initiation and clearance of faults on a 1100 KV system', IEEE Trans. on Power Apparatus and Systems, Vol.PAS-89, pp. 1744-1751, 1970.
25. C. Boonyubol, C. Calabrese and J.R. Tudor, 'A mathematical analysis of transmission line transients related to fault surges', IEEE Trans. on Power Apparatus and Systems, Vol.PAS-89, pp. 1207-1215, 1970.
26. C.H. Thomas and R.A. Hedin, 'Switching surges on transmission lines by differential analyzer simulation', IEEE Trans. on Power Apparatus and Systems, Vol.PAS-88, pp. 636-645, 1969.
27. L.M. Wedepohl and S.E.T. Mohamed, 'Transient analysis of multiconductor transmission lines with special reference to nonlinear problems', Proc. IEE, Vol.117, No.5, pp. 979-988, May 1970.
28. M.J. Battisson, S.J. Day, N. Mullineux and J.R. Reed, 'Calculation of transients on transmission lines with sequential switching', Proc. IEE, Vol.117, No.3, pp. 587-590, March 1970.

29. M.J. Battison, S.J. Day, N. Mullineux, K. Parton and J.R. Reed, 'Some effects of the frequency dependent transmission line parameters', Proc.IEE, Vol.116, No.7, pp. 1209-1216, July 1969.
30. A.J. McElroy and R.M.Porter, 'Digital computer calculation of transients in electrical networks', IEEE Trans. on Power Apparatus and Systems, Vol.PAS-82, pp. 88-96, 1963.
31. H. Ishihara, 'Surge analysis by Digital computer', Elec. Engg. in Japan, JIEE, Vol.86, No.7, pp.62-71, July 1966.
32. W. Cheng, Analysis of Linear Systems (Book), Addison Wesley Publishing Company, Inc. (1959).
33. P.L. Arlett and R. Murray-Shelley, 'The teaching of travelling wave technique using an improved graphical method-I', Int.J. Elec.Engg. Educ., Vol.4, pp. 213-230, 1966.
34. P.L. Arlett and R. Murray-Shelley, 'The teaching of travelling wave technique using an improved graphical method-II', Int. J. Elec.Engng. Educ., Vol.4, pp. 327-349, 1966.
35. G.I. Attabekov, The Relay protection of high voltage networks (Book), Pergamon Press, 1960.
36. G. Holmdahl and R. Lundin, 'Digital solution of travelling wave problem in three phase systems', PSCC Proceedings, pt.3, 2nd Power System Computation Conference, report 5.12, 1966.
37. L. Paris, 'Basic considerations of magnitude reduction of switching surges due to line energisation', 31 PP 66-423, Presented at the IEEE Summer Power Meeting, New Orleans, La, July 10-15, 1966.
38. H.B. Thoren, 'Reduction of switching overvoltages in EHV and UHV systems', 70 TP 606, Presented at the IEEE Summer Power Meeting and EHV Conference, Los Angeles, Calif., July 12-17, 1970.
39. J.K.Dillard, J.M.Clayton and L.A.Kiler, 'Controlling switching surges on 1100 KV transmission systems', 70 TP 65 Paper presented at the IEEE Winter Power Meeting, New York, N.Y., Jan.26-30, 1970.

40. E.W.Boehne, 'Energisation surges in capacitive circuits',  
70 CP 235, presented at the IEEE Winter Power  
Meeting, New York, N.Y., Jan. 26-30, 1970.
41. P.A. Baltensperger and T. Djindjevic, 'Damping of  
switching overvoltages in EHV networks -  
New economic aspects and solutions', IEEE Trans.  
on Power Apparatus and Systems, Vol.PAS-89,  
No.7, pp. 1504-1512, Sept./Oct. 1970.
42. A.R. Hileman, P.R. Lablanc and G.W.Brown, 'Estimating the  
switching surge performance of transmission lines',  
IEEE Trans. on Power Apparatus and Systems,  
Vol.PAS-89, No.7, pp. 1455-1469, Sept./Oct. 1970.
43. J. Umoto and T. Hene, 'Numerical analysis of surge  
propagation on single conductor systems consi-  
dering corona losses', Elec.Engg. in Japan,  
(JIEE), Vol.89, No.5, pp. 21-28, May 1969.
44. R.G.Colclaser, L.E.Berkabile and D.E. Buettner, 'The  
effect of capacitors on the short line fault  
component of transient voltage', Presented at  
IEEE Winter Power Meeting 1970.
45. H. Sato, 'A digital method for determining inherent  
transient recovery voltages in power systems',  
IEEE Trans. on Power Apparatus and Systems,  
Vol.PAS-87, No.8, pp. 1706-1713, Aug. 1968.
46. A. Clerici and A. Tachini, 'Influence on switching surges  
of the switched line zero sequence impedance',  
Paper No. 70 TP 504, presented at the IEEE Summer  
Power Meeting and EHV Conference, Los Angeles,  
Calif., July 12-17, 1970.
47. K.R.Shah, C.Calabresse and J.R. Tudor, 'Determination of  
fault surge waveshaps with particular reference  
to fault detection', 70 TP 334, Presented at  
IEEE Summer Power Meeting and EHV Conference,  
Los Angeles, Calif., July 12-17, 1970.
48. Jean, A. Robert and Khuong Tran-Dunh, 'New digital  
simulation for ground mode switching surges  
response of EHV transmission systems', IEEE  
Trans. on Power Apparatus and Systems, Vol.PAS-88,  
No.5, pp. 597-603, May 1969.
49. G. Carrara, L. Dellera and G. Sartonio, 'Switching surges  
with very long fronts (above 1500  $\mu$ s): Effect of  
fault shape on discharge voltage', IEEE Trans.on  
Power Apparatus and Systems, Vol.PAS-89, No.3,  
pp. 453-456, March 1970.

50. H. Ishihara, 'Surge calculations in nonlinear circuits by analogue computer', Elec. Engng. in Japan, JIEE, Vol.86, No.2, pp. 39-46, Feb. 1966.
51. H.W.Dommel, 'Nonlinear and time varying elements in digital simulation of electromagnetic transients', Presented at the 1971 PICA conference held at New York in May 1971.
52. A.C. Legate, 'Comparison of field switching surge measurements with transient network analyser measurements', Presented at the IEEE Winter Power Meeting, New York, January 26-30, 1970.
53. H.B.Thoren and L. Carlson, 'A digital computer program for the calculation of switching and lightning surges on power systems', IEEE Trans. on Power Apparatus and Systems, Vol.PAS-89, No.2, pp. 212-218, Feb.197
54. Alan Budner, 'Introduction of frequency dependent line parameters into an electromagnetic transients program', IEEE Trans. on Power Apparatus and System. Vol.PAS-89, pp. 88-97, Jan. 1970.
55. M. Ramamoorthy, 'Transient analysis of multiconductor transmission lines with special reference to nonlinear problems' - Discussion, Proc. IEE, Vol.118, No.5, pp. 795-796, June 1971.
56. Discussion on " Calculation of transients on transmission lines with sequential switching", 'Transient analysis of multiconductor transmission lines with special reference to nonlinear problems' and 'frequency dependent parameters in transmission line analysis' Proc. IEE, Vol. 118, No.12, pp. 1815-1819, Dec.1971
57. L.M. Wedepohl and D. Wilcox, 'Transient analysis of underground power transmission systems - System model and wave propagation characteristics - Proc. IEE, 120, No.2, pp. 253-258, Feb. 1973.
58. A. Ametani, 'Modified travelling wave techniques to solve electrical transients on lumped and distributed constant circuits - Refraction coefficient method', Proc. IEE, Vol.120, No.4, pp. 497-504, April 1973.
59. E.Bolton, D. Birtwhistle, P. Bownes, M.G. Dwek and G.W.Routledge, 'Overhead-line parameters for circuit breaker application', Proc. IEE, Vol.120, No.5, pp. 561-573, May 1973.



60. M. Ramamoorthy, 'Approximate method for including ground effects in wave propagation transmission lines', Proc. IEE, Vol.120, No.6, pp.702-703, June 1973.
61. J.P. Bickford and R.M.K.El-Devieny, 'Energisation of transmission lines from inductive sources - Effects of nonsimultaneous closure also investigated', Proc. IEE, Vol.120, No.8, pp. 883-890, August 1973.
62. D. Birtwhistle, G.E. Gardner, B. Jones and R.J. Urwin, 'Transient recovery voltage and thermal performance of an airblast circuit breaker', Proc. IEE, Vol.120, No.9, pp. 994-1000, Sept. 1973.
63. C. Singarajah, 'Voltage surges induced on overhead lines by lightning strokes', Proc. IEE, Vol.120, No.10, pp. 1259-1260, Oct.1973.
64. M. Nakagawa, A. Amatani and K. Iwamoto, 'Further studies on wave propagation in overhead lines with earth return: impedance of stratified earth', Proc. IEE, Vol.120, No.12, pp. 1521-1528, Dec. 1973.
65. S.J. Balser, J.R. Eaton and P.C. Krause, 'Single pole switching - A comparison of computer studies with field test results', IEEE Trans. on Power Apparatus and Systems, Vol.PAS-93, pp.100-108, Jan./Feb. 1974.
66. G.L. Wilson, R.F. Challan and D.J. Bosack, 'Transmission line models for switching studies: Design criteria Part I - Effect of nontransposition and frequency', IEEE Trans. on Power Apparatus and Systems, Vol. PAS-93, pp. 383-389, Jan./Feb.1974.
67. G.L. Wilson and K.A. Schmidt, 'Transmission line models for switching studies: Design criteria Part II - Selection of section length, model design and test', IEEE Trans. on Power Apparatus and Systems, Vol. PAS-93, pp. 389-396, Jan./Feb. 1974.
68. D.P. Carroll and F. Nozari, 'An efficient computer method for simulating transients on transmission lines with frequency dependent parameters, IEEE Trans. on Power Apparatus and Systems, Vol.PAS-94, pp. 1167-1177, July/Aug. 1975.
69. N.S. Rau, 'A new approach to the selection of insertion resistance to control switching overvoltages', IEEE Trans. on Power Apparatus and Systems, Vol.PAS-94, pp. 1367-1375, July/Aug. 1975.

70. R.G. Colclaser, J.E. Beehler and T.F. Garrity, 'A field study of the short-line-fault component of transient recovery voltage', IEEE Trans. on Power Apparatus and Systems, Vol. PAS-94, pp. 1943-1954, Nov./Dec. 1975.
71. R.G. Wasley and S. Selvavinayagamoorthy 'Approximate frequency response values for transmission line transient analysis', Proc. IEE, Vol. 121, No. 4, pp. 281-286, April 1974.
72. J.P. Bickford and R.M.K. El-Dewieny, 'Energisation of transmission lines from mixed sources', Proc. IEE, Vol. 121, No. 5, pp. 355-360.

## APPENDIX A

## SYSTEM DATA

Length of the line 240 Kms.

Source inductance 0.1 H/phase

Earth conductivity 100 Ohm-m.

50 Hz line parameter matrices for the untransposed configuration are as follows:

$$R = \begin{bmatrix} 0.079658 & 0.049180 & 0.048136 \\ 0.049180 & 0.078826 & 0.048053 \\ 0.048136 & 0.048053 & 0.077874 \end{bmatrix} \times 0.62 \text{ ohm/Km.}$$

$$L = \begin{bmatrix} 0.002493 & 0.001132 & 0.000829 \\ 0.001132 & 0.002434 & 0.000979 \\ 0.000829 & 0.000979 & 0.002291 \end{bmatrix} \times 0.62 \text{ H/Km.}$$

$$C = \begin{bmatrix} 1.89230 & -0.35843 & -0.10716 \\ -0.35843 & 1.81560 & -0.34268 \\ -0.10716 & -0.34268 & 1.74110 \end{bmatrix} \times 0.62 \times 10^{-8} \text{ f/Km.}$$

For the case of the transposed line, the line parameters are obtained by finding the average values of the diagonal and off-diagonal elements of these matrices separately, corresponding to the untransposed case.

## APPENDIX B

## LINE PARAMETERS CALCULATION - CARSON'S FORMULAE

$$\text{Self impedance of conductor} = r_c + 0.00159f \\ + j0.004657f \log_{10} \frac{2160V(\rho/f)}{\text{GMR}}$$

$$\text{Mutual impedance between two conductors} = 0.00159f \\ + j0.004657f \log_{10} \frac{2160V(\rho/f)}{d_{ab}}$$

where  $r_c$  = resistance of the conductor per mile

$f$  = frequency in Hz

$\rho$  = earth resistivity in ohm-m

GMR = geometric mean radius of the conductor  
in feet

$d_{ab}$  = distance between the conductors in feet.

## APPENDIX C

## SYSTEM DATA - BOONYUBOL'S EXAMPLE

Positive sequence resistance of the line = 0.03 ohm/mile  
Positive sequence inductance of the line = 1.56 mH/mile  
Positive sequence capacitance of the line = 0.0189  $\mu$ f/mile  
Zero sequence resistance of the line = 0.316 ohm/mile  
Zero sequence inductance of the line = 5.76 mH/mile  
Zero sequence capacitance of the line = 0.0138  $\mu$ f/mile  
Frequency of supply = 60 Hz  
Length of the line = 180 miles

The fault is simulated at mid span.

The source impedance has been taken as zero.

The fault has been assumed to occur on phase 'a' at the instant when phase 'a' voltage is at positive peak.

## APPENDIX D

## SYSTEM DATA FOR FAULT STUDIES

Length of the line      480 Kms.

The line is fed on both the ends by similar sources, which are purely inductive of value 0.05 H.

Earth conductivity    = 100 ohm-m.

The computed line parameter matrices at 50 Hz for the untransposed configuration are given below. As these matrices are symmetric, only the lower triangular elements are given.

$$[R] = \begin{bmatrix} 0.079658 & & & & & \\ 0.049180 & 0.078826 & & & & \\ 0.048136 & 0.048053 & 0.077874 & & & \\ 0.049658 & 0.049180 & 0.048136 & 0.079658 & & \\ 0.049180 & 0.048826 & 0.048053 & 0.049180 & 0.078826 & \\ 0.048136 & 0.048053 & 0.047874 & 0.048136 & 0.048053 & 0.077874 \end{bmatrix}$$

x 0.62 ohm/Km.

$$[L] = \begin{bmatrix} 0.002493 & & & & & \\ 0.001132 & 0.002434 & & & & \\ 0.000829 & 0.000979 & 0.002291 & & & \\ 0.000972 & 0.000876 & 0.000754 & 0.002493 & & \\ 0.000876 & 0.000848 & 0.000786 & 0.001132 & 0.002434 & \\ 0.000754 & 0.000786 & 0.000829 & 0.000829 & 0.000979 & 0.002291 \end{bmatrix}$$

x 0.62 H/Km.

$$[C] = \begin{bmatrix} 1.39230 & & & & & \\ -0.35843 & 1.81560 & & & & \\ -0.10716 & -0.34268 & 1.74110 & & & \\ -0.12082 & -0.08571 & -0.06246 & 1.89230 & & \\ -0.08571 & -0.10012 & -0.12187 & -0.35843 & 1.81560 & \\ -0.06246 & -0.12187 & -0.26750 & -0.10716 & -0.34268 & 1.74110 \end{bmatrix} \times 0.62 \times 10^{-8} \text{ f/Km.}$$

For the transposed configuration, the self elements of the line parameter matrices are obtained by taking the average value of the self elements of the corresponding parameter matrices of the untransposed case, given above. Similarly, the mutual elements between the phases of each circuit and the mutual elements between the two circuits for the transposed line are the average values of the corresponding elements of the untransposed case.

## APPENDIX E

## URAM AND MILLER'S METHOD - THEORY

The Uram and Miller's method is a time domain method, in which by making certain assumptions, an incremental solution of the transmission line equations for the voltage and current at each instant at any point on a transmission line, subsequent to a switching operation is made possible.

The voltage and current vectors at any point on a transmission line, subsequent to a switching operation are governed by the equations

$$-\frac{\partial \underline{v}(x,t)}{\partial x} = [R] \underline{i}(x,t) + [L] \frac{\partial \underline{i}(x,t)}{\partial t}$$

$$-\frac{\partial \underline{i}(x,t)}{\partial x} = [C] \frac{\partial \underline{v}(x,t)}{\partial t}$$

neglecting the conductance to ground of the transmission line.

Taking the Laplace transform with respect to  $t$ , these equations become

$$-\frac{d\underline{V}(x,s)}{dx} = \{ [R] + s[L] \} \underline{I}(x,s) \quad (\text{E.1})$$

$$-\frac{d\underline{I}(x,s)}{dx} = s[C] \underline{V}(x,s) \quad (\text{E.2})$$

These two equations can be combined to get

$$\frac{d^2 \underline{V}(x,s)}{dx^2} = [Z][Y] \underline{V}(x,s) \quad (\text{E.3})$$



where  $[Z] = \{ [R] + s[L] \}$

and  $[Y] = s[C]$

The above coupled matrix differential equation can be decoupled by performing the modal transformation,

$$\underline{V}(x,s) = [T] \underline{F}(x,s)$$

where  $[T]$  is an eigenvector matrix of the matrix product  $[Z][Y]$ .

Equation (E.3), after the modal transformation, takes the form

$$\frac{d^2 \underline{F}(x,s)}{dx^2} = [T]^{-1} [Z][Y][T] \underline{F}(x,s)$$

where  $[T]^{-1}[Z][Y][T]$  is a diagonal matrix.

The solution of this equation for the  $i$ th modal component can be written as

$$F_i(x,s) = K_{1i}(s) e^{-\sqrt{(Z_{mi} Y_{mi})}x} + K_{2i}(s) e^{\sqrt{(Z_{mi} Y_{mi})}x}, i=1,N.$$

where  $K_{1i}(s)$  and  $K_{2i}(s)$  are constants, independent of  $x$  and  $Z_{mi} Y_{mi} = i$ th diagonal element of the diagonal matrix  $[T]^{-1}[Z][Y][T]$ .

In the vector notation, the solution can be written as

$$\underline{F}(x,s) = \underline{K_1(s)} e_{\underline{x}}^- + \underline{K_2(s)} e_{\underline{x}}^+$$

where

$$\underline{K}_1(s) e_x^- = [K_{11}(s) e^{-V(Z_{m1} Y_{m1})x} \dots K_{1N}(s) e^{-V(Z_{mN} Y_{mN})x}]^T$$

and

$$\underline{K}_2(s) e_x^+ = [K_{21}(s) e^{V(Z_{m1} Y_{m1})x} \dots K_{2N}(s) e^{V(Z_{mN} Y_{mN})x}]^T$$

Transforming back to the phase quantities

$$\underline{V}(x,s) = [T] \underline{F}(x,s) = [T] \{ \underline{K}_1(s) e_x^- + \underline{K}_2(s) e_x^+ \}$$

From equation (E.1), the solution for the transformed phase current vector can be written as

$$\underline{I}(x,s) = [T] [\Omega]^{-1} \{ \underline{K}_1(s) e_x^- - \underline{K}_2(s) e_x^+ \}$$

where  $[\Omega] =$

$V(Z_{m1}/Y_{m1})$	0	...	0
0	$V(Z_{m2}/Y_{m2})$	...	0
...	...	...	...
0	0	...	$V(Z_{mN}/Y_{mN})$

From these general transformed voltage and current vector solutions, the expressions for the sending end and receiving end transformed voltage and current vectors can be written as

$$\underline{V}_s(s) = [T] \{ \underline{K}_1(s) + \underline{K}_2(s) \} \quad (E.4)$$

$$\underline{I}_s(s) = [T][\Omega]^{-1} \{ \underline{K}_1(s) - \underline{K}_2(s) \} \quad (E.5)$$

$$\underline{V}_R(s) = [T] \{ \underline{A}(s) + \underline{B}(s) \} \quad (E.6)$$

$$\underline{I}_R(s) = [T][\Omega]^{-1} \{ \underline{A}(s) - \underline{B}(s) \} \quad (E.7)$$

where the  $i$ th components of the vectors  $\underline{A}(s)$  and  $\underline{K}_2(s)$  are related to the  $i$ th components of  $\underline{K}_1(s)$  and  $\underline{B}(s)$  by the expressions

$$A_i(s) = K_{1i}(s) e^{-\sqrt{(Z_{mi} Y_{mi})} \ell}$$

$$\text{and } K_{2i}(s) = B_i(s) e^{-\sqrt{(Z_{mi} Y_{mi})} \ell}$$

In the above expressions

$\ell$  = the length of the line

$$\begin{aligned} \sqrt{(Z_{mi} Y_{mi})} &= \sqrt{[(R_{mi} + sL_{mi})sC_{mi}]} \\ &= s\sqrt{(L_{mi} C_{mi})} \left(1 + \frac{R_{mi}}{sL_{mi}}\right)^{\frac{1}{2}} \end{aligned}$$

where  $R_{mi}$ ,  $L_{mi}$  and  $C_{mi}$  are the resistance, inductance and capacitance per unit length respectively offered by the line for the  $i$ th mode of propagation.

$$\text{If } \frac{R_{mi}}{sL_{mi}} \ll 1, \sqrt{(Z_{mi} Y_{mi})} = s\sqrt{(L_{mi} C_{mi})} + \frac{R_{mi}}{2} \sqrt{\left(\frac{C_{mi}}{L_{mi}}\right)}$$

$$\sqrt{\left(\frac{Y_{mi}}{Z_{mi}}\right)} = \sqrt{\left(\frac{C_{mi}}{L_{mi}}\right)} \left(1 + \frac{R_{mi}}{sL_{mi}}\right)^{-\frac{1}{2}}$$

$$\text{If } \frac{R_{mi}}{sL_{mi}} \ll 1, \sqrt{\left(\frac{Y_{mi}}{Z_{mi}}\right)} = \sqrt{\left(\frac{C_{mi}}{L_{mi}}\right)}.$$

$$\text{Hence } A_i(s) = K_{1i}(s) e^{-(R_{mi}/2)\sqrt{(C_{mi}/L_{mi})}\ell} e^{-s\sqrt{(L_{mi} C_{mi})}\ell} \quad (\text{E.8})$$

$$K_{2i}(s) = B_i(s) e^{-(R_{mi}/2)\sqrt{(C_{mi}/L_{mi})}\ell} e^{-s\sqrt{(L_{mi} C_{mi})}\ell} \quad (\text{E.9})$$

When equations (E.4) - (E.7) are transformed back to time domain, the sending end and receiving end voltage and current vectors become

$$\underline{v}_s(t) = [T] \{ \underline{k}_1(t) + \underline{k}_2(t) \} \quad (\text{E.10})$$

$$\underline{i}_s(t) = [T][\Omega]^{-1} \{ \underline{k}_1(t) - \underline{k}_2(t) \} \quad (\text{E.11})$$

$$\underline{v}_R(t) = [T] \{ \underline{a}(t) + \underline{b}(t) \} \quad (\text{E.12})$$

$$\underline{i}_R(t) = [T][\Omega]^{-1} \{ \underline{a}(t) - \underline{b}(t) \} \quad (\text{E.13})$$

where  $[\Omega] =$

$$\begin{bmatrix} V(L_{m1}/C_{m1}) & 0 & \dots & 0 \\ 0 & V(L_{m2}/C_{m2}) & 0 & \dots & 0 \\ \dots & \dots & \dots & \dots & \dots \\ 0 & 0 & \dots & V(L_{mN}/C_{mN}) \end{bmatrix}$$

By the shifting property of Laplace transforms, when functions  $A_i$  and  $K_{2i}$  are related by expressions as in equations (E.8) and (E.9) to the functions  $K_{1i}(s)$  and  $B_i(s)$  in the Laplace domain, the corresponding inverse transformed functions in time domain are related by the expressions

$$a_i(t) = e^{-(R_{mi}/2)V(C_{mi}/L_{mi})t} k_{1i}(t-\tau_i) u(t-\tau_i), \quad i=1, N$$

$$k_{2i}(t) = e^{-(R_{mi}/2)V(C_{mi}/L_{mi})t} b_i(t-\tau_i) u(t-\tau_i), \quad i=1, N$$

where  $\tau_i$  = the travel time of the  $i$ th mode of propagation  
of the travelling wave to traverse the length  
of the line

$$= \sqrt{(L_{mi} C_{mi})} l .$$

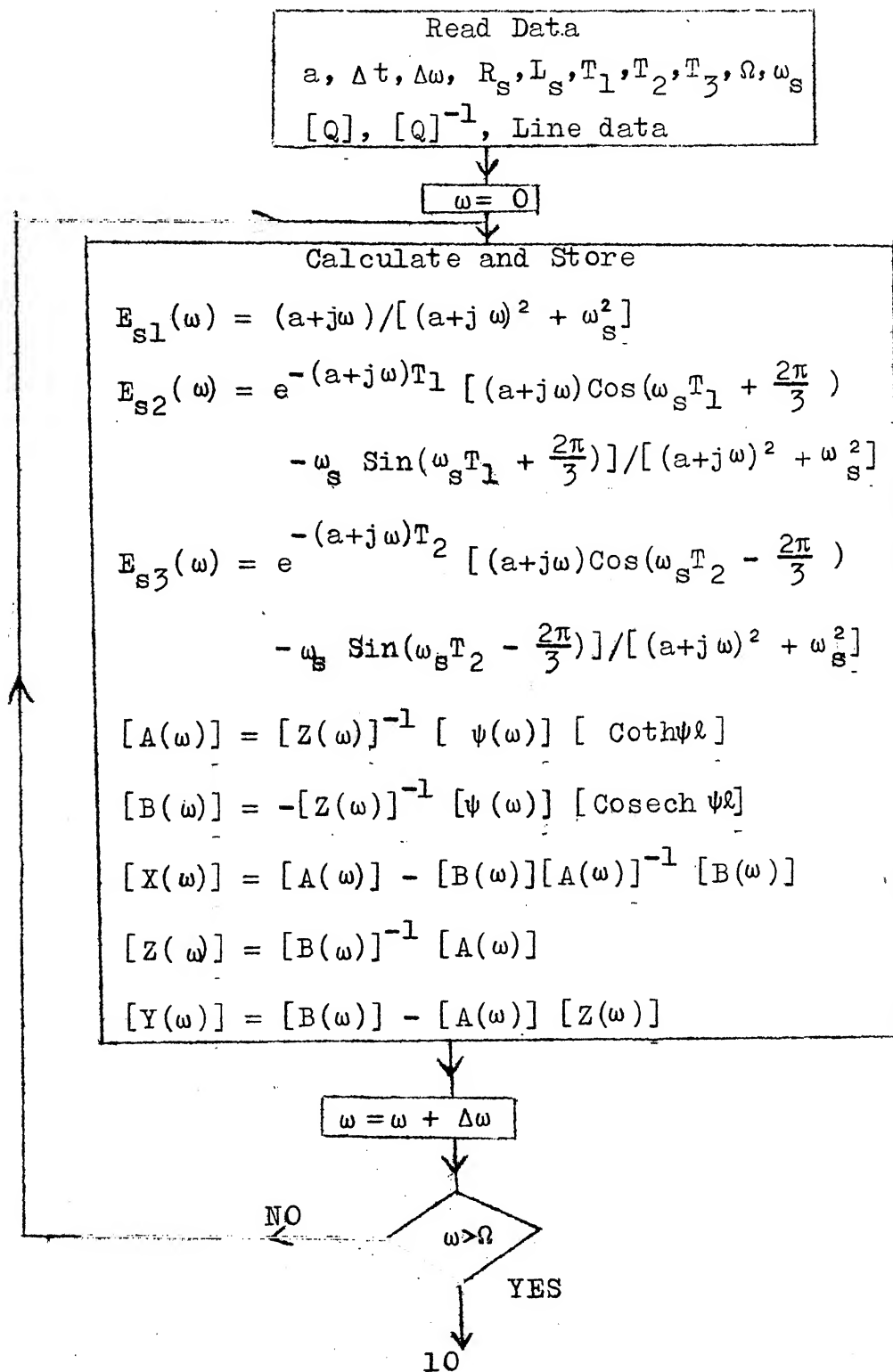
Thus the voltage and current vectors at each instant of time at any point on a transmission line, subsequent to a switching operation can be expressed in terms of the values of the four function vectors  $\underline{k}_1(t)$ ,  $\underline{k}_2(t)$ ,  $\underline{a}(t)$  and  $\underline{b}(t)$  at that instant. Among these four function vectors,  $\underline{a}(t)$  and  $\underline{k}_2(t)$  have been shown to be the attenuated delay functions of the other two function vectors  $\underline{k}_1(t)$  and  $\underline{b}(t)$  respectively. The function vectors  $\underline{k}_1(t)$  and  $\underline{b}(t)$  can be expressed in terms of the function vectors  $\underline{a}(t)$  and  $\underline{k}_2(t)$  by the terminal conditions of the line. For the case of the line, which was relaxed before the switching operation, initially till the time equal to the travelling time of the line, the delayed functions are zero.

$$\text{i.e. } a_i(t) = 0, \quad i = 1, N \quad \text{for } 0 < t < \tau_i$$

$$\text{and } k_{2i}(t) = 0, \quad i = 1, N \quad \text{for } 0 < t < \tau_i.$$

Thus an incremental solution of the transmission line equations in time domain is possible for an initially relaxed line.

## APPENDIX F

FLOW CHART FOR COMPUTATION OF SEQUENTIAL CLOSING TRANSIENTS  
BY MODIFIED FOURIER TRANSFORM METHOD

10

$$IIII = 1$$

$$\omega = 0$$

$$T_{\max} = T_1$$

$$\underline{v}_s(t) = 0, 0 < t < T_3$$

$$\underline{v}_R(t) = 0, 0 < t < T_3$$

$$IIII = 1$$

YES

1

$$[Y_s(\omega)] = \begin{bmatrix} 1/[R_s + (a+j\omega)L_s] & 0 & 0 \\ 0 & 0 & 0 \\ 0 & 0 & 0 \end{bmatrix}$$

NO

$$IIII = 2$$

YES

2

$$\omega = 0$$

$$T_{\max} = T_2$$

$$\omega = 0$$

$$T_{\max} = T_3$$

7

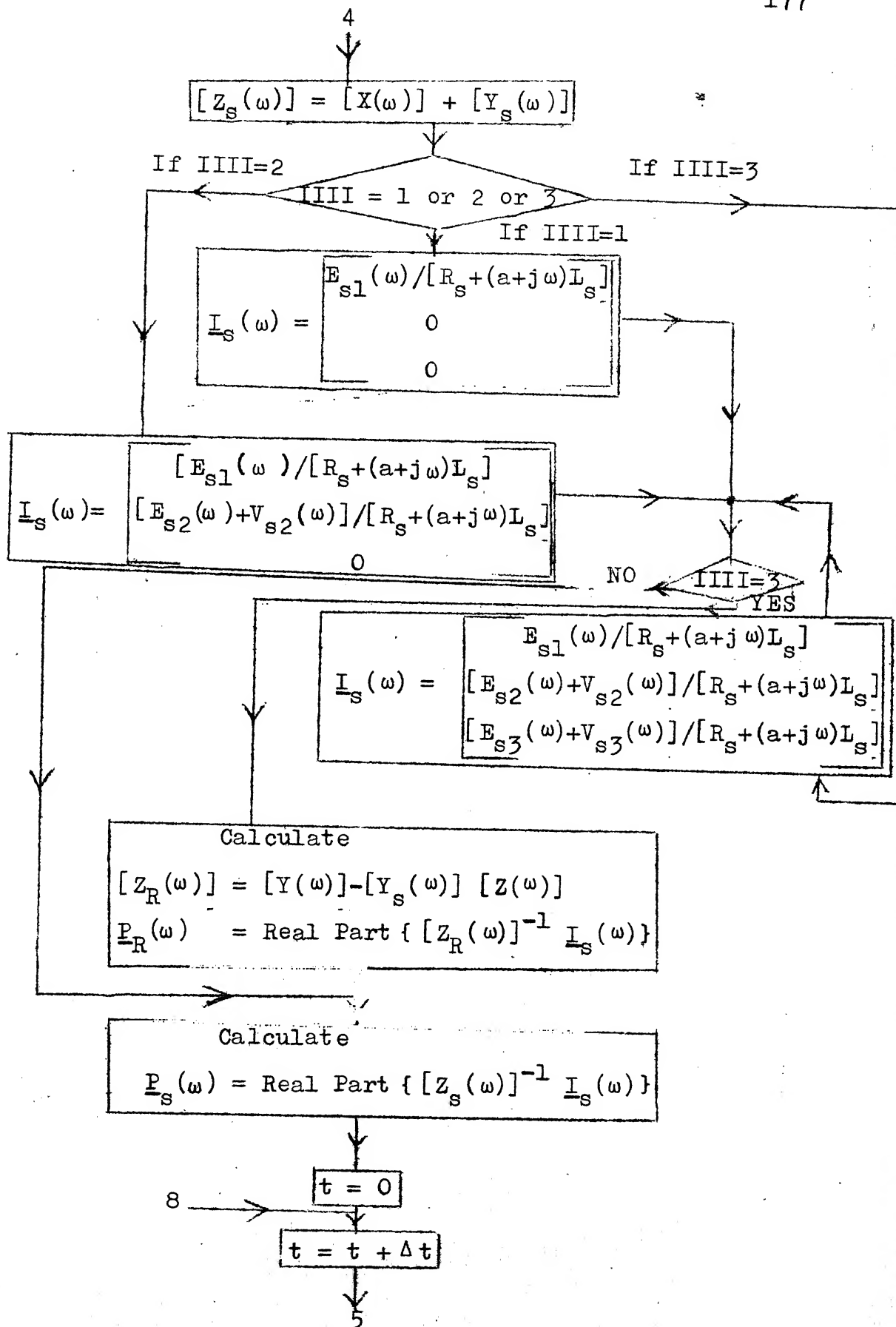
Calculate  $V_{s2}(\omega)$ ,  $V_{s3}(\omega)$ , the modified Fourier transforms of  $v_{s2}(t)$  in  $0 < t < T_1$  and of  $v_{s3}(t)$  in  $0 < t < T_2$

Calculate  $V_{s2}(\omega)$ , the modified Fourier transform of  $v_{s2}(t)$  in the interval  $0 < t < T_1$

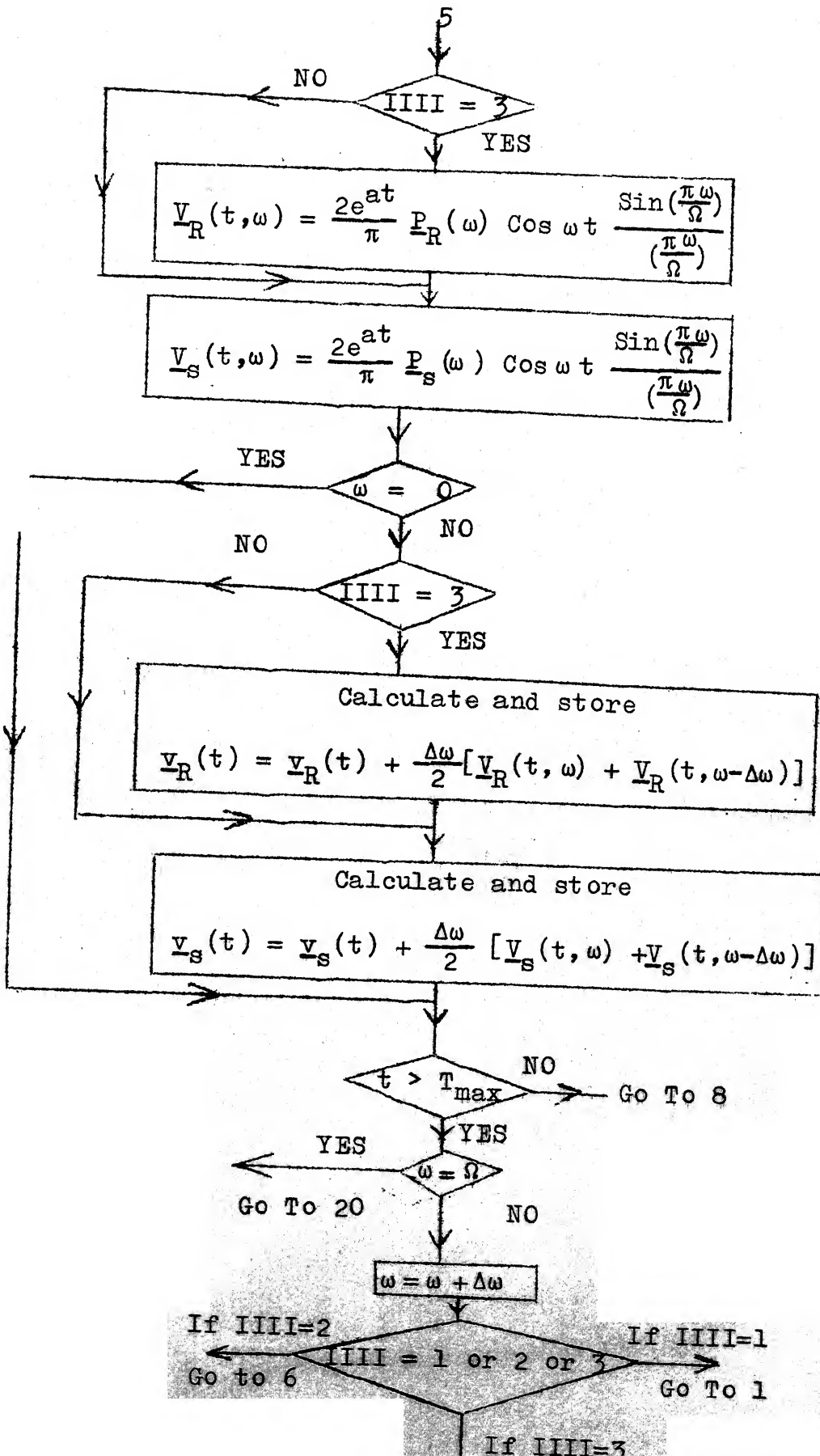
$$[Y_s(\omega)] = \begin{bmatrix} 1/[R_s + (a+j\omega)L_s] & 0 & 0 \\ 0 & 1/[R_s + (a+j\omega)L_s] & 0 \\ 0 & 0 & 0 \end{bmatrix}$$

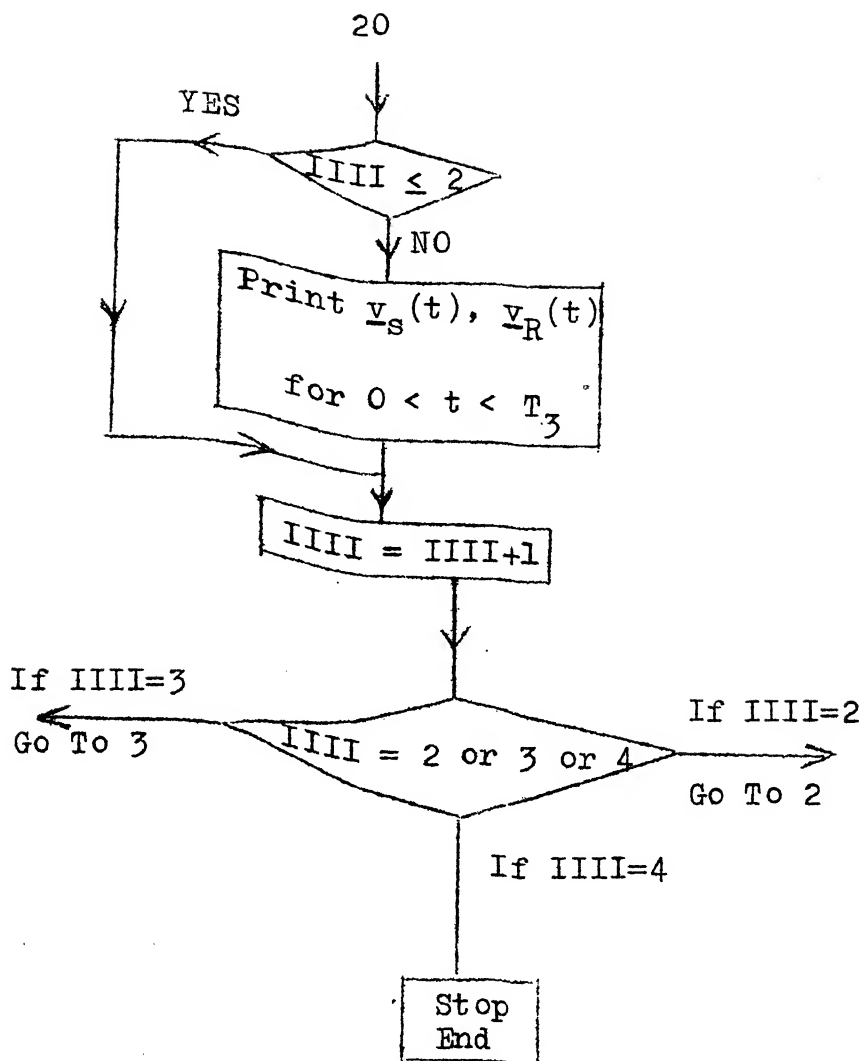
$$[Y_s(\omega)] = \begin{bmatrix} 1/[R_s + (a+j\omega)L_s] & 0 & 0 \\ 0 & 1/[R_s + (a+j\omega)L_s] & 0 \\ 0 & 0 & 1/[R_s + (a+j\omega)L_s] \end{bmatrix}$$

4









## APPENDIX G

## OBRA-LUCKNOW LINE DATA

Length of the line                      400 Kms

Shunt reactors of reactance value    3200 ohms at both the ends.

Source reactance at Obra end is 67.8 ohms, which takes into account both the local generation, short circuit power supplied through transmission lines on lower voltage levels and the short circuit power of the 400 KV transformers.

The line parameters are as follows:

Positive sequence resistance	0.027 ohm/Km
Positive sequence inductive reactance	0.331 ohm/Km
Positive sequence capacitance	$10.95 \times 10^{-9}$ f/Km
Zero sequence resistance	0.261 ohm/Km
Zero sequence inductive reactance	1.31 ohm/Km
Zero sequence capacitance	$8.42 \times 10^{-9}$ f/Km.

## CURRICULUM VITAE

1. Candidate's name: R. Balasubramanian

2. Academic Background:

<u>Degree</u>	<u>Specialisation</u>	<u>Institute</u>	<u>Year</u>
B.E.	Electrical Engineering	P.S.G.College of Technology, Madras University	1968
M.Sc.(Engg.)	Power Systems	Annamalai University	1970

3. Publications:

- i) Calculation of transient due to fault initiation on a double circuit transmission line, Accepted for publication in the Proceedings IEE, London.
- ii) Calculation of energising transient on a double circuit transmission line, Submitted for publication in Proceedings IEE-IERE (India).
- iii) Accurate evaluation of energising transients on double circuit EHV transmission lines, Submitted for presentation in IEEE Winter Power Meeting, 1977.

**A 51191**

[illegible][illegible]

EE-1976-D-BAL-ACC